Universidade de Aveiro  Departamento de Química
Ano 2018

MARISA
CONCEIÇÃO
REIS PINHO

EFEITO DA OBESIDADE NO LIPIDOMA DA GLÂNDULA MAMÁRIA E A SUA RELAÇÃO COM O DESENVOLVIMENTO DE CANCRO

Universidade de Aveiro Departamento de Química
Ano 2018

MARISA
CONCEIÇÃO
REIS PINHO

EFEITO DA OBESIDADE NO LIPIDOMA DA GLÂNDULA MAMÁRIA E A SUA RELAÇÃO COM O DESENVOLVIMENTO DE CANCRO

EFFECT OF OBESITY IN THE MAMMARY GLAND LIPIDOME AND ITS RELATION WITH CANCER DEVELOPMENT

Dissertation in Biochemistry – specialization in biomolecular methods, written under the scientific guidance of Prof. Doctor Maria do Rosário Gonçalves Reis Marques Domingues, Associated Professor with aggregation of the Department of Chemistry University of Aveiro and Doctor Luisa Alejandra Helguero Shepherd Assistant Professor at the Department of Medical Sciences, University of Aveiro

o júri

presidente                    Professora Doutora Rita Maria Pinho Ferreira
                              Professora auxiliar, Universidade de Aveiro


                              Doutora Iola Melissa Fernandes
                              Equiparada a investigadora principal, Universidade de Aveiro


                              Professora Doutora Luisa Alejandra Helguero
                              Professora auxiliar, Universidade de Aveiro

**Palavras-chave**

**Resumo**

A prevalência de excesso de peso e obesidade têm vindo a aumentar mundialmente e está associada ao desenvolvimento de diversas patologias como: doenças cardiovasculares, hipertensão, diabetes mellitus e outras doenças crônicas. Adicionalmente, mais recentemente, estudos epidemiológicos mostraram que a obesidade está associada ao aumento do risco de desenvolver diversos tipos de cancro, incluindo o cancro de mama. Os lípidos têm diversas funções, incluindo sobrevivência celular, proliferação, sinalização celular e morte, uma vez que estão envolvidos no armazenamento de energia química, sinalização celular, membranas celulares e interações célula-célula. Por este motivo, quaisquer alterações no ambiente lipídico podem ter consequências graves na resposta celular normal a uma situação, contribuindo para o desenvolvimento de cancro. Como tal, o objetivo deste trabalho foi estudar as alterações no lipidoma da glândula mamária relacionadas com a obesidade e como essas alterações se podem relacionar com o aumento do risco de desenvolver cancro de mama na obesidade. Para tal foram usadas glândulas mamárias obtidas de um modelo animal onde a obesidade foi induzida pela dieta. As técnicas de análise utilizadas foram Q-TOF (para triacilgliceróis), GS-MS (para os ácidos gordos) e LC-MS (para os fosfolípidos). Os resultados mostraram um aumento nos níveis dos triacilgliceróis que mais ricos nos ácidos gordos C18:2 (n-6). Esses ácidos gordos foram reportados que quando oxidados produzem aldeídos que podem formar aductos promutagénicos com o DNA, podendo desta forma contribuir o desenvolvimento da carcinogénese. Adicionalmente, os níveis de fosfatidilcolinas mais saturadas e com mais carbonos diminuíram, dando origem a membranas celulares mais fluidas, característica das células cancerígenas, além de uma diminuição nos níveis de ceramidas, lípido que tem atividade antiproliferativa, mostrando assim que o processo apoptótico pode estar afetado na obesidade. Por último, também relatamos uma diminuição nos níveis de fosfatidiletanolamina e plasmenil etanolamina, que pode estar relacionado com a diminuição na proteção antioxidante de lipídios de membrana. Em suma, na obesidade existe uma alteração no lipidoma da glândula mamária que contribui para uma maior predisposição de mutações de DNA assim como a alteração na resposta apoptótica e autofágica da célula, o que por sua vez pode contribuir para o aumento do risco de desenvolvimento de cancro da mama.

Abstract

The prevalence of overweight and obesity is increasing worldwide and has been associated several comorbidities like cardiovascular diseases, hypertension, diabetes mellitus and other chronic diseases. In addition, more recently epidemiological studies have shown that obesity is associated with increased risk of many types of cancer, including breast cancer. Lipids have many functions, including cellular survival, proliferation, cell signaling and death, since they are involved in chemical-energy storage, cellular signaling, cell membranes, and cell–cell interactions. For this reason, any alterations in the lipid environment can bring severe alterations to the normal cell response to a situation, contributing to cancer development. Therefore, the objective of this work was to study the alterations in the lipidome of the mammary gland related to obesity and how those alterations may be related to the increase risk of developing breast cancer in obesity. For such, the mammary gland used were obtain from an animal model where obesity was induced by diet. The techniques used where Q-TOF (for triacylglycerol), GS-MS (for the fatty acids) and LC-MS (for the phospholipids). Our results show an increase in the levels of the triacylglycerol richer in fatty acid C18:2 (n-6). Those fatty acids have been reported to when oxidized produce aldehydes that form can form promutagenic adducts with DNA in human cells and thus may contribute to human cancers. In the phospholipids analyses we saw a decreased in the levels of phosphatidylcholines, more saturated and with more carbons, giving origin to more fluid cell membranes, a characteristic associated to cancer cells. In addition, we also saw a decreased in the levels of ceramides a lipid that has an anti-proliferative activity, showing this way that the normal apoptotic cells response may be impaired in obesity. Lastly, we also report a decrease in the levels of phosphatidylethanolamine and plasmyl-phosphatidylethanolamine which can be associated to a decrease in the antioxidant protection of membrane lipids. In sum, in obesity there is a modifications in the mammary gland lipidome that contributes for a higher predisposition to DNA mutations as well as, for an alteration in the apoptotic and autophagy response of cells, being that this may contribute to a higher risk of developing breast cancer.

# Table of contents:

# Abbreviations:

**α-MSH -** alpha-melanocyte stimulating hormone

**AA** – arachidonic acid

**ACC** – acetyl-CoA carboxylase

**ACL** - average chain length

**ACLY** – ATP-citrate lyase

**ACO** - acyl CoA oxidase

**ACS** – acyl-CoA synthetase

**ANGPTL4** – angiopoietin-like 4

**AP** - adipocyte precursor

**ATGL** – adipose triglyceride lipase

**AVL** - average chain length

**BMI** – body mass index

**CAT** - catalase

**DAGs** – diacylglycerides

**DBI** - double bond index

**DIO** – diet-induced obese

**DIT** – diet-induced thermogenesis

**EFAs** – essential fatty acid

**FA** - fatty acids

**FASN** – fatty acid synthase

**FATP** – fatty acid transport protein

**FFAs** – free fatty acids

**GLs** - glycerolipids

**GPLs** - glycerophospholipids

**GPx** - glutathione peroxidase

**HChD** – high cholesterol diet

**HFD** – high fat diet

**HSL** – hormone-sensitive lipase

**IS** - internal standard

**LDL** -  low-density lipoprotein

**LPA** – lysophosphatidic acid

**LPL** – lipoprotein lipase

**MDA** - malondialdehyde

**MGL** – monoacylglycerol lipase

**MS** – mass spectrometry

**MUFAs** – monounsaturated fatty acids

**NCoR** - nuclear receptor corepressor

**ND** – normal diet

**NFkB** – nuclear factor kappa B

**NI** – not identified

**NZO** – The New Zealand obese mouse

**PA** – phosphatidic acid

**PAI-1** – plasminogen activator inhibitor-1

**PC** – phosphatidylcholine

**PCA** – principal component analysis

**PE** – phosphatidylethanolamine

**PG** – phosphatidylglycerol

**PI** – phosphatidylinositol

**PK** - polyketides

**PL** – phospholipids

**PLS-DA** – projection to latent structures discriminant analysis

**PPARs** – peroxisome proliferator-activated receptors

**PPER** – PPAR response element

**PRLs** - prenol lipids

**PS** – phosphatidylserine

**PUFAs** – polyunsaturated fatty acids

**ROS** - reactive species of oxygen

**S1P** – sphingosine-1-phosphate

**SCLs** - saccharolipids

**SFAs** – saturated fatty acids

**SLs** - sphingolipids

**SMs** – sphingomyelins

**SOD** - superoxide dismutase

**STs** - sulfatides

**STLs** - sterol lipids

**TAG** – triacylglycerol

**TCA** – tricarboxylic acid

**TNF** – tumor necrosis factor

**UCPs** – uncoupling proteins

**VEGF** - vascular endothelial growth factor

**WHO –** world health organization

**WAT –** white adipose tissue

**XICs –** extracted ion chromatogram

# List of tables:

# Figures list:

## 1.      Introduction

Obesity is a common but often underestimated condition of clinical and public health that has a major impact in many countries around the world. Body mass index (BMI) is a simple parameter and is most commonly used for classifying various degrees of overweight and obesity. It is calculated from the weight of the individual in kilograms divided by the square of the height in meters ($kg/m^2$).Based on the World Health Organization (WHO) criteria BMI <$18.5kg/m^2$ is considered underweight, 18.5–24.9 $kg/m^2$ ideal weight, 25–$29.9kg/m^2$ overweight or pre-obese and  lastly BMI $\geq 30kg/m^2$  obese. However, BMI may not correspond to the same degree of fatness in different populations due, in part, to different body proportions.[1]

Overweight together with obesity affects nowadays around a third of the world's population. However, the prevalence of this conditions is predominant in developed countries and has markedly increased between 1980–2008.[2] The higher the BMI the higher the risk of developing comorbidities such as diabetes, hypertension, hyperlipidemia and cancer.[3,4]The objective of this review it's to discuss how the lipid alterations seen in obesity can be related in breast carcinogenesis and if this lipid alterations could result in differential activation of the peroxisome proliferator activated receptors (PPARs).

## 2.      Animal models of obesity

The increasing  prevalence of obesity makes it imperative to use animal models that share similar characteristics of human obesity and its comorbidities in the pursuit for novel preventions and/or treatments.[5] Obesity can be considered polygenetic since more than one gene is associated to the tendency to develop this disease. Animal models can be partitioned into monogenetic models and polygenetic models. The monogenetic models are models in which only a single gene is lacking or dysfunctional in the entire animal. Monogenic animal models of obesity are useful because the obesity and the adiposity may be severe, resulting in a distinct phenotype. This distinct phenotype might be important for certain aspects of obesity research such as the expression of the leptin, insulin secretion and resistance.[6,7,8] The monogenic models are:

- KK-$A_y$ mice are a mouse model with peripheral insulin sensitivity and glucose intolerance.[9] The KK strain is an insulin resistant strain that results in diabetes and mild obesity.[10] When  an Agouti ($A_y$) mutation is induced into the KK strain the KK-$A_y$ mice are produced.[11] The Ay gene is ubiquitously expressed in the KK-Ay

mouse, and the agouti protein is thought to act as a melanocortin 4 receptor antagonist, thereby inhibiting the signals from alpha-melanocyte stimulating hormone (α-MSH) and affecting the regulation of energy balance.(12,13) Thus, KK-A$_y$ can be considered a mouse with a monogenic defect but in a polygenic background that results in a predisposition for obesity. The obesity is partially caused by hyperphagia, and the typical diabetes phenotype of KK-A$_y$ mice exhibits a hyperglycemia, hyperinsulinemia, and glucose intolerance.(14,15)

- *Ob/ob* mouse model lacks leptin production, it's a monogenic model used in obesity and diabetes. Worldwide several colonies of *ob/ob* mice exists, each of them with a different mutation showing variations of the phenotype.(16) Obesity is the first observable phenotypic characteristic of the *ob/ob* mouse, whereas insulin resistance and hyperglycemia follow the development of obesity. In addition, obesity is further increased in *ob/ob* mice because of a defect in thermogenesis in brown adipose tissue and therefore a larger deposition of ingested energy as fat.(17)'(18) Furthermore, lipogenesis, especially hepatic, is enhanced in *ob/ob* mice, which also adds to the disposition for an obese phenotype.(19)

- The Zucker rat has a homozygotes mutation (*fa/fa*). It develops an early onset obesity because of a defective leptin receptor.(20) Under normal conditions, leptin produced from adipose tissue signals acts via the leptin receptor to reduce food intake. In this rat, this regulatory path is nonfunctional, and despite high levels of circulating leptin, the rats remain hyperphagic.(21) In addition to obesity, the Zucker rat also develops insulin resistance, but glycemic levels remain normal, and they do not develop overt diabetes.(22)

In contrast to diseases caused by single-gene defects, many of the most common human pathologies, including obesity exhibit continuous phenotypic variation and a predominantly multifactorial and polygenic basis.(23) The polygenic models are another category of animal models that can be used in different models in obesity. They combine the contribution of the genetic (e.g. genes associated with lipid and insulin metabolism) with the environmental stimuli responsible for the different obesity phenotypes.(24) The polygenic animal models are:

- Diet-induced obese rats and mice (DIO) are more human-like models since the obesity is based on several factors, including an excessive intake of calories.

However, in the diet-induced obesity there is a large variation both with respect of the diet used as well as the strain used (strain which has a pronounced weight gain or strain considered obesity resistant).(25) Different predefined mouse and rat diets for obesity induction can vary in the percentage of calories from fat and carbohydrates, as well as the source of fat or carbohydrates, all of which can result in minor differences in phenotypes. In rodents, a high-fat and high-fructose diet has been shown to result in metabolic syndrome with obesity and changed body composition.(26,27)

- Cafeteria diet-induced obesity mainly results from hyperphagia that is partly compensated by increased energy expenditure, in particular diet-induced thermogenesis (DIT) due to sympathetic activation of brown fat. Overeating of cafeteria diets is due to increased average meal size as well as increased meal frequency.(28) This contrasts with overeating of palatable diets with no choice of foods, which mainly influences meal size.(29)

- UCD-T2DM rat is a polygenic rat model with adult-onset obesity, insulin resistance and late onset type 2 diabetes that maintains leptin signaling without dietary intervention.(30)

- The New Zealand obese (NZO) mouse is a polygenic model that develops hyperphagia and juvenile onset obesity, even when fed a low fat diet. In addition, as a number of genetic susceptibility loci that favor the development of adiposity and hyperglycemia have been identified in NZO mice. This animal model has been primarily used for pharmacogenetics studies.(31)

- Tallyho mouse is a model with moderate obesity and male-derived hyperglycemia.(32) The increased food intake and not reduced energy expenditure, is the reason for the obesity. In addition, Tallyho mice have hypothalamic leptin resistance and upregulation of NPY mRNA levels.(33)

**Table 1** summarizes all the characteristics of the different models discussed in this text.

*Table 1 - Comparison between the different animal models of obesity. MG- monogenetic model; PG – polygenic model*

| | | Obesity | Hyperphagia | Hyperinsulinemia | Glucose intolerance | Hyperglycemia |
|---|---|---|---|---|---|---|
| **MG** | KK-A$_y$ | X | X | X | X | X |
| | *Ob/ob* | X | X | X | X | Mild |
| | Zucker | X | X | X | X | ___ |
| **PG** | DIO / Cafeteria diet-induced obesity | X | ___ | X | X | ___ |
| | UCD-T2DM | X | X | X | X | X |
| | NZO | X | X | — | — | X |
| | Tallyho | X | X | — | — | X |

In sum, there are a number of valid surrogate animal models of human obesity that can be utilized in the discovery and developmental process. All these models differ from each other on different aspects, making each of them ideal for the study of distinct aspects of human physiology. Human obesity phenotype is mainly caused by the interaction between genetic and environmental factors, therefore, the model that best reflects this condition the DIO model.

In obesity the adipocyte hypertrophy and excessive adipose tissue accumulation promotes adiposopathy resulting on abnormal levels of local and circulating lipids, making these an important class of biomolecules to study their association with the comorbidities related to this disease.

## 3.    Lipid classes

Lipids area major class of biological molecules and play many key roles in different processes having structural (e.g., by stabilizing different membrane phenotypes and biochemical characteristics) and signaling function.(34,35) Lipids include nine categories: fatty acids (FAs), triacylglycerol (TAG), glycerophospholipids (GPLs), glycerolipids (GLs), prenol lipids (PRLs), saccharolipids (SCLs), sphingolipids (SLs), sterol lipids (STLs) and polyketides (PK) – **table 2**.(36) The majority of the FAs are esterified in the other lipid classes. Structurally, FAs are simple lipids, whereas GPLs, GLs, SLs, and STLs are more complex lipids.(37,38)
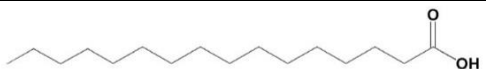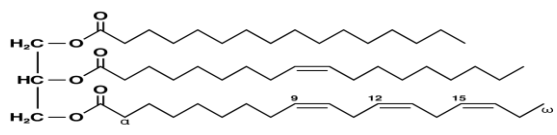
TAGs molecule is made up of 3 molecules of fatty acids that are connected to a glycerol molecule. While a glycerol molecule is made up of 3 carbon molecules with an OH bond on each, the fatty acid molecule is made up of a long chain of carbon and hydrogen (hydrocarbon) atoms with a carboxyl (-COOH) group at one end.(38)
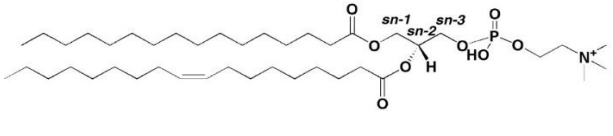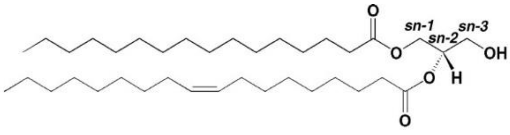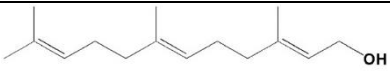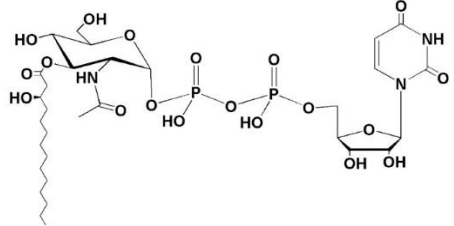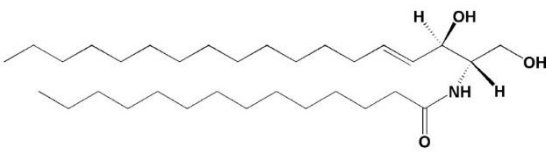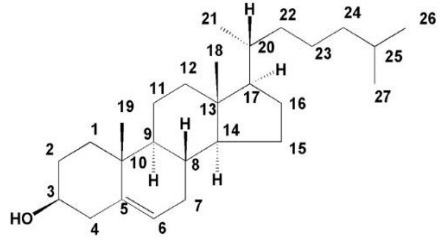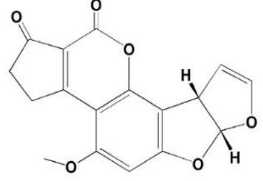
When it comes to GPLs, there are numerous classes that include numerous molecular species with different combinations of polar heads at the *sn-3* position and acyl moieties at the *sn-1* and *sn-2* positions, respectively, likephospholipids (PLs) and lysophospholipids.(39) Based on the type of polar heads at the *sn-3* position of the glycerol backbone, PLs be divided into: phosphatidic acid (PA), phosphatidylcholines (PC), phosphatidylethanolamine (PE), phosphatidylglycerol (PG), phosphatidylinositol (PI) and phosphatidyloserine (PS).

SLs are essential bioactive compounds of cellular membrane, and include ceramides, cerebrosides, gangliosides, sphingomyelins (SMs) and sulfatides (STs). SL structure is formed by a sphingoid base backbone: the head group attached to the primary hydroxyl group, N-acyl group and sphingoid-base backbone determines a change in structure of SLs. (41)

In addition, lipids contain FAs classified according to the presence or absence of double bonds as saturated (SFAs—without double bonds), monounsaturated (MUFAs—with one double bond) and polyunsaturated fatty acids (PUFAs—with two or up to six double bonds); further, as *cis* or *trans* bond, based on the configuration of the double bonds defines *n-3* or *n-6* PUFAs depending on the position of the first double bond from the fatty acid methyl-end.(43,44)

*Table 2 - Classification of lipids based on structures. The table lists different lipid classes and an example for each class: fatty acids (FAs), triacylglycerol (TAGs) glycerophospholipids (GPLs), glycerolipids (GLs), prenol lipids (PRLs), saccharolipids (SCLs), sphingolipids (SLs), sterol lipids (STLs) and polyketides (PK).*

| Lipid category | Example | Structure |
|---|---|---|
| FAs | Hexadecanoic acid |  |
| TAGs | (6Z,9Z,28Z,31Z)-19-(16,17,18-trihydroxy-15-oxooctadecyl)heptatriaconta-6,9,28,31-tetraene-18,20-dione |  |

| | | |
|---|---|---|
| **GPLs** | 1-hexadecanoyl-2-(9Z-octadecenoyl)-sn-glycero-3-phosphocholine |  |
| **GLs** | 1-hexadecanoyl-2-(9Z-octadecenoyl)-*sn*-glycerol |  |
| **PRLs** | 2E,6E-farnesol |  |
| **SCLs** | UDP-3-O-(3R-hydroxy-tetradecanoyl)-αD-N-acetylglucosamine |  |
| **SLs** | N-(tetradecanoyl)-sphing-4-enine |  |
| **STLs** | Cholest-5-en-3β-ol |  |
| **PK** | Aflatoxin B1 |  |

In conclusion, lipids are a class of biomolecules may be composed by FAs and can be divided into nine categories: FAs, TAGs, GPLs, GLs, PRLs, SCLs, SLs, STLs and PK. Each of these class of lipids have different functions that are essential for cell structure and functioning, contributing to the homeostasis of the organism. Any alterations of the normal lipid composition and profile can be associated with diseases such as cardiovascular diseases, cancer and others.(45,46)

## 4.    Metabolic Changes in obesity

The majority of adult mammalian tissues satisfy their lipid requirements through the uptake of free fatty acids (FFAs) and lipoproteins, like low-density lipoprotein (LDL), from the bloodstream. FAs and cholesterol biosynthesis are restricted to a subset of tissues, including liver, muscle and adipose tissues.(47,48,49) In the context of breast cancer, obesity and lipid biosynthesis are important because the mammary gland activates lipid metabolism during lactogenic differentiation and the mammary epithelium is embedded in subcutaneous fatty tissue. Thus, adiposopathies resulting from obesity likely contribute to the increase of breast cancer incidence observed in obese women.(50)

The first step in FA and cholesterol biosynthesis is the production of acetyl-CoA from citrate by the enzyme ATP-citrate lyase (ACLY). Acetyl-CoA  is then converted into malonyl-CoA by the enzyme acetyl-CoA carboxylase (ACC).(51) Acetyl-CoA and malonyl-CoA are then coupled to the acyl-carrier protein domain of the multifunctional enzyme fatty acid synthase (FASN). The repeated condensations of acetyl groups generate the saturated FA: palmitic acid, that can be further elongated and desaturated to generate a diverse spectrum of saturated and unsaturated FAs synthesized by mammalian cells and used as precursors for GLPs eicosanoids and more.(52) Most of the acetyl-CoA used for *de novo* FA and cholesterol biosynthesis is generated from glucose via the conversion of pyruvate to citrate in the tricarboxylic acid (TCA) cycle – **figure 1**.(53) Humans and mice are not able to generate some FAs (Essential FAs - EFAs), the omega *n-3* or *n-6* (e.g. linoleic acid and α-linoleic acid), need to be provided by the diet, however humans are able to synthetize longer omega *n-3* or *n-6* through a series of desaturations and elongations to these EFAs.(54,55)
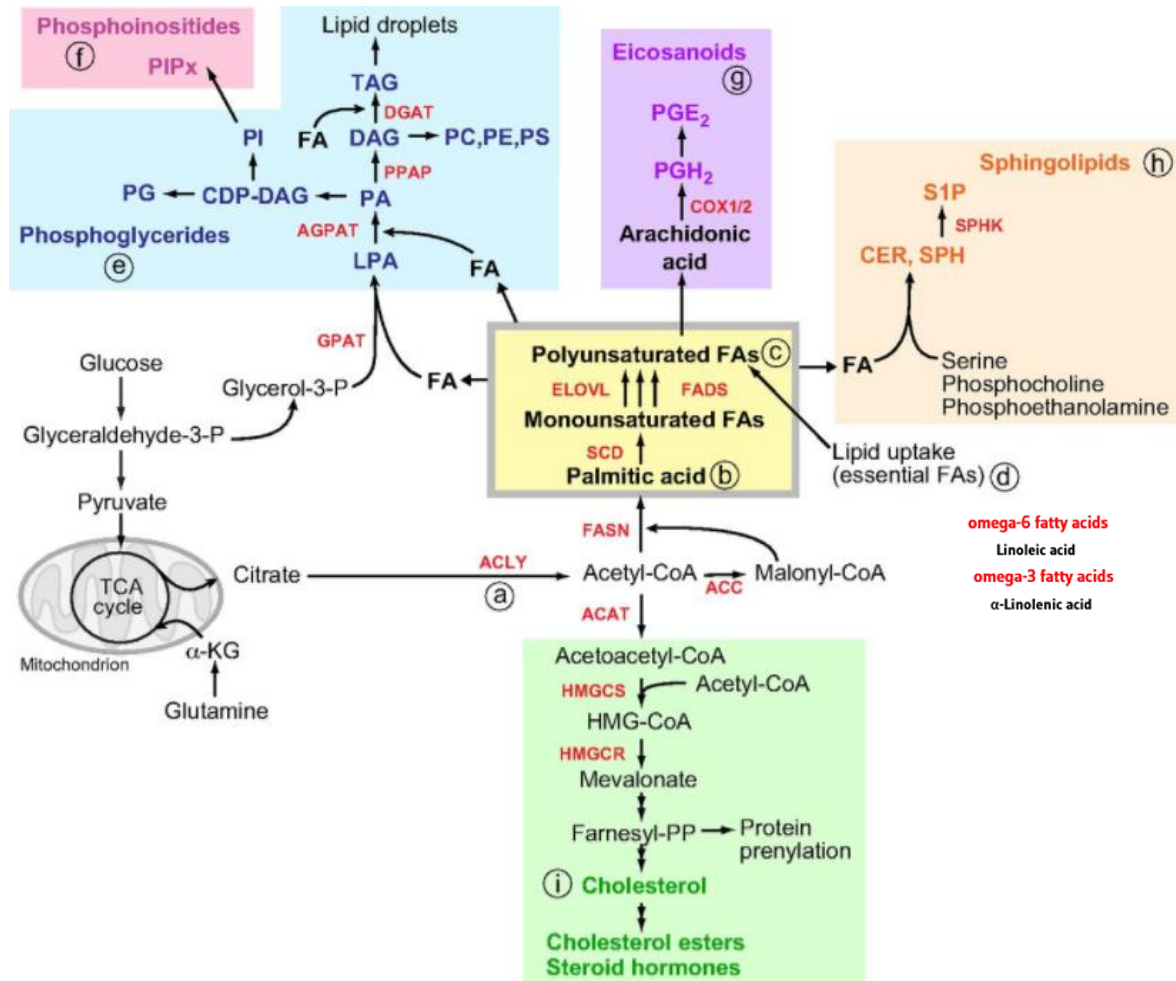
*Figure 1 - Schematic overview of the pathways involved in the synthesis of FAs (fatty acids), cholesterol, phosphoglycerides, eicosanoids and sphingolipids. The enzymes involved in lipid biosynthesis are indicated in red. (a) Glucose- or glutamine-derived citrate is first converted to acetyl-CoA by ACLY (ATP-citrate lyase). (b) For FA biosynthesis, acetyl-CoA is converted into malonyl-CoA. The repeated condensation of acetyl-CoA and malonyl-CoA by the multifunctional enzyme FASN (fatty acid synthase) leads to the generation of palmitic acid (16:0). The introduction of a double bond in the Δ9 position of the acyl chain by SCD (stearoyl-CoA desaturase) generates mono-unsaturated FAs. (c) Subsequent elongation and further desaturation produces FAs with different saturation levels. (d) Essential FAs need to be provided from dietary sources. (e,f) Saturated and unsaturated FAs are combined with glycerol-3-phosphate (glycerol-3-P) to generate (e) phosphoglycerides and (f) phosphoinositides. (g) Arachidonic acid, is used for the synthesis of eicosanoids. (h) Sphingolipids contain acyl chains and polar head groups derived from serine, phosphocholine or phosphoethanolamine. (i) Cholesterol biosynthesis is initiated by the conversion of acetyl-CoA to acetoacetyl-CoA. Addition of another acyl group by HMGCS (3-hydroxy-3-methylglutaryl-CoA synthase) produces 3-methylglutaryl-3-hydroxy-CoA, which is converted to mevalonate by HMGCR (3-hydroxy-3-methylglutaryl-CoA reductase). Subsequent reactions result in the production of farnesyl-pyrophosphate. Cholesterol also forms the structural backbone for steroid hormone biosynthesis. Enzyme abbreviations: ACAT, acetyl-CoA acetyltransferase; ACC, acetyl-CoA carboxylase; AGPAT, 1-acylglycerol-3-phosphate O-acyltransferase; COX1/2, prostaglandin-endoperoxide synthase (PTGS); DGAT, diacylglycerol O-acyltransferase; ELOVL, fatty acid elongase; FADS, fatty acid desaturase; GPAT, glycerol-3-phosphate acyltransferase; PPAP, phosphatidic acid phosphatase; SPHK, sphingosine-1-kinase. Metabolite abbreviations: α-KG, α-ketoglutarate; CDP-DAG, cytidine diphosphate-diacylglycerol; CER, ceramide; DAG, diacylglycerol; LPA, lysophosphatidic acid; PA, phosphatidic acid; PC, phosphatidylcholine; PE, phosphatidylethanolamine; PG, phosphatidylglycerol; PGE2, prostaglandin E2; PGH2, prostaglandin H2; PI, phosphatidylinositol; PIPx, phosphatidylinositol phosphate; PS, phosphatidylserine; S1P, sphingosine-1-phosphate; SPH, sphingosine; TAG, triacylglyceride. (Adapted from(56) and(57))*

In addition, FAs can be used to generate many different types of lipids. They are converted into diacylglycerides (DAGs) and TAGs via the glycerol phosphate pathway. However, intermediates of this pathway can be converted into different phosphoglycerides, including PC, PE, PS, PI e PG. In addition to phophoglycerides, sphingolipids, and eicosanoids are also generated from FAs.(58,59)

An increase in lipid biosynthesis is a major contributor to increased fat mass, while its reduction may be protective against the development of obesity. In the case of obesity, carbohydrates consumed in thus excess for the hepatic glycogen storage capacity must be converted into lipids for subsequent storage. White adipose tissue (WAT) is the primary lipid-storing tissue. High-carbohydrate diets and high-fat diet have been shown to activate a lipogenic response in liver tissue since they stimulate the expression of both PGC-1β and SREBP1 in liver. PGC-1β coactivates the SREBP transcription factor family and stimulates lipogenic gene expression. Also high-fat diets contribute to obesity, as the caloric excess must be stored, adipose tissue expands to accommodate this increase in exogenous lipids and endogenous lipid synthesis.(60,61)

Another important event besides lipid biosynthesis is the breakdown of lipids such as the hydrolysis of triglycerides into glycerol and FFA (lipolysis) – **figure 2.** The main enzymes responsible for lipolysis are adipose triglyceride lipase (ATGL), hormone-sensitive lipase (HSL) and monoacylglycerol lipase (MGL).(62) A defect in HSL expression linked to an impaired lipolytic capacity is observed in subcutaneous adipocytes of obese subjects.(63) In individuals that have obese relatives the maximum expression of HSL is lower as well as the lipolytic capacity of adipocytes, suggesting a defect in fat cell lipolysis caused by an impaired expression of HSL in normal weight individuals with a family history of obesity.(64,65) This information suggest that impaired lipolysis could therefore constitute an early event in the development of obesity. In addition to the alteration of the levels of hormone-sensitive lipase in obesity, the adipose triglyceride lipase protein expression and TAG hydrolase activity were also shown to be reduced in subcutaneous AT of obese subjects.(66)
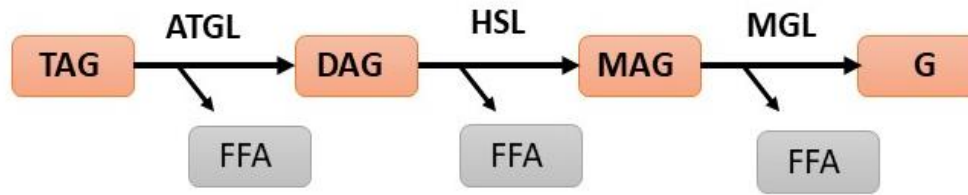
*Figure 2 - Schematic delineation of the coordinate breakdown of TAG (triacylglycerols) into DAG (diacylglycerol) promoted by ATGL (adipose triacylglyceride lipase). Later, HSL (hormone-sensitive lipase) produces MAG (monoacylglycerol) from DAG, and lastly MGL (monoglyceride lipase) transforms MAG into G (glycerol). These enzymes promote the release of FFA (free fatty acids).*

Obesity and excessive accumulation of adipose tissue are well known risk factors for several types of cancer, including breast cancer. Especially in obesity, the dysfunctional adipose tissue releases increased amounts of FFAs. Furthermore, it was shown that breast cancer cells and adipocytes, which are a major component of the stromal environment of mammary tumors are able to directly interact with each other. On a molecular level, studies show that adipocytes exert tumor-promoting effects on breast cancer cells.[67,68,69] The elevated levels of FAs can be used by cancer cells for the production of lipids that serve as oncogenic lipid signaling molecules, such as lysophosphatidic acid (LPA), prostaglandins and sphingosine-1-phosphate (S1P).[70,71,72]

In the adipose tissue, oleic acid (C18-1 *n-9*) is the most abundant fatty acid esterified to TAGs and for this reason has been studied for its potential role in cancer progression.[73,74] Recently it was demonstrated that oleic acid induces the expression of angiopoietin-like 4 (ANGPTL4) in breast cancer cells, resulting in anoikis resistance and metastasis via upregulation of fibronectin.[75] In addition, the expression of ANGPTL4 was also induced by palmitic acid and linoleic acid.[76,77] In another study, it was showed that AMPK is activated in highly metastatic breast cancer cells treated with oleic acid. AMPK promoted the rates of fatty acid oxidation and ATP synthesis in these cells, enabling increased cell growth and cell migration. In low metastatic cancer cells, oleic acid reduced cell proliferation and migration, indicating a selective tumor-promoting function of oleic acid on highly metastatic cancer cells.[78] It was shown that, in highly aggressive breast cancer cells, oleic acid enhanced cell proliferation via activation of G protein-coupled receptor 40.[79]

In conclusion, adult mammalian tissues do the uptake of FFAs and lipoproteins from the bloodstream. In addition, de *novo* lipogenesis is a complex and highly regulated metabolic pathway that when it's stimulated by the excess of carbohydrates contributes to the development of obesity. Another important mechanism is lipolysis and in obesity it was shown an alteration in the expression of the enzymes involved in this mechanism affecting the breakdown of the TAGs. However besides FA, also lipids are involved in cancer and obesity and for the study of the lipids alterations and we are able to study them through the analysis of the lipidome of breast cells.

## 4.1 Lipidome of normal breast vs breast cancer

The importance of the lipids is that they play essential roles in cellular functions, such as survival, proliferation and death, since they are involved in chemical-energy storage, cellular signaling, cell membranes, and cell–cell interactions in tissues. These cellular processes are strongly related to several carcinogenesis pathways, such as transformation, progression, and metastasis.(80,81,82,83) The study of lipids profile in normal cells and lipid alterations in cancer cells helps to elucidate metabolic alterations in this disease and discover potential biomarkers that can be used later in clinic situations.(80)

One important lipids group are the PUFAs. They are involved in the inflammatory process, which is in turn related to cancer cell survival and motility.(84,85) PUFAs play an essential role in normal physiology. Omega-3 PUFAs, are precursors for the production of anti-inflammatory eicosanoids and specialized pro-resolving lipid mediators (e.g, resolvins, protectins and maresins).(86) In contrast, eicosanoids from the *n-6* PUFA–arachidonic acid (AA) axis are predominantly linked to pro-inflammatory mediators.(87) In recent years, epidemiologic studies have explored the role of *n-3* and *n-6* PUFAs on cancer risk and shown that diets with a low *n-3:n-6* ratio are associated with a higher risk of several cancer types.(88) Remarkably, in obese woman, an elevated intake of *n-3* PUFAs as well as a higher dietary intake ratio of *n-3:n-6* PUFAs is correlated with reduced breast cancer risk.(89) Especially in obesity, increased intake of *n-3* PUFAs might be a useful to reduce obesity-associated inflammation and related tumor risk.(90) A study using WAT from French women with either breast cancer or benign breast tumor showed that a decreased risk of breast cancer was associated with higher content of *n-3* PUFA (18:3, 20:5, 22:6). In contrast, a high content of *n-6* PUFA was associated with either a trend (20:4, 20:3) or an increased risk (18:2, 20:2) risk of developing breast cancer – **figure 3**.(91)
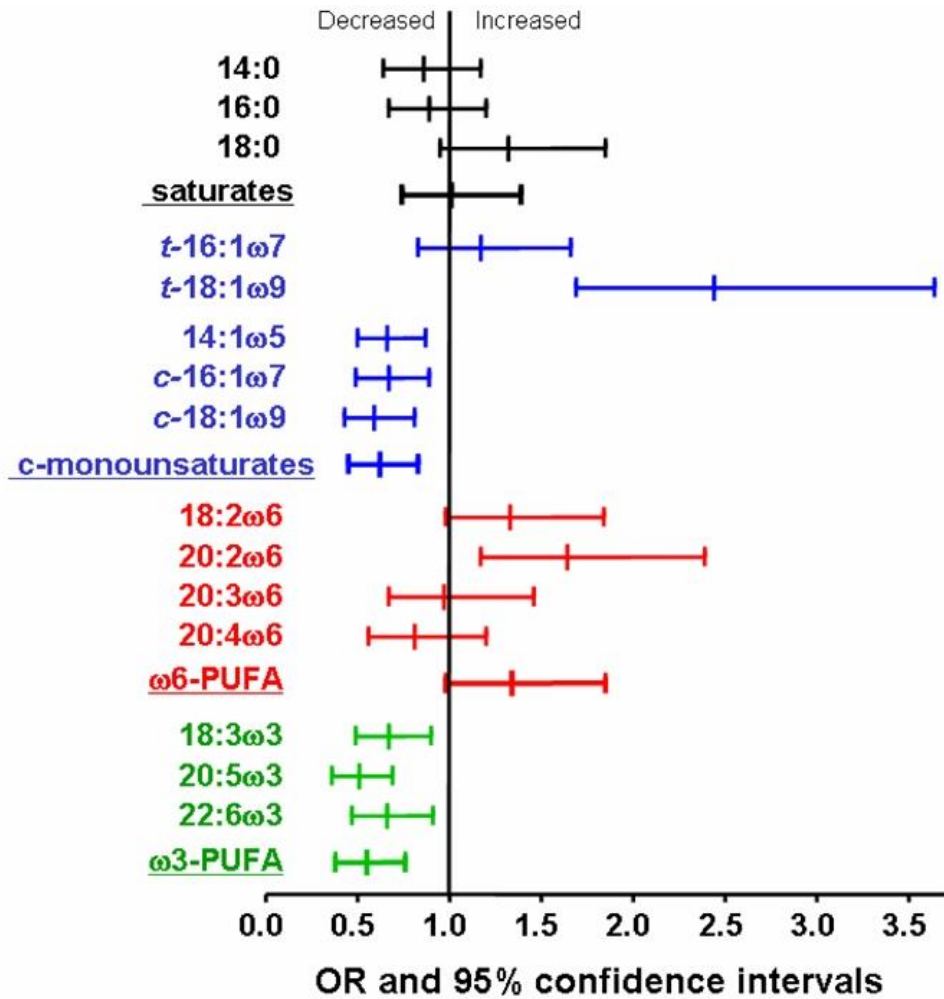
*Figure 3 – When comparing benign (control) and malign (disease) mammary gland tissue samples, a decreased risk of breast cancer was associated with higher content of n-3 PUFA. In contrast, a high content of n-6 PUFA was associated with either a trend or an increased risk. Cis-monounsaturates were all protective, whereas trans-monounsaturates were not, or were strongly associated with an increased risk. No association with breast cancer risk was detected for saturated fatty acids. (91)*

The previous analysis didn't take into account the inter-individual differences in the WAT content of each FA. For this purpose used the data from 329 patients (cases and control) organized according to the age and BMI from lower to higher was used and FAs values are represented as different colors for from green (low) to red (elevated). Between the two study groups it's possible to see that the major differences are in the lower right corner where in the group of cases the values of *n-6* PUFA are more elevated and the ratio of *n-6* to *n-3* FA (lower panel) when compared to the controls – **figure 4**. This study showed that lipid profile array provides indication of the combinations of WAT FAs levels associated with the risk of breast cancer.(92)
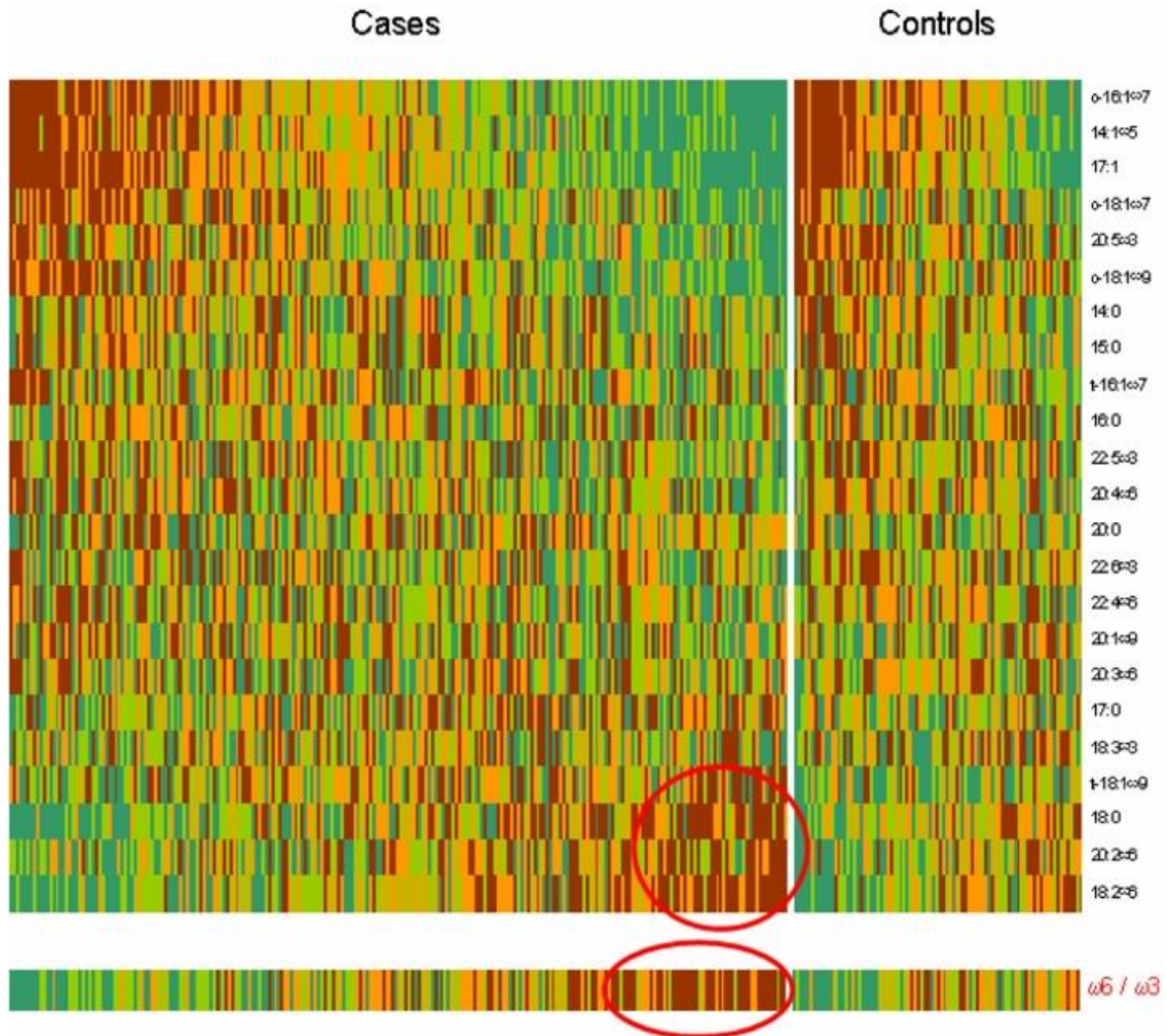
*Figure 4 - When comparing benign (control) and malign (disease) mammary gland tissue samples. Fatty acid level array in patients with benign (controls) or malignant (cases) breast tumors. In this representation, each lane represents a patient and each line represents one fatty acid. Fatty acid values are represented as different colors for from green (low) to red (elevated). Lower panel represents the ω6(n-6)/ω3(n-3) ratio of polyunsaturated fatty acids. (90)*

The changes in the lipidome of the cancer breast tissue were studied using ESI-MS, where it's possible to observe that in the breast cancer tissue there is a statistical significant decreased in the relative abundance of the molecular species of PI (34:4); PE (36:4), (38:5), (38:4); PC (34:2), (36:4). (38:5), (38:4), (38:3); SM (34:2), (36:2), (40:2). In contrast, the species of PE (34:1), (36:1); PC (38:6) have a higher relative abundance in breast cancer samples when compared to normal tissue samples.(93) **Figure 5** shows the significant differences between normal breast and breast cancer tissue, which confirms the fact that tumor tissue can be easily discriminated from normal cells for all studied cell lines based on their lipidomic composition.
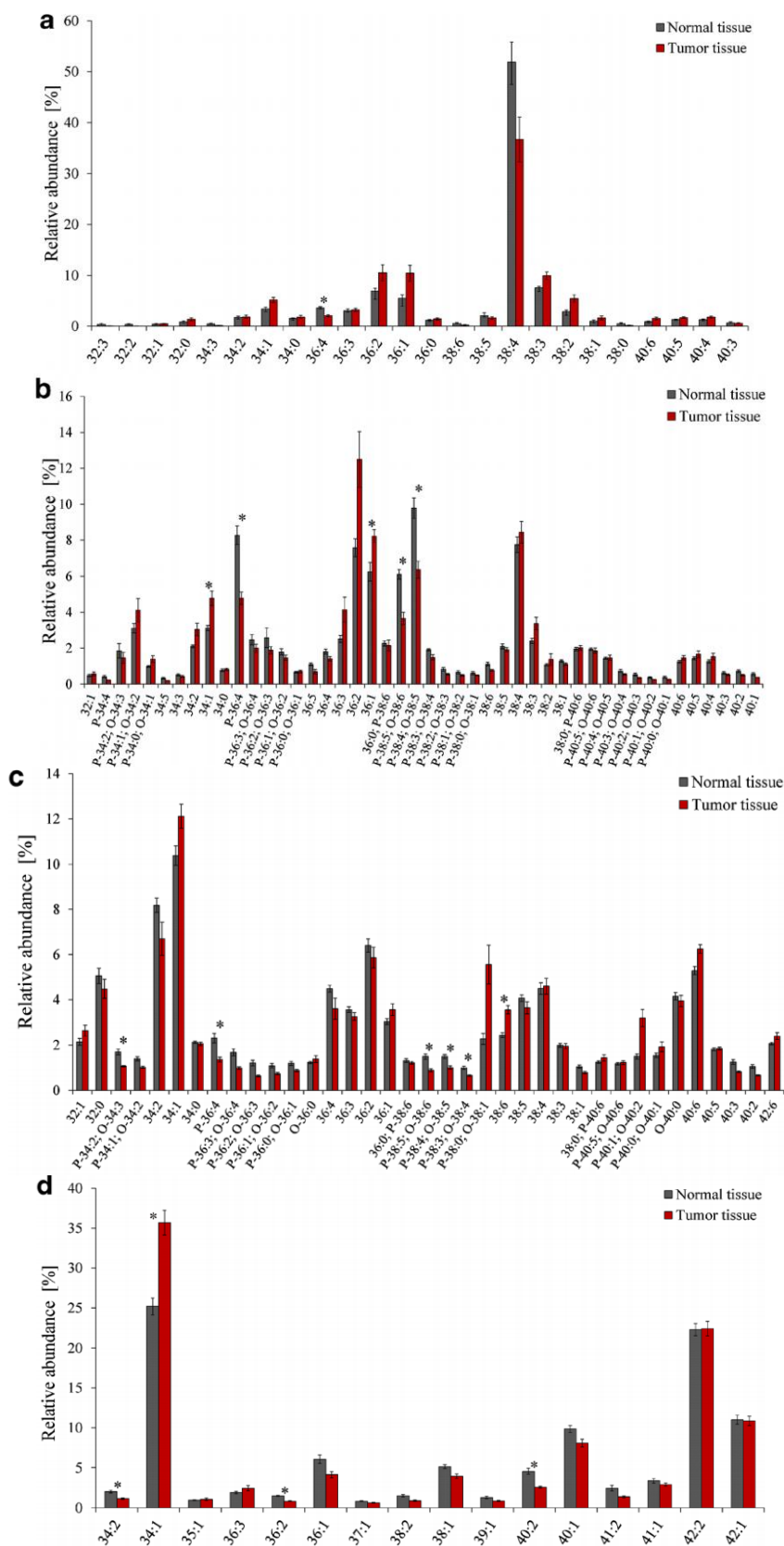
Figure 5 - Relative abundances [%] of individual molecular species of the phospholipid classes (a) PI, (b) PE, (c) PC, and (d) SM in normal and tumor tissues of ten breast cancer patients. Abundances were determined using relative abundances of [M-H]– and [M-CH3]– (PE) ions in negative-ion mass spectra or [M+H]+ ions (PI, PC and SM) in positive-ion mass spectra obtained by HILICHPLC/ESI-MS. Statistically significant differences according to T test are indicated by an asterisk * (93)

With the goal to determine the degree of similarity between tumor cell lines and tumor tissues and to identify the most dysregulated lipids observed for both models, *Cífková et al.* used breast normal and cancer cell lines and compared the results obtained with a study performed previously by them using normal and tumor cell lines (**figure 5**). The 10 most upregulated (A) and 10 most downregulated (B) lipids are represented in the **figure 6,** considering their relative abundance. The most pronounced upregulated lipids are low unsaturated PL like PC (32:1), PC (34:1); PI (34:1) as well as highly PUFA like PI (40:6), PE (40:6), PC (40:6) and PE (38:4) (**figure 6(A)).** In contrast, phospholipids containing PUFA with the formulas 36:4 and 38:4 (except PE (38:4)) are downregulated (**figure 6(B)).**The differences of the relative abundance between the breast tissue and cell lines can be related to the fact that there are changes in breast tissues that could be caused by other factors in addition to cancer, such as inflammation and immune response. However, we are able to see in PI (32:1), PE (32:1), PI (36:4) and PE (36:4) that there are some differences in the tendency of the change in the PLs. (94)
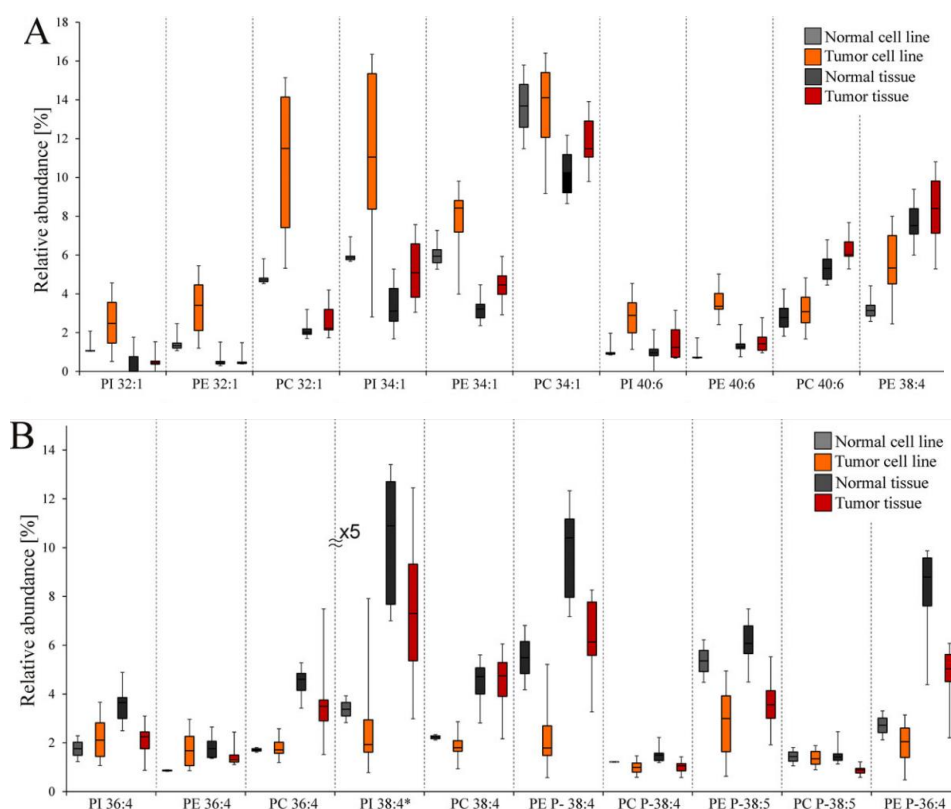


*Figure 6 - Box plots describing the most important (A) upregulated and (B) downregulated lipids in normal and tumor breast cell lines and tissues of breast cancer patients. In case of PI 38:4, y axes values are five times more than shown numbers. (94)*

Doria et al. after a previous study on mouse normal breast cells and breast cancer ones, applied TLC ESI-MS on human normal breast cells and breast cancer cell lines, in an effort to describe alterations of PL profiles between cancer and normal cell lines driving the progression of carcinogenesis. Non-malignant cells showed the highest differences in PE content, relative to total amount of PLs, whereas PA presented highest relative abundance in metastatic cells. In addition, higher levels of PCs and PI (40:5) were found in migratory cells, with metastatic ability.(95) Later a different group, using the GC-MS and direct infusion MS for the lipidomic analysis of breast cancer cell lines (MDA-MB-231 and MCF-7) with different degrees of invasiveness found that PS (38:4), PI (38:4), and PC (38:4) were significantly higher in the highly metastatic MDA-MB-231 cells than in slightly metastatic MCF-7 cells. In contrast, the levels of PE (36:2) and PI (36:1) were markedly lower in cells with high metastatic potential than in slightly metastatic ones.(96) In a study using MALDI-IMS, 34 pairs of surgical breast tissues (34 breast tumors with 34 adjacent normal samples) where analyzed with the aim of differentiating between tumors and normal tissues shown that PC (34:1) was overexpressed in breast cancer.(97) In addition, using high resolution MALDI-IMS on nine breast tumor samples and one normal breast tissue, it was showed that several PIs were specifically localized into cancer cell clusters, with a heterogeneous distribution, which identified two different populations of cancer cells: the first predominantly expressed PI (36:1), the second PI (38:3), being that the latter population was associated with tumor invasion.(98)

A MALDI-IMS approach was employed for investigating the effects of hypoxia and necrosis on the heterogeneous lipid composition in breast tumor model. The results showed that the lipid distributions into the tumor tissue were characterized by spatial heterogeneity: in particular PC (36:0), PC (34:1), PC (36:2) and PC (36:1) were localized in accessible tumor areas, whereas LPC (16:0) were localized in necrotic tumor regions. In addition, the results also revealed that palmitoylcarnitine, stearoylcarnitine, PC (38:1) and SM (d18:1/16:0) are mainly localized in the hypoxic tumor regions. (99)

In sum, in this pathology PUFAs play a major role, where *n-3* PUFAs have a protective effect on the development of the breast cancer and a higher content on *n-6* PUFAs increases the risk for the development of breast cancer. In addition, when comparing normal *vs.* cancer breast tissue we are able to see some alterations in the PLs relative abundance. Cancer cells shown the biggest differences in the relative abundance of PE (some are higher

and some are lower). In addition, PI is also associated with the invasion power off tumor cells. Nevertheless this field of study is not very explored and as consequence there aren´t enough studies relating breast cancer to lipidomic alteration. This type of studies can be very useful in the clinical field on diagnose and the prognosis of this disease. In addition we are also able to see that the lipid profile of breast tissue is similar to the breast cancer cells lines however, in the breast tissue we have a small contribution of the other structures composing the breast, besides cancer cells. Therefore, this epithelial-stromal communication resorting to specific lipid molecules as signaling mediators can influence cancer development and progression.

Lipid mediators can trigger physiological responses by activating nuclear hormone receptors, such as the PPARs (peroxisome proliferator-activated receptors). PPARs, in order, control the expression of networks of genes involved in all aspects of lipid metabolism. In addition, PPARs are tumor growth modifiers, via the regulation of cancer cell apoptosis, proliferation, and differentiation, and through their action on the tumor cell environment, namely, angiogenesis, inflammation, and immune cell functions.(100)

## 5. Peroxisome proliferator-activated receptor

PPARs are proteins belonging to the superfamily of phylogenetically related proteins termed nuclear hormone factor.(101) They show low natural ligand specificity, being activated by many long-chain saturated and unsaturated FAs and some PLs. Lipids act, directly or after metabolic processing, as signaling molecules implicated in the regulation of lipid and of carbohydrate metabolism. It is now established that PPARs are involved in such regulatory processes by acting as lipid sensors. PPAR agonists have different and specificities properties (e.g. different distribution profiles, distinctive gene expression profiles) for individual PPAR receptors, which lead to different clinical outcomes.(102,103)

The family of PPARs is represented by the following 3 members: PPAR-α (mostly expressed in liver and skeletal muscle), PPAR-δ (most cell types), and PPAR-γ (adipose tissue), each of which mediates the physiological actions of a variety of FA and fatty acids derived molecules. Whereupon activated, PPARs translocates to the nucleus and heterodimerizes with RXR.(104) PPARs bind to the target genes at a PPAR response element (PPRE), where they initiate transcription through the recruitment of the transcriptional machinery – **figure 7**.(105) PPARs can also negatively regulates some genes, through the blocking the transcription machinery from bonding to the promoter site. Some

transcription factors such as NFκB signal activators and transducers of transcription STAT-1 and AP-1 signaling are able to bind the activated PPARs trough DNA-independent protein-protein interactions resulting also in the transcriptional repression.(106)
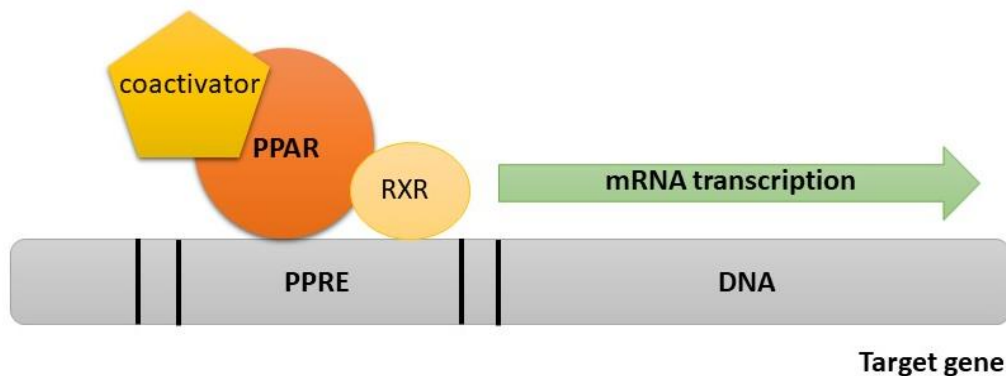


*Figure 7 - Mechanism of gene transcription by PPARs. PPARs - Peroxisome proliferator-activated receptors; RXR - Retinoid X receptor; PPER - PPAR response element.*

## 5.1 Role of PPARs in energetic metabolism

PPARα plays an essential role in intracellular FAs metabolism and tissues. A high expression of this receptor induce an increase of the FA catabolism. PPARα regulates the expression of genes coding for enzymes implicated in PPARα ligand metabolism and also modulates genes involved in FA uptake, activation to acyl-CoA esters, mitochondrial β-oxidation and ketone body synthesis.(107,108,109) The Expression of putative FAs transporter genes, such as the gene for fatty acid transport protein (FATP), are regulated by PPARα. The entrance of FAs through the cell membrane is controlled by the activity of FATP and by acyl-CoA synthetase (ACS) which traps FAs inside the cells by their conversion to ester derivatives, controlling this way the intracellular FAs concentration.(110) Furthermore, PPARα deficient mice fed with a HFD showed a substantial accumulation of lipids in liver highlighting the crucial role PPARα plays in lipid metabolism.(111,112)

The rate of mitochondrial FA uptake is one of the major FA metabolism regulators. PPARα has been demonstrated to affect mitochondria uptake of FA by up-regulating the expression of muscle and liver-type α-carnitine palmitoyltransferase I genes.(113,114) PPARα activators, through their effect on the expression of FA transporter and FA oxidation genes, direct the FA flux to the β-oxidation pathway dismissing the FA pool to be incorporated to triglyceride TG-rich lipoproteins. Consequently, PPARα maintains lipid homeostasis by controlling the FA flux from peripheral tissues, such as adipose tissue to the

liver. A study made with PPARα-deficient mice fasted for 24 hours showed that they display hypoglycemia, hypoketonemia, and elevated plasma FA levels.(111) Furthermore another studies revealed that PPARα might increase energy expenditure by up-regulating the expression of uncoupling proteins (UCPs).(115,116)

In the adipose tissue, PPARα mediates leptin-induced lipolysis.(117) Indeed, hyperleptinemia in rodents depletes adipocyte fat, while it up-regulates enzymes involved in FA oxidation, UCPs and PPARα, which are normally in low amounts in adipocytes. In addition to PPARα, PPARγ modulates lipid homeostasis and maintaining the mature adipocyte phenotype in the adipose tissue. PPARγ regulates gene expression of AP2, phosphoenol pyruvate carboxykinase, ACS, FATP and LPL (lipoprotein lipase).(118 ,119,120,121,122) The induction of LPL promotes FA delivery to adipocytes while induction of FATP and ACS results in enhanced FA uptake by the adipocyte. These actions contribute to enhanced TG synthesis and accumulation in adipose tissue.

Another receptor it's PPARδ that is expressed ubiquitously and is implicated in fatty acid oxidation, and in the response of macrophages for very low-density lipoprotein.(123,124) It also prevents exhaustion of hematopoietic stem cells by lowering oxidative stress and preventing symmetric cell divisions.(125,126) Following ligand binding, it undergoes a conformational change and mediates transcription of genes such as PPARD itself, ANGPTL4 and antioxidant genes such as CAT (catalase) that serve as 'signatures' for PPARδ activity.(127)

In the end, PPARα plays a major role in lipid metabolism, mainly in tissue with a high FA metabolism, controlling the intracellular FA concentration and FA flux from such as adipose tissue to the liver. In addition, PPARα also mediates leptin-induced lipolysis. PPARγ also plays a role in the energetic metabolism by controlling lipid homeostasis and regulating the expression of a set of genes related to the TG synthesis and accumulation in the adipose tissue. The capability of this receptors to stimulate β-oxidation it's an important mechanism in cancer cells since it helps them to obtain energy and develop.

## 5.2 PPAR natural ligands

PPARs have the capability to accommodate and bind a variety of natural and synthetic lipophilic acids, like for example essential fatty acids (EFA) (e.g. fibric acids in atherosclerosis). These acids act as PPAR agonists that transcript the genes involved in glucose and lipid homeostasis.(128,129,130) In addition, eicosanoids are natural ligands of

PPARs – e.g. leukotriene B4 stimulates PPARα,and prostaglandin PGJ2 activates PPARγ.(131) The natural ligands of PPARα are highly polyunsaturated *n-3* FA, that readily undergo oxidation and stimulate PPARs.(132) These FAs reveal an anti-inflammatory effect that results from the inhibition of their own oxidation caused by activated NF-κB in a PPARα-dependent pathway.(133,134) PPARα also mediates the anti-inflammatory actions of palmitoylethanolamide, the naturally occurring amide of palmitic acid and ethanolamine.(135) In addition to *n-3* FA, the oxidated LDL in endothelial cells are strong stimulators of PPARα.(136)

Particular FAs are considered natural modulators of PPARγ however, their association with the receptor does not always lead to PPAR activation and target gene transcription. For example, the activation of PPARγ by PUFAs (mainly docosahexaenoic acid and eicosapentaenoic acid) promotes a functional response in tumor cells.(137) Phytanic acidis also a natural PPARγ agonist that reveals a similar activity to *n-3* PUFA and increases glucose uptake and insulin sensitivity.(138) In addition, also long-chain MUFAs with chain lengths longer than 18 carbons may upgrade obesity-related metabolic dysfunction through increased expression of PPARγ and decreased inflammatory marker expression in white adipose tissue.(139)

*Table 3–Lipids natural ligands of PPAR*

| | **PPAR-α** | **PPAR-δ** | **PPAR-γ** |
|---|---|---|---|
| **Natural ligands** | Unsaturated fatty acids | Unsaturated fatty acids | Unsaturated fatty acids |
| | Leukotriene B4 | Carbaprostacyclin | 15- hydroxyeicosatetraenoic acid |
| | 8-hydroxyeicosatetraenoic acid | LDL | 9- and 13- hydroxyoctadecadienoic acid |
| | | | 15-deoxy 12,14- prostaglandin J2 |
| | | | prostaglandin PGJ2 |

## 5.3 PPARs in cancer

Although acute inflammation is a necessary protective process, unresolved chronic inflammation seen in obesity may promote cancer development by providing an appropriate

environment for tumor growth.(140,141) Depending on the context, PPAR ligands can inhibit the expression of genes encoding proinflammatory molecules like for example tumor necrosis factor (TNF), interleukin 1β, interleukin 6 and matrix metalloprotease 9.(142,143) PPAR ligands use their anti-inflammatory effects by inhibiting numerous transcription factors, such as NF-kB.(144)

In addition, many tumors are characterized by alterations in lipid homeostasis with associated changes in the expression and activity of lipogenic and lipolytic enzymes regulated by PPARs.(145,146) PPAR subtypes are linked with tumorigenic processes in breast cancer cells through differential effects on cellular proliferation, apoptosis and differentiation.(145)

Peroxisome proliferators increase the peroxisome volume and number, resulting in an increase in hydrogen peroxide ($H_2O_2$) levels.(147) These effects may be mediated in part by the increased expression of peroxisomal enzymes that produce $H_2O_2$, such as acyl CoA oxidase (ACO) being that PPAR$\alpha$ upregulates the expression levels of ACO.(148,149) In addition, excessive $H_2O_2$ levels are degraded by CAT, the activity of which is decreased in obesity.(150) A rise in the intracellular levels of $H_2O_2$ may lead to DNA damage.(151) A stably transfected African green monkey kidney cells (CV-1) overexpressing rat ACO increased $H_2O_2$ production, formed transformed *foci*, and grew efficiently in soft agar when the cells were treated with linoleic acid. When these cells were transplanted into nude mice, these cells formed solid tumors, suggesting a role of PPARα in tumorigenesis.(152)

In the other hand, the role of PPARδ in oncogenesis is controversial. Some studies show that PPARδ activation upregulated vascular endothelial growth factor (VEGF) transcription, expression, and peptide release in intestinal epithelial tumor cells, and subsequently activated PI3K-Akt signaling, whose activation it's connected to the inhibition of apoptosis, angiogenesis and insensitivity to antiproliferative signals.(153,154) Similar results were obtained in the human endothelial cells.(155) It was also showed that activation of PPARδ promotes mouse mammary carcinogenesis.(156) In addition, it was also reported that PPARδ selective agonists stimulated the proliferation of human breast cell lines.(157) In contrast with those results, *Girroir et al.* reported that activation of the same receptor inhibited the growth of the human breast cancer cell line, MCF7, and human melanoma cell line, UACC903.(158)

Also PPARγ plays a role in carcinogenesis, and the activation of PPARγ by ligands led to either inhibition of cell proliferation or induction of apoptosis.(159,160) PPARγ induces apoptosis in HT-29 by inhibiting NFκB activity, which upregulates various antiapoptotic genes, and suppressing the expression of BCL-2, which protects cells against apoptosis.(161) In addition, they also inhibit the cell growth of several breast cancer cell lines (e.g. MCF7, MDA-MB-231, BT474, and T47D) and mammary gland tumor development.(162,163)

In conclusion, PPARs play a major role in the lipid metabolism as well as in inflammation and energy balance. These processes are modified in obesity, which is a disease associated with the modification of local and systemic lipid metabolism as well as a state of low grade inflammation. Since PPAR are lipid sensors, the alterations in the lipid environment can lead to abnormal actions of this receptor, promoting this way the development and growth of cancer cells in the breast. This way, it's important to develop further studies with the goal to elucidate the role of PPARs for developing new efficiently and safety chemotherapeutic agents for cancer treatment.

## 6.    Aim of the study

For years, the dietary intake and increased BMI/obesity have been studied for their contribution to breast cancer risk, however the relation between dietary factors (specifically dietary fat) and breast cancer risk is not very clear. There are a few studies that make associations between breast cancer risk and adult intake of total fat and other types of dietary fat. However, there is a need for a better understanding of the contributions of lipids in diet to breast cancer risk.

The aim of this work was to characterize the lipidome of mammary glands from obese and lean mice and compare them to detect changes associated to different obesity inducing diets.

More specifically the aims of this study are:
- Detect changes in the lipids profile associated to obesity;
- Detect the effect of the different diets in the mammary gland lipidome;

Additionally, with the resource to the literature our main goals are to:
- Associate FA changes to potential PPAR selective activation;
- Associate the lipidome changes to risk of cancer development.

## 7.    Methods

### 7.1  Animal model and diets

We used a DIO C57bl/6j mouse model, since it offers a more human-like model, where the obesity is based on several factors, including an excess intake of calories. The model used is specified in **figure 8**.
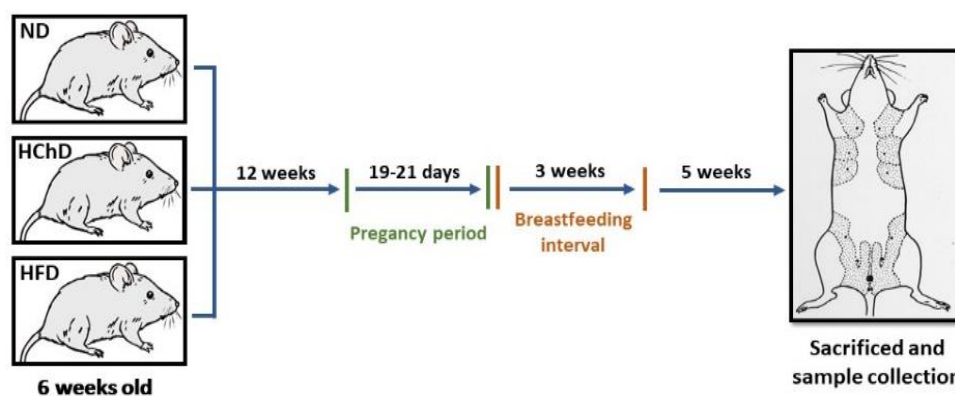


*Figure 8–Animal model of obesity developed by our collaborators at Karolinska Institutet and used in this master thesis.*

Twelve 6 week-old mice were divided into 3 distinct groups. During 12 weeks each of the groups where put on different diets during all the living period respectively as, normal diet (ND), high cholesterol diet (HChD) and high fat diet (HFD).After 12 weeks all the 12 mice got pregnant. They breastfeed for 3 weeks and after additional 5 weeks they were sacrificed and the mammary gland collected. The samples were stored at -80˚C.

All the different diets where purchased from Research Diets (USA). The ND (Product Data - D12450H) had 4.3% of energy derived from fat, 19.2% from protein, and 67.3% from carbohydrate, the HFD (Product Data - D12451) had 24% of energy derived from fat, 24% from protein, and 41% from carbohydrate and the HChD (Product Data - D12108C) had 20% of energy derived from fat, 23% from protein, and 45% from carbohydrate and a 1.25% of cholesterol.

### 7.2  Reagents

Chloroform (CHCl3), methanol (MeOH) and n-hexane were purchased from Fisher scientific (Leicestershire, UK). Perchloric acid was purchased from Panreac (Barcelona, Spain), Perchloric acid from Chem-Lab NV (Zedelgem, Germany). Ascorbic acid and sodium chloride were from VWR chemicals (Levven, Belgium).Purified water (Synergy,Millipore Corporation, Billerica, MA, USA) was used whenever necessary.

Phospholipid internal standards 1,2-dimyristoyl-sn-glycero-3-phosphocholine (dMPC), 1,2-dimyristoyl-sn-glycero-3-phosphoethanolamine (dMPE), 1,2-dimyristoyl-sn-glycero-3-phospho-(10-rac-glycerol) (dMPG), 1,2-dimyristoyl-sn-glycero-3-phospho-L-serine (dMPS), 1,2-dipalmitoyl-sn-glycero-3-phosphatidylinositol (dPPI), N-palmitoyl-D-erythro-sphingosylphosphorylcholine (NPSM), 1-nonadecanoyl-2-hydroxy-sn-glycero-3-phosphocholine (LPC), as well as standarts used in the GC and Q-TOF were purchased from Avanti Polar Lipids, Inc. (Alabaster, AL).The internal standard (C19:0) used in the GC-MS was purchased from Merk, Darmstadt, Germany. SPE columns where purchased from Sigma–Aldrich, Darmstadt, Germany.

## 7.3  Lipid extraction

To extract total lipids, part of the mammary gland tissue was placed in a glass tube and weighted. The samples were homogenize with 1 ml of milliQ-water. Then, the solution of 2:1 CHCl3:MeOH mixture (v/v) was added to a final relation of 8:4:3 CHCl3:MeOH:H2O and homogenized for 3 min. The glass tubes were placed on ice for 30 min and vortexed a few times during this period. After that time, the mixtures where vortexed for 30 sec after which they were centrifuge for 5 min at 1500 rpm, in order to separate organic (bottom) and aqueous phases. The organic phase was collected to a different glass tube. Re-extraction of the aqueous phase by addition of 2,5 ml CHCl3, followed by vortexing for 30 sec and centrifugation during 5 min at 1500 rpm, collect the organic phase again and repeat this step again in order to assure to collect the biggest amount of lipids of the sample. The lipid extract was dried under a nitrogen steam, ressuspended in 0.300 mL, vortexed and transfer to a vial. This step was repeated twice in order to transfer total lipid extract for the vial. The lipid extract was dried in the vials under a nitrogen steam, weight and stored in -20˚C.

## 7.4  Fractionation of the total lipid extracts using Solid-Phase Extraction

The total lipid extracts from the mammary gland were fractionated  by solid phase extraction (SPE) to obtain two major fractions, one with the neutral lipid that contain TAG and another fraction correspondent to the PLs. The columns were conditioned with 7.5 mL of n-hexane and loaded with half of the lipid extract obtain in the lipid extraction diluted in n-hexane/chloroform/methanol (95:3:2 v/v/v). The first fraction containing TAG was collected with 7.5 ml of CHCl3 in a glass tube and the fraction containing PLs into a glass

tube was collected using first 5 ml of methanol/hexane (6:1 v/v) and then 2.5 ml of methanol/hexane (1:1 v/v). Both fractions were collected in a glass tube, dried under nitrogen, dissolved in $CHCl_3$andtransferredto an amber glass vial. In addition, vials with 1 mg of TAG were. All the vials where stored at -20 C before analysis by MS.PL were analyzed by LC-MS while TG were analyzed by ESI-MS. FA profile through GC-MS.

## 7.5  Phospholipid quantification

Quantification of PL in the total lipid extracts and in the fractions obtained after SPE (Solid-phase extraction) was performed according to Bartlett and Lewis method.(164) Samples were put on acid-washed glass tubes and 0.125 mL of perchloric acid (70%, m/V) and were incubated for 60 min at 180 °C in a heating block. After incubation samples were let to cool down and after which 0.825 mL of water were added together with0.125 mL of ammonium molybdate (2.5%, m/V) and 0.125 mL of ascorbic acid (10%, m/v). After each addition, the mixture was well homogenized in a vortex mixer and incubated during 10 min at 100 °C in a water bath. Eight standards with varying concentration from 0.1 to 1.5 µg of phosphate (standard solution of 2.5% NaMoO4.H2O) underwent the same treatment as the samples. Absorbance of standards and samples were measured at 797 nm, at room temperature, in a microplate via spectrophotometer that allowed to estimate the amount of phosphorous. The amount of PL of each sample was calculated by the relation of the amount of phosphorus in each spot to the phosphorus amount of the standard solutions applied in the microplate.

## 7.6  LC-MS

The Phospholipid fractions obtained after SPE of the total lipids extracts from the mammary gland were analyzed by using a high-performance LC (HPLC) system (Ultimate 3000 Dionex, Thermo Fisher Scientific, Bremen, Germany) with an autosampler coupled online to the Q-Exactive® hybrid quadrupole Orbitrap® mass spectrometer (Thermo Fisher Scientific, Bremen, Germany). The solvent system consisted of two mobile phases as follows: mobile phase A [acetonitrile:methanol:water 50:25:25 (v/v/v) with 1 mM ammonium acetate] and mobile phase B [acetonitrile:methanol 60:40 (v/v) with 1 mM ammonium acetate]. Initially, 40% of mobile phase A was held isocratically for 8 min, followed by a linear increase to 60% of A within 7 min and a maintenance period of 5 min, returning to the initial conditions in 5 min, followed by a re-equilibration period of 10 min

prior next injection. HPLC-MS was performed with an internal standard. A volume of 5 µL of each sample, containing 5 µg of lipid extract, 4 µL of each internal standard: PE (0.02 µg/100 µL), SM (0.02 µg/100 µL), LPC (0.02 µg/100 µL),PG (0.012 µg/100 µL), and 79 µL of solvent system (60% of eluent B and 40% of eluent A) was introduced into the Ascentis®Si column (15 cm × 1 mm, 3 µm, Sigma-Aldrich) with a flow rate of 40 µL min−1 and at 30 ºC. The mass spectrometer with Orbitrap® technology was operated in simultaneous positive (electrospray voltage 3.0 kV) and negative (electrospray voltage -2.7 kV) modes with high resolution with 70,000 and AGC target of 1e6, the capillary temperature was 250 ºC and the sheath gas flow was 15 U. In MS/MS experiments, a resolution of 17,500 and AGC target of 1e5 was used and the cycles consisted in one full scan mass spectrum and ten data-dependent MS/MS scans that were repeated continuously throughout the experiments with the dynamic exclusion of 60 seconds and intensity threshold of 1e4. Normalized collision energy™ ranged between 25, 30 and 35 eV. Data acquisition was carried out using the Xcalibur data system (V3.3, Thermo Fisher Scientific, USA). The mass spectra were processed and integrated into the MZmine v2.3 program. Each PL species was identified by the identification of the ion exact mass, and confirmed by MS/MS using Xcalibur data system.

## 7.7 TAG analysis by using ESI-MS

For the identification and structural characterization of TAG molecular species, the TAGs fractions were analyzed by ESI-MS and MS/MS in a quadrupole time-of-flight (Q-ToF) mass spectrometer (Waters, Manchester, UK), operating in positive ion mode. To estimate the relative amount of each TAG molecular species in each sample, an internal standard of TAG (1,3-ditetradecanoyl-2-(9Z-hexadecenoyl))-glycerol, TAG(14:0/16:1/14:0), was add to each. A stock solution of the TAG internal standard was prepared in chloroform (0.25 mg/mL) and added to the samples as follows: sample/internal standard/solvent (4:1:195, v/v/v). The solvent used was methanol with 5 mmol/L of aqueous ammonium acetate. On a syringe pump was placed a final volume of 200 µL and samples were then supplied to the electrospray source at a flow rate of 10 µL/min. The source temperature was 80˚C and the desolvation temperature was 150˚C.MS/MS spectra were acquired with a collision energy of 25 V.

### 7.8  FA-GC-MS

Fatty acids (FA) in PLs and in TGs fractions were analyzed by GC–MS after transmethylation. FA methyl esters (FAME) were obtained as follows: 10 µg of lipid (TAGs andPLs fractions) were transferred to a Pyrex glass tube and dried under nitrogen. Then, was added 1 mL of n-hexane containing a C19:0 internal standard (2 µg/mL), followed by 200 µL of a methanolic solution of potassium hydroxide (2 mol/L) and the mixture was well homogenized. Finally, was added 2 mL of a saturated solution of sodium chloride and the sample was centrifuged for 5 min at 2000 rpm to separate the phases. The organic (upper) phase, with the FAME was transferred to a micro tube and solution was dried under nitrogen.

### 7.9  Calculations and Statitical analysis

The calculations made where for double mass index (DBI) and average chain length (ACL). The ACL was calculated as $ACL = [(\Sigma\% \ Total_{14} \ x \ 14) + ... + (\Sigma\% \ Total_n \ x \ n)] / 100$ (n = carbon atom number). The DBI was calculated as $DBI = \Sigma$ mol % of unsaturated fatty acids x number of double bonds of each unsaturated fatty acid.

The data from the three different study groups (ND, HFD, HChD) obtained during ESI-MS (in an ESI-Q-TOF) and GC-MS where analyzed using one-way ANOVA and Tukey´s multiple post-test. Differences were considered significant if $p < 0.05$. The software used for this analyses was GraphPad Prism 6. In the HPLC data, for analyzing the normality of the data from the different study groups (ND, HFD, HChD) was used the Shapiro-Wilk test. Univariate statistical analysis was performed using ANOVA test following post hoc Tukey's honestly significant difference (HSD) test. After that, multivariate data processing and analyses were done using the SPSS software package (IBM SPSS Statistics Version 24). Principal component analysis (PCA), partial least squares discriminant analysis (PLS-DA) and hierarchical clustering were performed on auto scaled-scaled data using the R (R version 3.4.2) with the packages RFmarker Detector, FactoMineR63, Factoextra64 and Ropls65).

## 8. Results

In the last few years, there has been an increase of scientific research on the role of lipids, including TAG and PLs in the development of cancer. Therefore, in this work we evaluated the lipid profile of the mammary gland including the fat pad resulting from three diet groups (ND, HChD, HFD). For this, we used complementary lipidomic approaches, namely ESI-MS and MS/MS, GC-MS and HILIC-LC-MS and MS/MS approaches to analyze the TAG, FA and PL profiles, respectively.

Prior to the analysis, lipids were extracted using conventional methods and lipid extracts obtained were weighted (**Table 4**). The total lipid extract mass recovered after lipid extraction for 100 mg didn't show significant differences between groups. Total lipid extracts were fractionated by solid phase extraction and the fractions corresponding to TAG and to PL were recovered (**Table 4**). The HFD group shown a significant lower amount of PLs when compared to the ND group. When it comes to the TAG content, there were no significant differences seen between the study groups (**Table 4**).

*Table 4–Mean of the weight of the total lipid extract from each study group (ND – normal diet, HChD – high cholesterol and HFD – high fat diet), as well as the ug of PLs and mg of TAG, recover from the initial lipid extract. (\*\* p<0.01; compare to the ND)*

| Diet | Tissue weight (mg) | mg lipid extract/100 mg tissue | mg TAG / 100 mg tissue | ug PLs/ 100 mg tissue |
|---|---|---|---|---|
| ND | 73.03 ± 28.15 | 45.72 ± 22.96 | 7.72 ± 6.29 | 181.32 ± 115.11 |
| HChD | 139.45 ± 80.74 | 42.41 ± 15.16 | 22.00 ± 13.43 | 140.63 ± 22.57 |
| HFD | 291.05 ± 114.07 | 55.72 ± 19.43 | 12.78 ± 4.70 | 58.11 ± 15.12 \*\* |

### 8.1 Triacylglycerol profile

TAG profile was analyzed by ESI-MS, that allowed to identify and relatively quantify their molecular species, and the profile of their esterified fatty acids was analyzed by GC-MS after derivatization.

The profiling of TAG by ESI-MS allowed to identify 18 ions attributed to the [M+NH4]$^+$ ions of TAG, considering the C:N composition - **Table 5** and **Figure 9**.
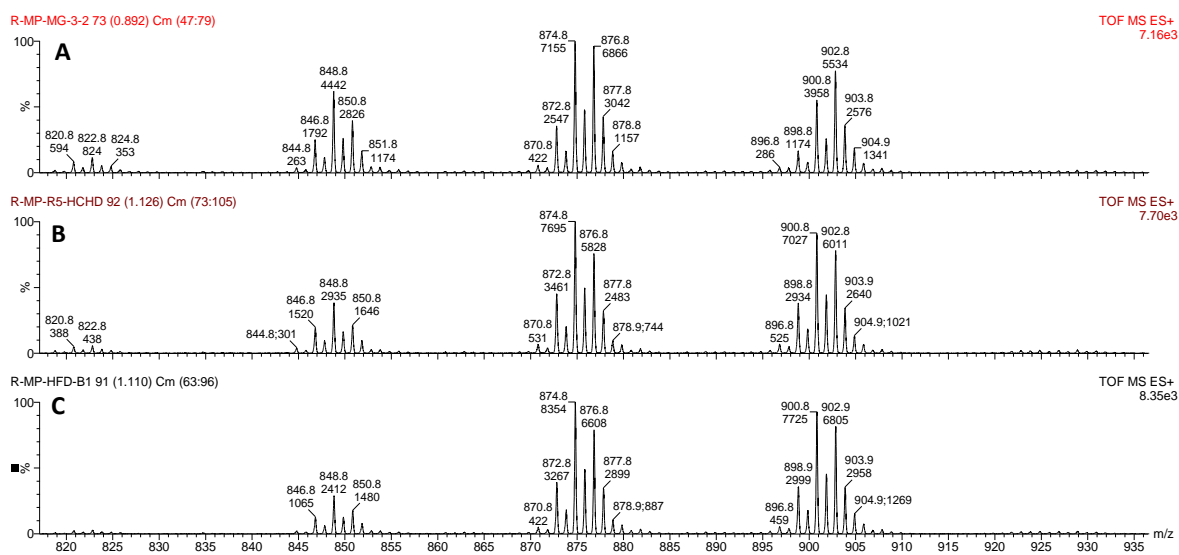
*Figure 9–ESI-MS spectra obtained from TAG fractions representative of each study group. The first one corresponds to the A- ND (normal diet); B - HChD (High Cholesterol Diet); C - HFD (High Fat Diet).*

Analysis of MS/MS data allowed to infer the FA composition of TAGs as was exemplified in **figure 10**. In this MS/MS spectrum we can see the product ion at *m/z* 607.7 formed by neutral loss of 280 Da. That allowed to identified one FA C18:2, while it was possible to see the *m/z* 605.7 formed by neutral loss of 282 Da that allowed to identified another FA C18:1. The third FA composition was inferred by the neutral loss of 284 Da, corresponding to the FA C18:0, corresponding to the *m/z* 603.7**.** This way we can infer that the TAG that has *m/z* of 904.8 was composed by the FA C18:0, C18:1 and C18:2.
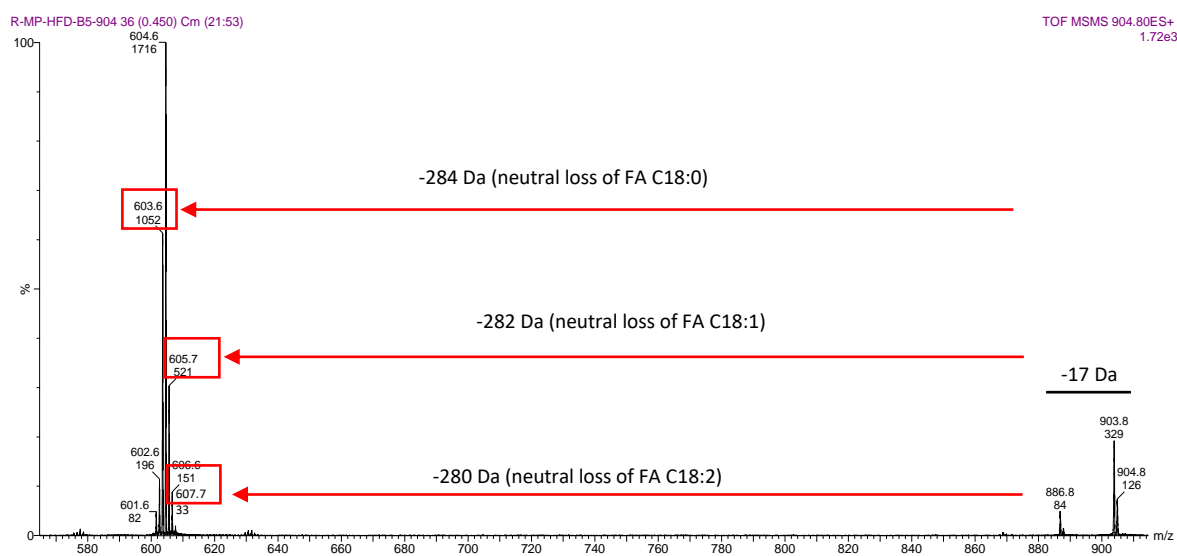


*Figure 10 – MS/MS Spectra the TAG (54:2). Firstly we have the loss of the ammonium corresponding to the loss of 17 Da. Then calculating the neutral loss of the different fatty acids that compose the corresponding TAG. In this case, the TAG (54:2) is composed by the FAs C18:0, C18:1 and C18:2.*

Using this approach for each ion, it was possible to pinpoint in these samples several ions that were assigned to more than one molecular species, as for example TAG (54:6) and TAG (56:6). These species were assigned as having 8 and 11 different molecular species. Thus a total of 18 TAG molecular species were identified in the neutral lipid fraction of the three study groups (ND, HChD, HFD) but correspond to a total of 86 different molecular species – **table 6**.

The most abundant TAG molecular species in all groups were TAG (52:2) identified as $[M+NH_4]^+$ at *m/z* 876.8, TAG (52:3) at *m/z* 874.8, and TAG (54:3) at *m/z* 902.8. These TAG molecular species made up about 48% of the TAG present in the neutral lipid fractions. Less abundant TAG molecular species were observed as $[M+NH4]^+$ ions at *m/z* 924.8 for TAG (56:6), *m/z* 896.8 for TAG (54:6) and *m/z* 844 for TAG (50:4), corresponding to TAG bearing minor FA (C18:3 and C20:1), along with more abundant FA - **Table 5**. These TAG represented about 1.5% of the TAG presented in the neutral lipid fractions. Comparing the three study groups, significant differences were seen in the relative abundances of seven TAG species, among which three TAG showed a decrease in HChD and HFD groups when compared to the ND. Those were TAG (50:2), TAG (50:1) and TAG (52:2). In contrast, the TAG (54:5) and TAG (54:4) where significantly higher in the HChD and HFD, when compared to the ND. In addition the TAG (52:4) was higher in the HChD, when compared to the ND and the TAG (52:3) was higher in the HFD when compared to the ND – **Figure 11.**

*Table 5 - TAG identified by ESI-Q-ToF-MS as [M + NH4]+ adducts, their relative amount in percentage with standard deviation. (\* p < 0.05; \*\* p<0.01; \*\*\* p < 0.001; \*\*\*\* p < 0.0001, compared to ND).*

| TAG | m/z | ND | HChD | HFD |
|---|---|---|---|---|
| 48:2 | 820.8 | 1.3 ± 0.2 | 0.8 ± 0.1 | 0.6 ± 0.2 |
| 48:1 | 822.8 | 2.0 ± 0.1 | 1.0 ± 0.2 | 0.7 ± 0.2 |
| 50:4 | 844.8 | 0.6 ± 0.1 | 0.6 ± 0.1 | 0.5 ± 0.1 |
| 50:3 | 846.8 | 3.8 ± 0.7 | 3.2 ± 0.3 | 2.6 ± 0.6 |
| 50:2 | 848.8 | 10.0 ± 0.7 | 6.7 ±0.5 \*\*\*\* | 5.9 ± 1.2 \*\*\*\* |
| 50:1 | 850.8 | 7.1 ± 0.5 | 4.2 ± 0.5 \*\*\*\* | 3.8 ± 0.7 \*\*\*\* |
| 50:0 | 852.8 | 0.9 ± 0.1 | 0.6 ± 0.1 | 00.5 ± 0.1 |
| 52:5 | 870.8 | 0.8 ± 0.2 | 1.2 ± 0.1 | 1.0 ± 0.2 |
| 52:4 | 872.8 | 5.3 ± 1.3 | 7.7 ± 0.6 \*\* | 6.9 ± 1.0 |

| 52:3 | 874.8 | 16.2 ± 0.7 | 18.0 ± 0.5 | 18.1 ± 0.4 * |
|---|---|---|---|---|
| 52:2 | 876.8 | 17.2 ± 1.5 | 14.1 ± 0.5 **** | 15.1 ± 1.0 * |
| 52:1 | 878.8 | 3.4 ± 0.6 | 1.9 ± 0.3 | 2.1 ± 0.3 |
| 54:6 | 896.8 | 0.6 ± 0.1 | 1.3 ± 0.1 | 1.1 ± 0.1 |
| 54:5 | 898.8 | 2.6 ± 0.5 | 6.6 ± 0.7 **** | 6.3 ± 0.7 **** |
| 54:4 | 900.8 | 9.2 ± 0.4 | 15.6 ±0.9 **** | 16.4 ± 1.6 **** |
| 54:3 | 902.8 | 14.6 ± 2.0 | 13.5 ± 0.7 | 14.9 ± 1.5 |
| 54:2 | 904.8 | 4.3 ± 1.1 | 2.6 ± 0.2 | 3.0 ± 0.6 |
| 56:6 | 924.8 | 0.3 ± 0.1 | 0.5 ± 0.1 | 0.4 ± 0.1 |
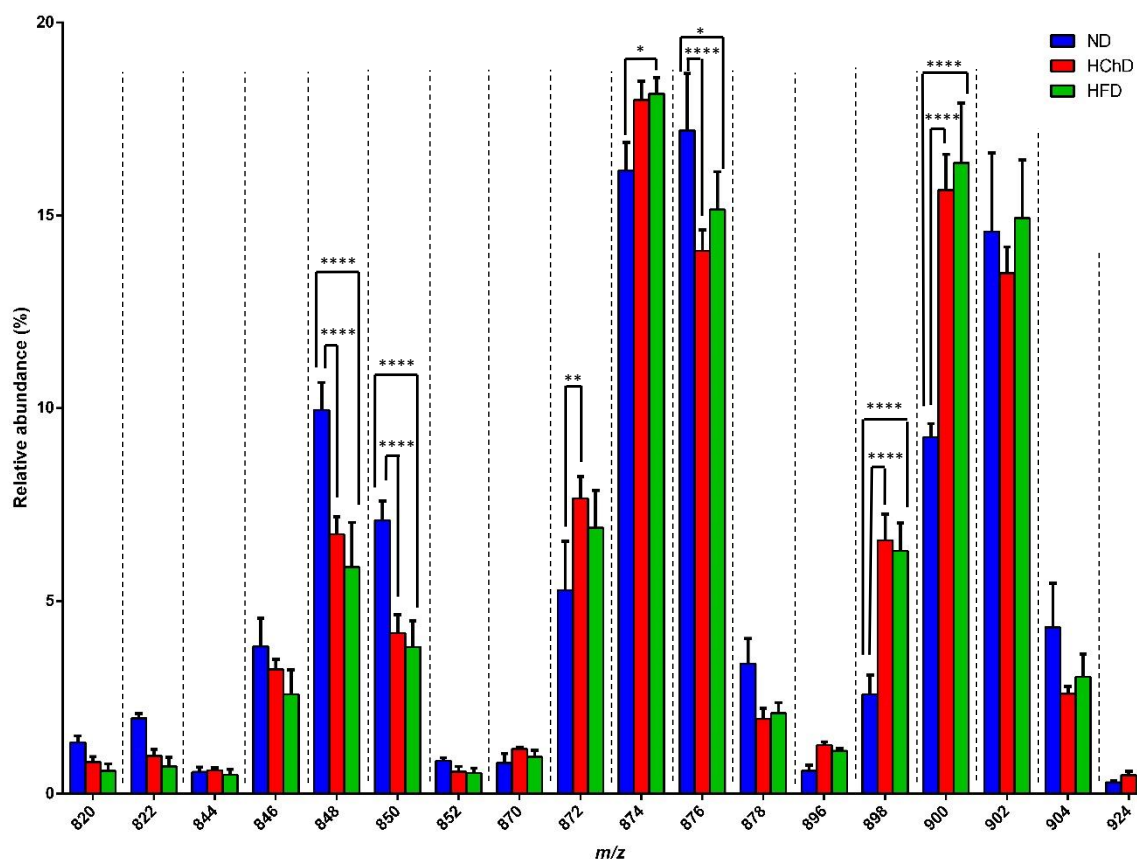


Figure 11–Graph representing the relative abundance of each TAG species with the standard deviation. In blue is the ND –Normal Diet, in red HChD- High Cholesterol Diet and in green HFD – High Fat Diet. (* $p < 0.05$; ** $p<0.01$; *** $p < 0.001$; **** $p < 0.0001$).

*Table 6 - Molecular species of triacylglycerols (TAG) and their composition in FA identified by ESI-Q-ToF-MS and MS/MS as [M + NH4]+ adducts.*

| TAG | COMBINATIONS OF FA | | | | | | | | | |
|------|------|------|------|------|------|------|------|------|------|------|
| 48:2 | 18:2/16:0/14:0 | 18:2/12:0/18:0 | 12:0/18:1/18:1 | 16:0/16:1/16:1 | 18:1/14:0/16:1 | 18:0/14:1/16:1 | | | | |
| 48:1 | 18:1/14:0/16:0 | 16:1/16:0/16:0 | 18:0/14:0/16:1 | 18:0/14:1/16:0 | | | | | | |
| 50:4 | 14:0/18:2/18:2 | 18:2/16:1/16:1 | 18:3/14:0/18:1 | 18:3/16:0/16:1 | 18:1/18:2/14:1 | | | | | |
| 50:3 | 18:1/16:1/16:1 | 18:3/16:0/16:0 | 18:2/14:0/18:1 | 18:2/16:0/16:1 | | | | | | |
| 50:2 | 14:0/18:1/18:1 | 18:0/16:1/16:1 | 18:2/16:0/16:0 | 18:1/16:0/16:1 | | | | | | |
| 50:1 | 18:1/14:0/18:0 | 18:1/16:0/16:0 | 18:0/16:0/16:1 | 14:1/18:0/18:0 | | | | | | |
| 50:0 | 18:0/16:0/16:0 | 14:0/18:0/18:0 | | | | | | | | |
| 52:5 | 16:1/18:2/18:2 | 18:3/16:0/18:2 | 18:3/18:1/16:1 | 20:4/16:1/16:0 | | | | | | |
| 52:4 | 16:0/18:2/18:2 | 18:3/16:0/18:1 | 18:3/16:1/18:0 | 18:2/16:1/18:1 | | | | | | |
| 52:3 | 16:1/18:1/18:1 | 18:2/16:0/18:1 | 18:2/16:1/18:0 | | | | | | | |
| 52:2 | 16:0/18:1/18:1 | 18:2/16:0/18:0 | 18:0/18:1/16:1 | | | | | | | |
| 52:1 | 18:1/16:0/18:0 | | | | | | | | | |
| 54:6 | 18:3/18:1/18:2 | 18:2/18:2/18:2 | 22:5/16:1/16:0 | 22:6/16:0/16:0 | 20:3/18:3/16:0 | 20:3/18:2/16:1 | 20:4/18:2/16:0 | 20:4/18:1/16:1 | | |
| 54:5 | 18:1/18:2/18:2 | 18:3/18:1/18:1 | 18:3/18:0/18:2 | 20:3/18:1/16:1 | 20:3/18:2/16:0 | 20:4/18:1/16:0 | 20:4/18:0/16:1 | 20:2/18:3/16:0 | | |
| 54:4 | 18:0/18:2/18:2 | 18:2/18:1/18:1 | 20:2/18:2/16:0 | 20:2/18:1/16:1 | 20:3/18:1/16:0 | 20:3/18:0/16:1 | | | | |
| 54:3 | 18:2/18:0/18:1 | 18:1/18:1/18:1 | 20:2/16:0/18:1 | 20:3/16:0/18:0 | | | | | | |
| 54:2 | 18:0/18:1/18:1 | 18:2/18:0/18:0 | 20:1/16:0/18:1 | | | | | | | |
| 56:6 | 22:4/16:0/18:2 | 22:5/16:0/18:1 | 22:6/16:0/18:0 | 20:2/18:3/18:1 | 20:2/18:2/18:2 | 20:3/18:2/18:1 | 20:3/18:3/18:0 | 20:4/18:0/18:2 | 20:4/18:1/18:1 | 16:0/20:3/20:3 | 16:0/20:2/20:4 |

The FAs identified in the TAG fraction are represented in the **table 7**. In all groups the FAs identified were C14:0, C16:0, C16:1 (*n-7*), C16:1 (*n-9*), C18:0, C18:1 (*n-9*), C18:2(*n-6*), C18:3(*n-3*) and C20:1. In HFD there was a statistically significant increase of the saturated FA C16:0 when compared with the control group ND. In addition the C18:1 (*n-9*) (palmitoleic acid) increased in the HFD when compared to HChD and the level of C18:2 (*n-6*) (linolelaidic acid) was higher in HChD and HFD groups when compared to the ND. In addition, there was no difference in the average chain (ACL) length between the groups, however the double bound index (DBI) is significant higher in the HChD and HFD when compared to the ND group and significant higher in the HFD group when compared to the HChD - **Figure 12.**

*Table 7 - Fatty acid (FA) composition in percentage with standard deviation of TAG from the three study groups: normal diet (ND), high cholesterol diet (HChD) and high fat diet (HFD), and their relative abundance. (\* $p < 0.05$; \*\* $p<0.01$; \*\*\* $p < 0.001$; \*\*\*\* $p < 0.0001$, compared to ND); ((\*) $p < 0.05$, compared to the HChD). ACL - average chain length; DBI - double bond index; NI – not identified*

|  | ND | HChD | HFD |
|---|---|---|---|
| C14:0 | 3.5 ± 0.4 | 2.8 ± 0.8 | 2.5 ± 0.7 |
| C16:0 | 24.1 ± 1.8 | 21.6 ± 1.2 | 19.9 ± 1.9 \*\*\* |
| C16:1 (n-7) | 2.1 ± 0.7 | 1.5 ± 0.3 | 1.5 ± 0.1 |
| C16:1 (n-9) | 6.5 ± 0.9 | 5.1 ± 0.7 | 4.3 ± 0.9 |
| C18:0 | 7.0 ± 2.0 | 7.0 ± 1.6 | 5.8 ± 0.9 |
| C18:1(n-9) | 41.0 ± 3.6 | 40.1 ± 1.4 | 43.7 ± 2.0 (\*) |
| C18:2(n-6) | 13.6 ± 17.0 | 19.0 ± 0.7 \*\*\*\* | 20.2 ± 0.8 \*\*\*\* |
| C18:3(n-3) | 1.1 ± 0.2 | 1.3 ± 0.3 | 1.2 ± 0.2 |
| C20:1 | 1.0 ± 0.3 | 0.8 ± 0.1 | NI |
| C20:2(n-6) | NI | 0.9 ± 0.3 | 0.9 ± 00.2 |
| **ACL** | 16.64 ± 0.11 | 16.84 ± 0.10 | 16.94 ± 0.08 |
| **DBI** | 81.20 ± 2.50 | 91.11 ± 1.63 \*\*\*\* | 95.37 ± 3.67 \*\*\*\* (\*) |
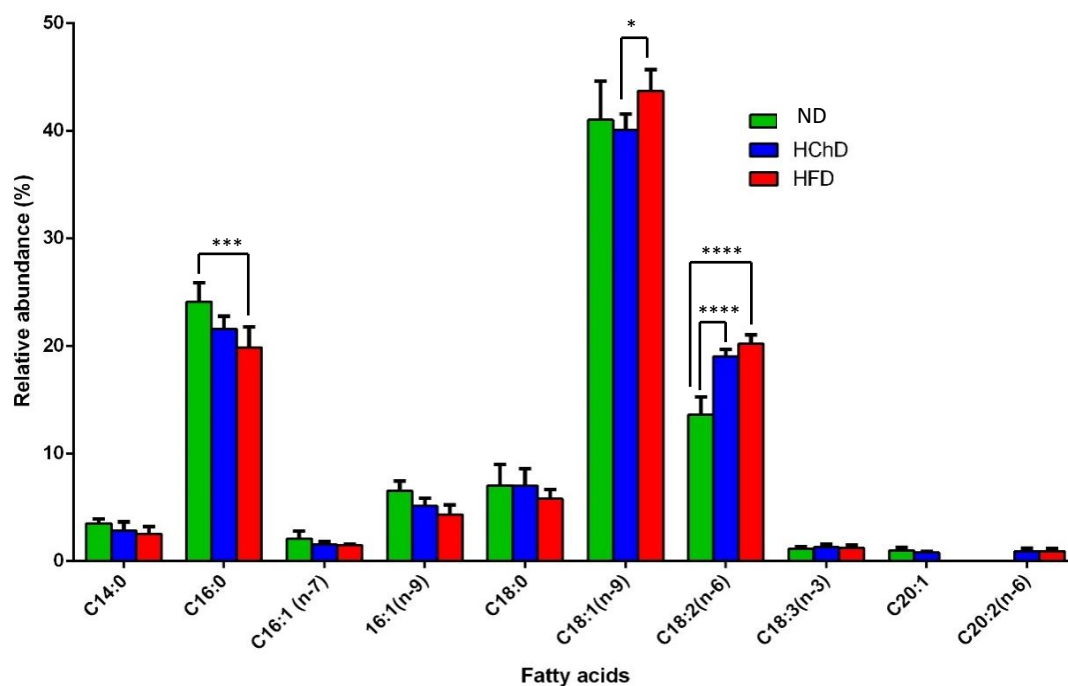
*Figure 12 – Graph representing the relative abundance in percentage with standard deviation of each FA identified with the standard deviation. In green is the ND –Normal Diet, in blue HChD- High Cholesterol Diet and in red HFD – High Fat Diet(\* p < 0.05; \*\* p<0.01; \*\*\* p < 0.001; \*\*\*\* p < 0.0001).*

## 8.2 Phospholipids profile

In relation to the PLs profile, data from LC-MS and MS/MS analysis of the phospholipid fraction obtained after SPE allowed the identification and relative quantification of PL species belonging to 6 different classes: PC, PE, LPC, LPE Cer and SM. Two-hundred and eight PLs species were identified in all samples.

The molecular species of PC and LPC classes were identified in the positive mode, and identified in the MS spectra as [M+H]$^+$ ions for all classes detected. The most abundant PC molecular species were PC (36:2) at *m/z* 786.601 followed by PC (34:2) at *m/z* 758.570, in all the conditions. In addition, in all the conditions, LPC (18:0) at *m/z* 524.372 was the most abundant followed by LPC (16:0) at *m/z* 496.340.The molecular species of SM were analyzed in the LC-MS spectra in positive ion mode and also identified as [M+H]$^+$ ions. The most abundant molecular specie in all conditions was SM (d34:1), corresponding to the ion *m/z* 703.575. The molecular species of PE were analyzed in the LC-MS spectra in the positive mode, with formation of the [M+H]$^+$ ions as well as in the negative mode as [M-H]$^-$ . In the positive mode the most abundant molecular species were PE (38:5), corresponding to the ion *m/z* 766.538 and the PE (38:4), corresponding to the ion *m/z* 768.55, in all species. LPE species were analyzed in the LC-MS spectra in the positive ion mode

where the most abundant molecular species in all conditions were LPE (18:0) and LPE (18:1), corresponding in the positive mode to the ion *m/z* 482.325 and m/z 480.309 and in the negative mode to m/z 480.309 and *m/z* 378.293, respectably. Additionally, the molecular species of Cer were also analyzed in the positive ion mode, where the most abundant molecular specie in all the conditions was Cer (d35:1), corresponding to the ion *m/z* 552.536.

For the relative quantification of all the lipid species identified, the peak areas of the extracted ion chromatograms (XICs) of each PL and Cer species within each class were normalized using the peak area of the internal standard (IS) selected for the class.

After testing the normality of the data using shapiro wilk test, data were subsequently autoscaled and then subjected to a principal component analysis (PCA) to display the clustering trends of the three experimental groups: ND, HChD and HFD. The PCA shows a separation of the HFD and HChD from the control group in a two-dimensional score plot which represented the analyses describing 63.8% of the total variance, including principal component 1 (50.5%) and principal component 2 (13.5%), where principal component 1 was the major discriminating component - **Figure 13**.

From the loading values, the major contributors of the component 1 were Cer (42:1), LPC (18:2), PC (34:4) and LPC (20:5), whereas Cer (42:1), Cer (38:1), PC (P-44:6), PC (O-42:6) and PC (O-42:5) where the main contributors for component 2.
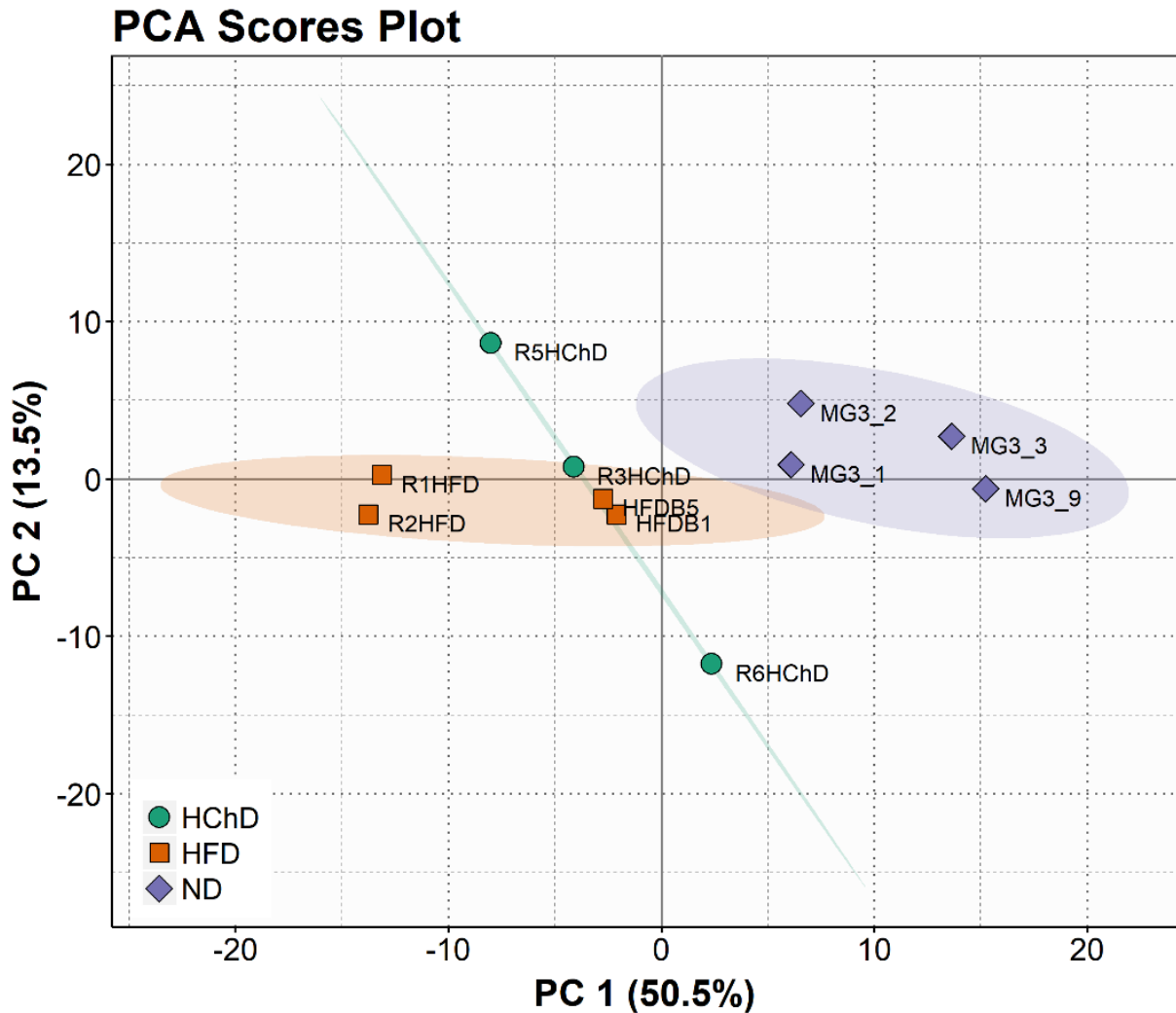
*Figure 13 - Principal component analysis score plot of phospholipid profiles obtained from the three study groups: normal diet (ND), high cholesterol diet (HChD) and high fat diet (HFD).*

A projection to latent structures discriminant analysis (PLS-DA) was performed in order to maximize the phenotypic classification of samples, which showed the performance statistics of R2X = 0.60413, R2Y = 0.95482 and a prediction parameter Q2 of 0.23334 (X) and 0.37711 (Y). The three groups were well separated in the resulting two-dimensional score plot - **Figure 14**. The PLS-DA score plot described 60.4% of the total variance, including component 1 (48.5%) and component 2 (11.9%). Along with the component 1 the HFD samples were scattered at the central region of the plot, the HChD samples were scattered to the bottom part of the plot and lastly the ND was scattered to the top part of the plot.
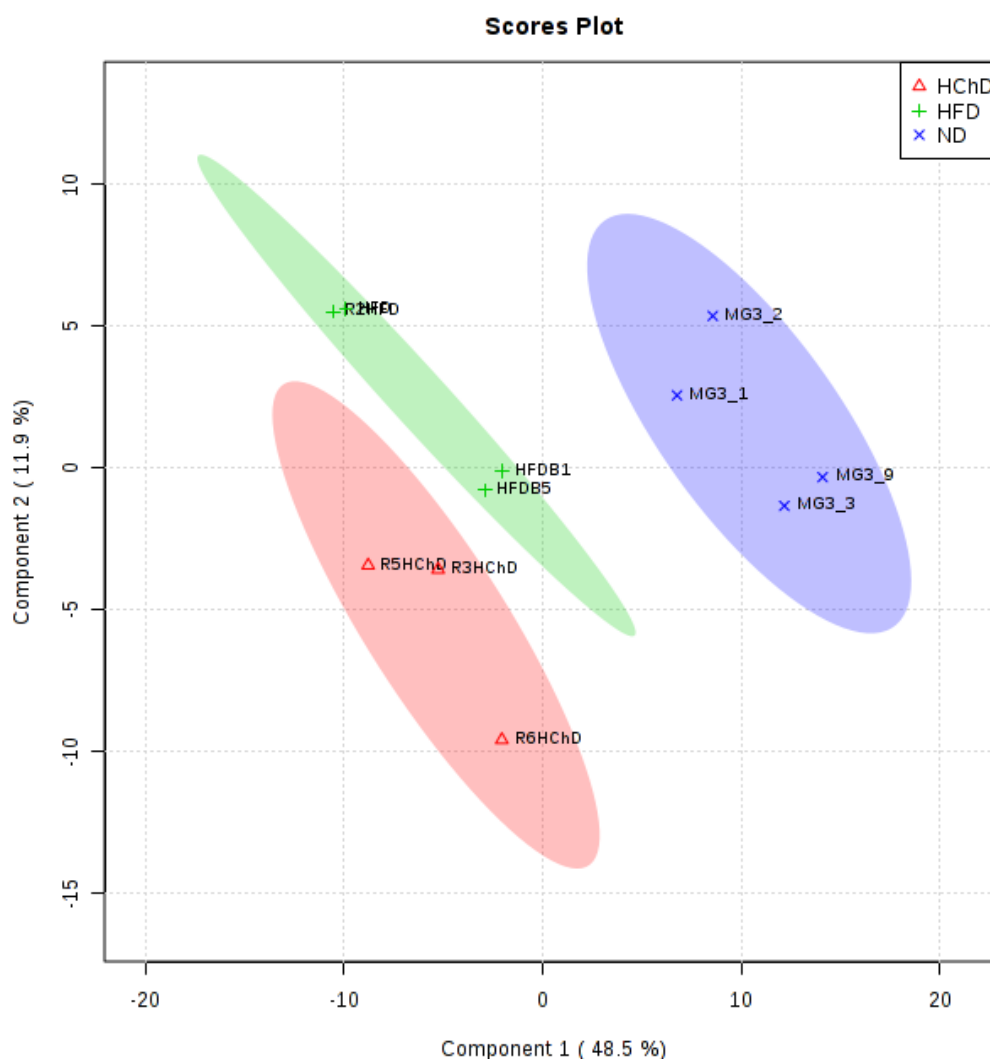
*Figure 14 - Partial least squares regression score plot of phospholipid profiles obtained from the three study groups: normal diet (ND), high cholesterol diet (HChD) and high fat diet (HFD).*

Some PC species showed significant variations. It was observed statistically significant decreased levels of PC (30:0), PC (30:1), PC (32:0), PC (32:1), PC (32:2), PC (34:1), PC (34:3), PC (34:4), PC (36:3), PC (36:4), PC (36:5), PC (36:6), PC (40:7), PC (38:6) and PC (42:1) in HFD and HChD in comparison with control (ND) (p<0.05). Additionally, it was observed a statistically significant decrease of the levels of PC (34:2) in HChD in comparison with control (ND) and a statistically significant decrease of the levels of PC (42:10) in the HFD in comparison with control (ND) (p<0.05) – **Figure 15**.

In relation to LPC it was observed statistically significant decrease of the levels of LPC (14:0), LPC (16:0), LPC (16:1), LPC (18:0),LPC (18:1), LPC (18:2), LPC (18:4), LPC (20:0), LPC (20:3), LPC (20:4), LPC (20:5), LPC (22:4), LPC (22:5), LPC (22:6) and LPCo

(16:1), in HFD and HChD in comparison with control (ND) (p<0.05). In addition, it was observed a statistically significant decrease of the levels of LPC (22:1), LPCo (18:0), LPCo (18:1) and LPCo (20:0) in HFD in comparison with control (ND) (p<0.05) - **Figure 15**.

It was observed statistically significant decrease of SM (d34:1), SM (d38:1), SM (d38:3), SM (d40:1), SM (d42:1), SM (d42:2), SM (d44:1) and SM (d44:2) in HFD in comparison with control (ND) (p<0.05). Interestingly, in the SM (d44:2) was also statistically significant decreased in the HDF when compared to HChD (p<0.05). In addition, in the case of Cer, it was observed statistically significant decrease of the levels of Cer (d38:1) and Cer (d42:1) in HFD in comparison with control (ND) (p<0.05). The molecular species Cer (d34:1), Cer (d36:2), Cer (d40:1) and Cer (d42:2) were decreased in the HChD when compared to ND (p<0.05). When comparing the ND with the HFD it was observed statistically significant difference in the specie Cer (d34:2) that was decreased and in the specie Cer (d36:2) that was increased (p<0.05). Additionally, there were statistically significant differences between the HFD and the HChD, where the species Cer (d36:2) and Cer (d40:2) were increased and the species Cer (d34:1), Cer (d38:1) and Cer (d42:1) were decreased in the HFD in comparison with HChD - **Figure 15**.

For PE, it was observed statistically significant decrease of the levels of PE (34:1), PE (34:3), PE (34:4), PE (40:5), PE (40:6), PE (42:9), PE (42:10), PE(P-34:2), PE(P-36:2) and PE(P-38:4) in HFD and HChD in comparison with control (ND) (p<0.05). In addition, it was observed a statistically significant decrease of the levels of PE (34:2), PE (38:1), PE (38:4), PE (38:5), PE (40:4), PE (40:8), PE (40:10), PEo(40:9), PE(P-36:3), PE(P-38:2), PE(P-38:5), PE(P-40:1), PE(P-40:3), PE(P-40:4) and PE(P-40:7) in HFD in comparison with control (ND) (p<0.05). In the negative mode, the most abundant molecular specie was PE (38:4), corresponding to the ion *m/z* 766.539. It was observed statistically significant decreased of the levels of PE (32:0), PE (34:1), PE (38:1), PE (40:4), PE (40:5), PE (40:7) and PE (40:8)in HFD and HChD in comparison with control (ND) (p<0.05). In addition, it was observed statistically significant decreased of the levels of PE (34:3), PE (38:4), PE (38:5), PE (40:3), PE (P-34:1), PE (P-38:4), PE (P-40:3), PE (P-40:4), PE (P-40:6), PEo(40:6) and PEo(38:3) in the HFD when compared to ND (p<0.05). Finally, it was observed statistically significant decrease of the levels of PE (40:5), PE (P-34:1), PE (P-38:4), PE (P-40:3), PE (P-40:4), PEo(40:6) and PEo(38:3) in the HChD when compared to HFD (p<0.05)**- Figure 16**.

For LPE, it was observed statistically significant decreased in the positive mode of the levels of LPE (14:0), LPE (16:1), LPE (18:0), LPE (18:1),LPE (18:2), LPE (20:4), LPE (22:4), LPE (22:6), LPE (P-16:0), LPE (P-18:0), LPE (P-20:0), LPE (O-16:0) and LPE (O-18:0) in HFD and HChD in comparison with control (ND) ($p<0.05$). In addition, it was observed a statistically significant decrease of the levels of LPE (P-20:0) when comparing the HFD with the HChD ($P<0.05$) -**Figure 15**. In the negative mode, the most abundant molecular specie was LPE (22:5), corresponding to the ion *m/z* 526.293. It was observed statistically significant decreased of the levels of LPE (14:0), LPE (16:0), LPE (16:1), LPE (18:0), LPE (18:1), LPE (18:2), LPE (20:1), LPE (20:4), LPE (20:5), LPE (22:6) and LPE(P-18:0) in the HFD and HChD when compared to ND ($p<0.05$). Additionally, LPE (20:2), LPE (22:4) and LPE (P-16:0), where decreased in HFD when compared to ND ($p<0.05$) - **Figure 16**.
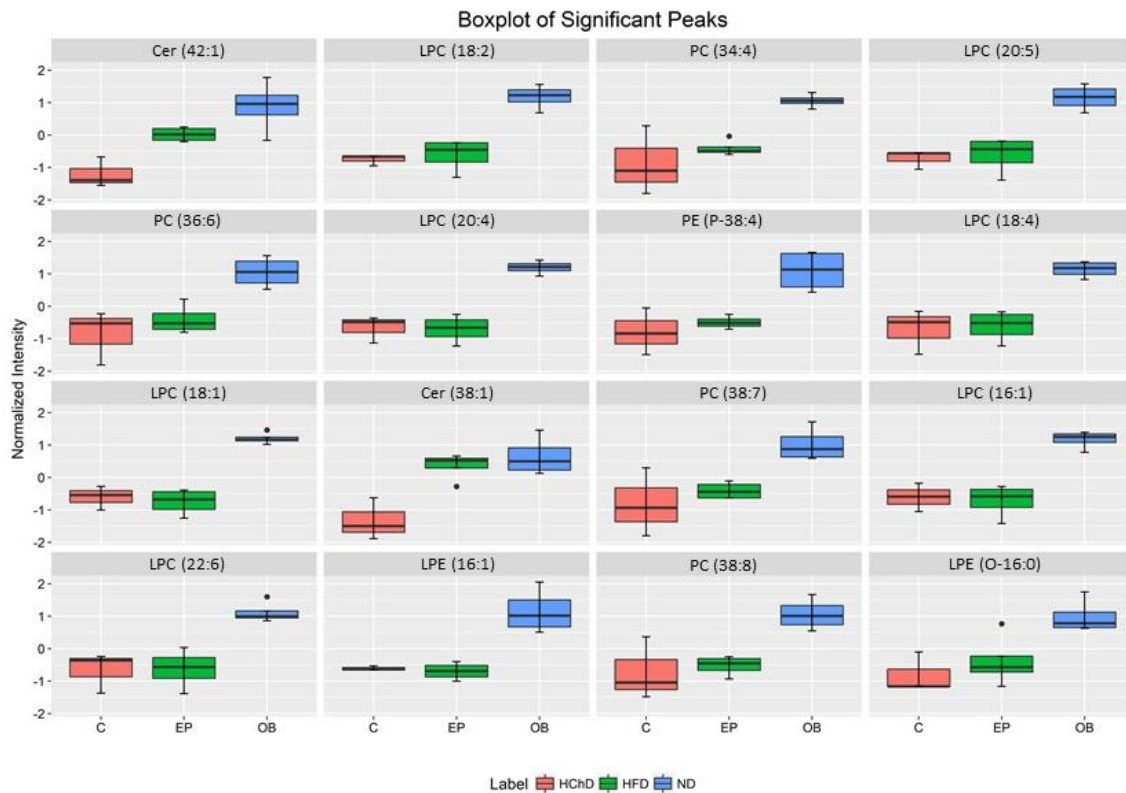


*Figure 15 - Box plots of 16 phospholipid molecular species that where identified as the most discriminates in the positive ion mode from the ND (normal diet), HChD (high cholesterol diet) and HFD (high fat diet). The values are represented as mean ± standard deviation.*
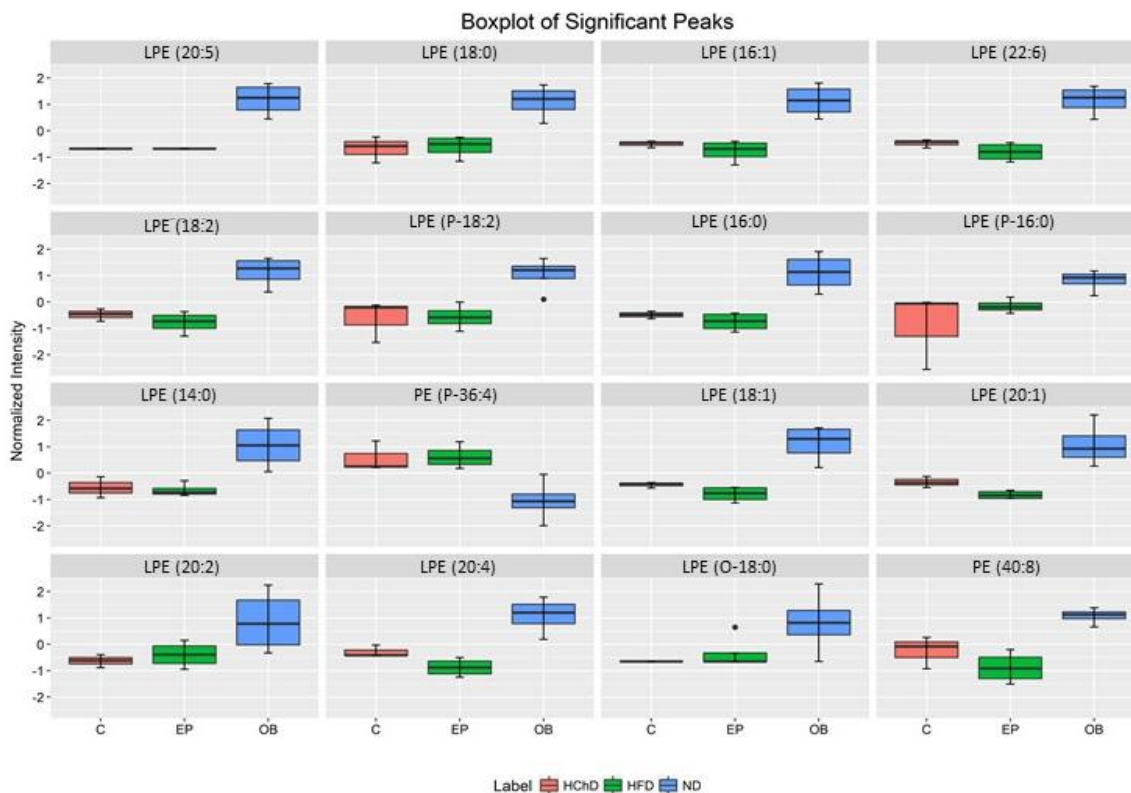
Figure 16 - Box plots of 16 phospholipid molecular species that where identified as the most discriminant in the negative mode from the ND (normal diet), HChD (high cholesterol diet) and HFD (high fat diet). The values are represented as mean ± standard deviation.

The FAs composition of PLs was analyzed by GC-MS and the results obtained are shown in **table 8**. The FAs identified were C14:0, C16:0, C16:1, C18:0, C18:1 (*n-9*), C18:2(*n-6*), C18:3(*n-6*), C20:0, C20:3(*n-3*), C20:4(*n-6*), C22:4(*n-6*), C22:5(*n-3*) and C22:6. Significant variations in the relative abundance of some individual FAs were observed and are shown in the **figure 17**. In PLs, the most abundant FAs were the C16:0 (palmitic acid) and the C18:0 (stearic acid). The less abundant FAs were C22:4 (*n-6*) and C22:5 (*n-3*) – **Table 8.** The C18:0 was statistically lower in the HFD when compared to the ND group. In addition, the ACL wasn't significant different between groups, however the DBI was significant higher in the HFD when compared to the ND.

Table 8- Fatty acid (FA) identification and relative quantitation (%) of PLs from the three study groups: normal diet (ND), high cholesterol diet (HChD) and high fat diet (HFD) and their relative abundance. Results are shown as mean ± SD (*** p < 0.001, compared to ND). ACL - average chain length; DBI - double bond index

| FA | ND | HChD | HFD |
|---|---|---|---|
| C14:0 | 2.4 ± 0.2 | 3.4 ± 0.9 | 3.3 ± 0.4 |
| C16:0 | 38.0 ± 1.6 | 35.0 ± 1.3 | 35.6 ± 3.7 |

**Universidade de Aveiro**
**Ano 2018**

| | | | |
|---|---|---|---|
| *C16:1* | 1.4 ± 0.2 | 2.3 ± 1.1 | 2.0 ± 0.1 |
| *C18:0* | 33.0 ±1.0 | 30.1 ± 2.5 | 26.1 ± 2.4 *** |
| *C18:1 (n-9)* | 10.5 ± 1.4 | 10.8 ± 2.7 | 12.0 ± 1.6 |
| *C18:2 (n-6)* | 5.6 ± 0.7 | 8.0 ± 1.1 | 8.2 ± 2.0 |
| *C18:3 (n-6)* | 1.3 ± 0.0 | 1.2 ± 0.0 | 1.1 ± 0.2 |
| *C20:0* | 1.4 ± 0.2 | 1.7 ± 0.4 | 1.8 ± 0.5 |
| *C20:3 (n-3)* | 2.4 ± 2.4 | 5.8 ± 0.0 | 0.9 ± 0.2 |
| *C20:4 (n-6)* | 3.7 ± 2.2 | 3.4 ± 3.2 | 5.3 ± 1.9 |
| *C22:4 (n-6)* | 0.7 ± 0.1 | 1.1 ± 0.3 | 0.9 ± 0.2 |
| *C22:5 (n-3)* | 0.7 ± 0.1 | 1.2 ± 0.3 | 1.0 ± 0.3 |
| *C22:6* | 1.7 ± 0.2 | 2.5 ± 0.9 | 1.9 ± 1.1 |
| ***ACL*** | 17.35 ± 0.03 | 17.42 ± 0.10 | 17.43 ± 0.17 |
| ***DBI*** | 55.91 ± 4.03 | 70.37 ± 4.40 | 77.29 ± 18.75* |
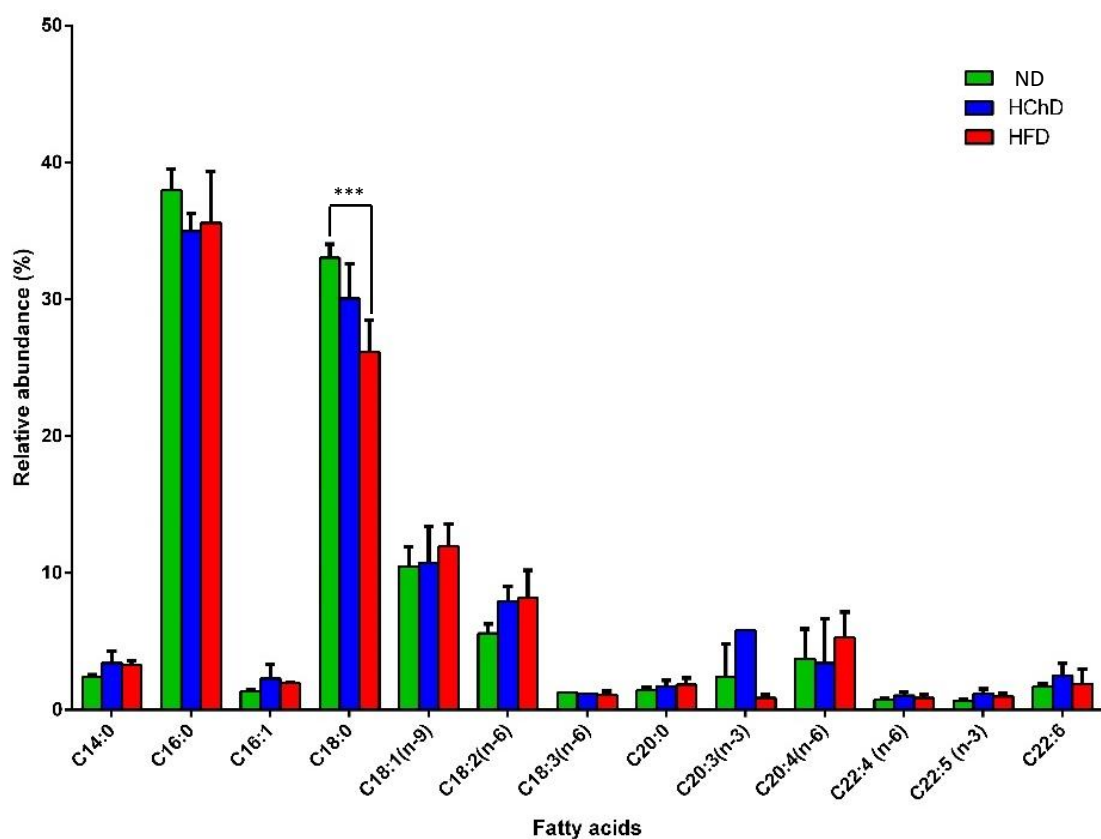


*Figure 17 - Graph representing the relative abundance in percentage, with standard deviation of each FA identified. In blue is the ND –Normal Diet; HChD- High Cholesterol Diet and HFD – High Fat Diet. (\*\*\* p < 0.001).*

## 8.3  Summary

In conclusion, there were 7 TAGs that shown a significant difference according to the different diets. Those TAGs where TAGs the TAG (50:3), TAG (50:1), TAG (52:4), TAG (52:3), TAG (52:2), TAG (54:5) and TAG (54:4). When it comes to the FAs the values of the FA C16:0, C18:1 (*n-9*) and C18:2 (*n-6*) where the most changed in the TAGs factions and the FA C18:0 in the PLs faction. The PLs analysis, the species identified where in general decreased in the HChD and HFD when compared to the ND. This way we can confirm that differences related to the different diets exist in the lipidome of the mammary gland.

## 9.    Discussion

The lipidomic approach employed in the present study allowed an unprecedented insight on the lipid dynamics in the mammary gland during obesity. MS analysis revealed alterations in the lipids environment related to different diets.

In this present study, results from the tissue extraction didn't shown differences in the amount of lipid extract, as well as no differences in the TAG content between the groups. In contrast, when it comes to the content of PLs on the lipid extract it was significant higher in the ND when compared to the HFD, which is explained by the fact that histologic studies show that there is probably less epithelium in adipose tissue from HFD samples. (165)

The ND and HFD main source of fat was lard, while in the HChD is cocoa butter. The cocoa butter has a higher amount of SFAs, being the C18:0 the main FA while in the lard the main FA is C16:0. In contrast, the lard has increased amounts of MUFAs and PUFAs, being C18:1 and C18:2 the main FAs in booth of them.(166) This may explain the differences saw between HChD and HFD in the TAG FA C18:1.

Previous published work that evaluated the TAG content from subcutaneous adipose tissue from *ob/ob* mice shows a significance increase on the levels of TAG (52:2), which is in accordance with our results.(167) In addition, in the analyses of the TAG results, we are able to see that the their composition in the mammary gland tissue is influenced by the diet, being that the TAG profile from HChD and HFD are associated with higher levels of the TAG with more PUFAs. That was the case of the increase of TAG (52:4), (52:3), (54:5) and (54:4), assigned respectively as *m/z* 872.8, *m/z* 874.8, *m/z* 898.8 and *m/z* 900.8. These TAG are composed mainly by MUFAs and PUFAs, which goes to the encounter of the higher levels seen in the GC-MS analyses of the PUFA C18:2(*n-6*) and the significant increase in the DBI seen in the HFD and HChD when compared to the ND and it has been shown that the free radical damage and lipid peroxidation increase as a function of the degree of unsaturation of the fatty acid substrates present in the tissues.(168) In the literature it is reported that n-6 PUFAs (including C18:2 (*n-6*)) can facilitate carcinogenesis, since the lipid peroxidation of these PUFAS generates α, β – unsaturated aldehydes, such as malondialdehyde (MDA) and 4-hydroxy-2-nonenal. These electrophilic lipid oxidation products (small aldehydes) can form promutagenic exocyclic adducts with DNA in human cells and thus may contribute to human cancers.(169,170) Recent published work suggests

that *n-6* PUFAs promote colon and mammary tumourigenesis by up-regulating the expression of COX-2 and p21 *ras*.(171)

There are some studies that suggest that same FAs may influence PPARs receptors activity. The FA C20:4 has been pointed as a regulator of PPARγ activity as well, downregulating transcription of a PPARγ target gene GLUT4.(172) In addition, C18:2 and C22:6 are also reported to activate PPARγ.(173,174) Interestingly, these two FAs have shown a tendency to increase in the HChD and HFD but the difference between these two study groups and the ND wasn't statistically different. PPARγ has a well-established central role in differentiation and function of mature adipocytes.(175,176) Thus activation of PPARγ can have an impact on the role of adipose tissue and it is also known that the function of adipose tissues is severely altered in obesity.(177) However, this does not stem from a reduced expression of PPARγ, which remains unchanged or increased in adipose tissues from obese rats, mice, and humans.(178,179) In addition it is reported that PPARγ is up-regulated in breast cancer cells.(180) PPARγ agonists increase fat mass along with improving glucose control supports the notion that WAT mediates some of their effects on glucose homeostasis. Besides FAs, WAT produces several adipokines, which affect insulin signaling in other tissues, and whose expression is also altered by PPARγ activation. Examples are TNF-α, leptin, and resistin, secreted proportionally with WAT mass.(181) These molecules activate breast cancer progression.(182,183,184) In addition, the FA C22:6 is also reported to activate PPARα and the activation of this receptor in human breast cancer line promoted proliferation.(185,186)

In what concern the results obtained about the variation of PLs, profile, the multivariate analyses performed (PCA and PLS-DA) showed that the PL profiles of the mammary gland was significantly different for the different diets (ND, HChD and HFD). The two-dimensional plots of PCA (**Figure 13**), show differentiation between the two conditions (HChD and HFD), but discriminant when it compares to the ND group. This suggests that different diets induce particular and specific changes is the PL profile of the mammary gland, according to the fat content and the type of fat in the diet. In our study we focused in the PC, LPC, PE, LPE, SM and Cer, since the higher content of TAG on the extract make it difficult to analyse the PLs. For this reason we decided to study the abundant species in this type of tissue.(187)

*Dianning He* and co-authors studied the mammary gland of Female C3 SV40 Tag transgenic mice feed with different diets, including a low fat and HFD. They used magnetic resonance spectroscopy to evaluate possible effect of the diet composition in the mammary gland fat, were they verified a higher accumulation of lipid in the mammary gland of HFD group.(188) It is shown that in obesity, the accumulated adipose tissue induces the synthesis of pro-inflammatory cytokines, which promote increased generation of ROS (reactive species of oxygen) and nitrogen.(189) In addition, *Furukawa et al.* found that accumulation of excessive fat in WAT, caused by a HFD, triggered an increase in lipid peroxidation in the WAT itself. In the animal studies, it was observed that obesity causes an increase of the expression of NADPH oxidase in WAT, concomitantly with a decrease in the activities of antioxidant enzymes such as CAT and GPx.(190) Lipid peroxidation refers to the oxidative degradation of lipids, a process initiated by free radicals/ROS escaping the antioxidant system.(191) Oxygen radicals react with PUFAs residues in PLs resulting in the production of a plethora of products, many of them reactive toward protein and DNA.(192)

In what concern PLs and cancer, and adipose tissue we also saw alterations with the different diets which are concordant with alterations reported. The FAs content of the PLs was evaluated trough GC-MS and it shows a significant decreased in the SFA C18:0 and a slight increase in the levels of the PUFAs. In addition, the DBI values shown a significant increase HFD. Acyl chain length and saturation determine the fluidity of the membrane; phospholipids with longer and more saturated chain lengths tend to aggregate and form less fluid membranes. The PCs account for nearly 50% of membrane PLs and are necessary for membrane structure and compartmentalization in the cell, as well as interaction with integral membrane proteins.(193) For this reason, the saturation of PCs is very important for cell membrane saturation that may explain why the PC (40:1), PC (42:2), PC (42:1) and PC (44:4) were decreased in the mammary gland of the HChD and HFD groups and the DBI was statistically higher in the HFD when compared to ND. More cell fluidity is associated with cancer cells, and poor prognosis in lung cancer cells.(194) In a study made by *Kirsi H. Pietiläine*, that compared the PLs profile in adipose tissue from twins with very different BMI (one of the twins has a high BMI and the other one lower BMI) it was reported a significant decrease in the levels of PC (36:2) ($p<0.001$), PC (34:2) ($p<0.01$) and PC (36:3) ($p<0.05$) in the WAT of the twins with higher BMI.(195) Similar pattern of variation in PC profile was reported in adipose tissue of *ob/ob* mice in comparison with control.(167) Since

the levels of PC were decreased in general from the mammary gland of HChD and HFD, it only makes sense that the levels of LPC, whose origin is PC are also decreased, in particular LPC constituted with longer and more saturated FAs, like LPC (20:0), LPC (22:1)  and LPC (24:0). In addition, recently it has been demonstrated that treating cultured adipocytes with LPC stimulated glucose uptake in a dose-dependent manner via an insulin-independent mechanism involving activation of protein kinase C δ. Furthermore, these authors were also able to show that acute LPC treatment improved glycemia in mouse models of diabetes.(196) Thus, LPC reduction in obese mice and humans may play some role in contributing to the defects in glucose homeostasis observed in obesity.

When it comes to SM, a study made by *Fahumiya S.* (197) reported the decreased of the levels of SM with more significance in the species SM (d34:1), SM (d38:1), SM (d40:1), SM (d42:1) and SM (d42:1) in the adipose tissue of *ob/ob* mice when compared to lean mice, which is in accordance with our results of the lipidome of  the mammary gland tissue.  They also reported a decrease in the levels of ceramides in general, with the most significance in the levels on species Cer (d42:1), Cer (d36:2) and Cer (42:2) which are also in agreement with our results. In addition, our results are also concordant with a study made by *A.U. Blachnio-Zabielska* which shows a general decrease of the ceramide levels in WAT in obese mice, and this decrease was accompanied by an increase in S1P values.(198) Ceramides are involved in apoptosis and lethal autophagy, all of which decrease cancer cell viability.(199,200) When ceramides are added to cells in culture they show to have anti-proliferative activities.(201,202). S1P is a pro-proliferating agent.(203) These results suggest that in obesity the process of apoptosis might be impaired, favoring the inhibition of apoptosis of adipocytes and enhancement cell proliferation, which could be favored by cell proliferation of possible new tumor cells.

PE are the second most abundant phospholipid class in mammalian membranes ranging from 20 - 50%.(204) Importantly, PE does not spontaneously assemble in bilayers and rather incorporates into curved structures, such as the inverted hexagonal phase, and such it is mostly found in the inner leaf of the cell membranes add shape cell curvature. (205) In a study made by *Xavier Prieur* it was reported that the levels of the PE(36:3) and PE(P-36:4) where decreased in the adipose tissue of *ob/ob* mice in comparison with non obese mice. Similarly our results showed an overall decrease in the levels of PE in the HChD and HFD.(167) This results may suggest an abrormal cells functioning. There is also a

decreased in the levels of plasmenyl-PE. This type of PLs has been shown to have an antioxidant action by protecting cholesterol from oxidation by free radicals and lowering the oxidizability of membranes.(206) It acts as an endogenous antioxidants by scavenging radicals at the vinyl–ether linkage.(207) The importance of oxidative membrane damage is that can be modified by direct attack of the reactive species on the membrane components that are responsible for the functions. In the other hand we can have the consequences of the products of the lipid peroxidation, like it was discussed before.(208) Therefore, two different ways of oxidative modifications of cellular constituents have to be considered in general: the direct modification by reactive oxygen species and the indirect modification via reactive products of lipid peroxidation.

## 10.   Conclusion

The aim of this work was to detect changes in the lipidome of the mammary gland related to obesity and associate those changes to a higher risk of developing breast cancer. In this study, we reported for the first time the changes the lipidome of mammary gland related to obesity.

Herein, we are able to detect changes in the TAG content mainly the augmentation in the n-6 PUFAs in the obesity that can be related to the augmentation of the DNA mutation in obesity, promoting this way breast carcinogenesis. In addition we can also see an increase in several FA responsible for activating the receptors PPARs whose have been reported to be activated in several cancers, including breast cancer

Additionally, we also characterize the PLs content of the mammary gland as well as detected changes is it PL and Cer profiles related to obesity. We focused our study in the most abundant and most discuss PLs species that are PC, PE, LPC, LPE, SM and Cer. We detected an overall decreased in the levels of the PLs species that had a statistically difference in the mammary gland of HFD and HChD. Cer and PE decreased may can influence the normal cell functioning. Since PC are the major component of cell membrane any alterations in them may influence the membrane fluidity.

Finally, the alterations in the FA content of the TAG as well as in PLs. This alterations may promote an abnormal PPAR function, in particular PPARγ that it's the most common isoform in the mammary gland and favor breast carcinogenesis.

## 11.    References

1.      WHO :: Global Database on Body Mass Index [Internet]. [2018]. Disponível em: http://apps.who.int/bmi/index.jsp?introPage=intro_3.html

2.      Hruby A, Hu FB. The Epidemiology of Obesity: A Big Picture. PharmacoEconomics.  2015;33(7):673–89.

3.      Apovian CM. Obesity: definition, comorbidities, causes, and burden. Am J Manag Care. 2016;22(7 Suppl):s176-185.

4.      Calle EE, Rodriguez C, Walker-Thurmond K, Thun MJ. Overweight, obesity, and mortality from cancer in a prospectively studied cohort of U.S. adults. N Engl J Med. 2003;348(17):1625–38.

5.      Lutz TA, Woods SC. Overview of Animal Models of Obesity. Curr Protoc Pharmacol Editor Board SJ Enna Ed--Chief Al. 2012;CHAPTER:Unit5.61.

6.      Frederich RC, Löllmann B, Hamann A, Napolitano-Rosen A, Kahn BB, Lowell BB, et al. Expression of ob mRNA and its encoded protein in rodents. Impact of nutrition and obesity. J Clin Invest. 1995;96(3):1658–63.

7.      Wang B, P. CC, Pippin JJ. Leptin- and Leptin Receptor-Deficient Rodent Models: Relevance for Human Type 2 Diabetes. Curr Diabetes Rev.  2014;10(2):131–45.

8.      Corsetti JP, Sparks JD, Peterson RG, Smith RL, Sparks CE. Effect of dietary fat on the development of non-insulin dependent diabetes mellitus in obese Zucker diabetic fatty male and female rats. Atherosclerosis. 2000;148(2):231–41.

9.      Ikeda H. KK mouse. Diabetes Res Clin Pract. 1994;24:S313–6.

10.     Igel M, Taylor BA, Phillips SJ, Becker W, Herberg L, Joost HG. Hyperleptinemia and leptin receptor variant Asp600Asn in the obese, hyperinsulinemic KK mouse strain. J Mol Endocrinol. 1998;21(3):337–45.

11.     Iwatsuka H, Shino A, Suzuoki Z. General survey of diabetic features of yellow KK mice. Endocrinol Jpn. 1970;17(1):23–35.

12.     Klebig ML, Wilkinson JE, Geisler JG, Woychik RP. Ectopic expression of the agouti gene in transgenic mice causes obesity, features of type II diabetes, and yellow fur. Proc Natl Acad Sci U S A. 1995;92(11):4728–32.

13.     Stütz AM, Morrison CD, Argyropoulos G. The agouti-related protein and its role in energy homeostasis. Peptides.  2005;26(10):1771–81.

14.     Bray GA, York DA. Genetically transmitted obesity in rodents. Physiol Rev. 1971;51(3):598–646.

15.     Butler L, Gerritsen GC. A comparison of the modes of inheritance of diabetes in the chinese hamster and the KK mouse. Diabetologia. 1970;6(3):163–7.

16.     Herberg L, Coleman DL. Laboratory animals exhibiting obesity and diabetes syndromes. Metabolism. 1977;26(1):59–99.

17.     Trayhurn P, Jones PM, McGuckin MM, Goodbody AE. Effects of overfeeding on energy balance and brown fat thermogenesis in obese (ob/ob) mice. Nature. 1982;295(5847):323.

18.     Hogan S, Himms-Hagen J. Abnormal brown adipose tissue in obese (ob/ob) mice: response to acclimation to cold. Am J Physiol. 1980;239(4):E301–9.

19.     Memon RA, Fuller J, Moser AH, Smith PJ, Grunfeld C, Feingold KR. Regulation of putative fatty acid transporters and Acyl-CoA synthetase in liver and adipose tissue in ob/ob mice. Diabetes. 1999;48(1):121–7.

20.     Phillips MS, Liu Q, Hammond HA, Dugan V, Hey PJ, Caskey CJ, et al. Leptin receptor missense mutation in the fatty Zucker rat. Nat Genet. 1996;13(1):18–9.

21.     Aleixandre de Artiñano A, Miguel Castro M. Experimental rat models to study the metabolic syndrome. Br J Nutr. 2009;102(9):1246–53.

22.     Bray GA. The Zucker-fatty rat: a review. Fed Proc.  1977;36(2):148–53.

23.     Lutz TA, Woods SC. Overview of Animal Models of Obesity. Curr Protoc Pharmacol Editor Board SJ Enna Ed--Chief Al.  2012;CHAPTER:Unit5.61.

24.     Pomp D. Genetic Dissection of Obesity in Polygenic Animal Models. Behav Genet. 1997;27(4):285–306.

25.     Surwit RS, Feinglos MN, Rodin J, Sutherland A, Petro AE, Opara EC, et al. Differential effects of fat and sucrose on the development of obesity and diabetes in C57BL/6J and A/J mice. Metabolism. 1995;44(5):645–51.

26.     Wada T, Kenmochi H, Miyashita Y, Sasaki M, Ojima M, Sasahara M, et al. Spironolactone improves glucose and lipid metabolism by ameliorating hepatic steatosis and inflammation and suppressing enhanced gluconeogenesis induced by high-fat and high-fructose diet. Endocrinology.  2010;151(5):2040–9.

27.     Couturier K, Batandier C, Awada M, Hininger-Favier I, Canini F, Anderson RA, et al. Cinnamon improves insulin sensitivity and alters the body composition in an animal model of the metabolic syndrome. Arch Biochem Biophys. 2010;501(1):158–61.

28.     Pérez C, Fanizza LJ, Sclafani A. Flavor preferences conditioned by intragastric nutrient infusions in rats fed chow or a cafeteria diet. Appetite. 1999;32(1):155–70.

29.     Rogers PJ, Blundell JE. Meal patterns and food selection during the development of obesity in rats fed a cafeteria diet. Neurosci Biobehav Rev. 1984;8(4):441–53.

30.     Cummings BP, Digitale EK, Stanhope KL, Graham JL, Baskin DG, Reed BJ, et al. Development and characterization of a novel rat model of type 2 diabetes mellitus: the UC Davis type 2 diabetes mellitus UCD-T2DM rat. Am J Physiol Regul Integr Comp Physiol. 2008;295(6):R1782-1793.

31.     Joost H-G. The genetic basis of obesity and type 2 diabetes: lessons from the new zealand obese mouse, a polygenic model of the metabolic syndrome. Results Probl Cell Differ. 2010;52:1–11.

32. Kim JH, Sen S, Avery CS, Simpson E, Chandler P, Nishina PM, et al. Genetic analysis of a new mouse model for non-insulin-dependent diabetes. Genomics. 2001;74(3):273–86.

33. Rhee SD, Sung YY, Lee YS, Kim JY, Jung WH, Kim MJ, et al. Obesity of TallyHO/JngJ mouse is due to increased food intake with early development of leptin resistance. Exp Clin Endocrinol Diabetes Off J Ger Soc Endocrinol Ger Diabetes Assoc. 2011;119(4):243–51.

34. Kamal MM, Mills D, Grzybek M, Howard J. Measurement of the membrane curvature preference of phospholipids reveals only weak coupling between lipid shape and leaflet curvature. Proc Natl Acad Sci. 2009;106(52):22245–50.

35. Phosphoinositide (Lipid) Signaling Pathway | Cell Signaling Technology [Internet]. [2018]. Disponível em: https://www.cellsignal.com/contents/science-cst-pathways-pi3k-akt-signaling-resources/phosphoinositide-(lipid)-interactive-signaling-pathway/pathways-lipid-signaling/

36. Fahy E, Subramaniam S, Brown HA, Glass CK, Merrill AH, Murphy RC, et al. A comprehensive classification system for lipids. J Lipid Res. 2005;46(5):839–61.

37. Hayasaka T, Goto-Inoue N, Sugiura Y, Zaima N, Nakanishi H, Ohishi K, et al. Matrix-assisted laser desorption/ionization quadrupole ion trap time-of-flight (MALDI-QIT-TOF)-based imaging mass spectrometry reveals a layered distribution of phospholipid molecular species in the mouse retina. Rapid Commun Mass Spectrom RCM. 2008;22(21):3415–26.

38. Sugiura Y, Konishi Y, Zaima N, Kajihara S, Nakanishi H, Taguchi R, et al. Visualization of the cell-selective distribution of PUFA-containing phosphatidylcholines in mouse brain by imaging mass spectrometry. J Lipid Res. 2009;50(9):1776–88.

39. Eibl H. Synthesis of glycerophospholipids. Chem Phys Lipids. 1980;26(4):405–29.

40. Welti R, Wang X. Lipid species profiling: a high-throughput approach to identify lipid compositional changes and determine the function of genes involved in lipid metabolism and signaling. Curr Opin Plant Biol. 2004;7(3):337–44.

41. Bielawski J, Szulc ZM, Hannun YA, Bielawska A. Simultaneous quantitative analysis of bioactive sphingolipids by high-performance liquid chromatography-tandem mass spectrometry. Methods San Diego Calif. 2006;39(2):82–91.

42. Burdge GC, Calder PC. Conversion of alpha-linolenic acid to longer-chain polyunsaturated fatty acids in human adults. Reprod Nutr Dev. 2005;45(5):581–97.

43. Brenna JT. Efficiency of conversion of alpha-linolenic acid to long chain n-3 fatty acids in man. Curr Opin Clin Nutr Metab Care. 2002;5(2):127–32.

44. Mišurcová L, Ambrožová J, Samek D. Seaweed lipids as nutraceuticals. Adv Food Nutr Res. 2011;64:339–55.

45. Fernandez C, Sandin M, Sampaio JL, Almgren P, Narkiewicz K, Hoffmann M, et al. Plasma lipid composition and risk of developing cardiovascular disease. PloS One. 2013;8(8):e71846.

46.     Jiang J, Xu N, Zhang X, Wu C. Lipids changes in liver cancer. J Zhejiang Univ Sci B. 2007;8(6):398–409.

47.     Dempsey ME. Cholesterol Biosynthesis in Liver Tissue. Em: Chemistry and Brain Development [Internet]. Springer, Boston, MA; 1971 [ 2018]. p. 31–9. (Advances in Experimental Medicine and Biology). Disponível em: https://link.springer.com/chapter/10.1007/978-1-4684-7236-3_3

48.     Muscat GEO, Wagner BL, Hou J, Tangirala RK, Bischoff ED, Rohde P, et al. Regulation of Cholesterol Homeostasis and Lipid Metabolism in Skeletal Muscle by Liver X Receptors. J Biol Chem. 2002;277(43):40722–8.

49.     Miettinen TA, Tilvis RS. Cholesterol synthesis and storage in adipose tissue. Int J Obes. 1981;5(6):613–8.

50.     Breast cancer | World Cancer Research Fund International [Internet]. [2018]. Disponível em: http://www.wcrf.org/int/research-we-fund/continuous-update-project-findings-reports/breast-cancer

51.     Hu J, Komakula A, Fraser ME. Binding of hydroxycitrate to human ATP-citrate lyase. Acta Crystallogr Sect Struct Biol. 2017;73(Pt 8):660–71.

52.     Smith S, Witkowski A, Joshi AK. Structural and functional organization of the animal fatty acid synthase. Prog Lipid Res. 2003;42(4):289–317.

53.     Kuhajda FP. Fatty-acid synthase and human cancer: new perspectives on its role in tumor biology. Nutr Burbank Los Angel Cty Calif. 2000;16(3):202–8.

54.     Nakamura MT, Nara TY. Structure, function, and dietary regulation of delta6, delta5, and delta9 desaturases. Annu Rev Nutr. 2004;24:345–76.

55.     Jump DB, Depner CM, Tripathy S. Omega-3 fatty acid supplementation and cardiovascular disease. J Lipid Res. 2012;53(12):2525–45.

56.     Baenke F, Peck B, Miess H, Schulze A. Hooked on fat: the role of lipid synthesis in cancer metabolism and tumour development. Dis Model Mech. 2013;6(6):1353–63.

57.     Flock MR, Harris WS, Kris-Etherton PM. Long-chain omega-3 fatty acids: time to establish a dietary reference intake. Nutr Rev. 2013;71(10):692–707.

58.     Hannun YA, Obeid LM. Principles of bioactive lipid signalling: lessons from sphingolipids. Nat Rev Mol Cell Biol. 2008;9(2):139–50.

59.     Vanhaesebroeck B, Leevers SJ, Ahmadi K, Timms J, Katso R, Driscoll PC, et al. Synthesis and function of 3-phosphorylated inositol lipids. Annu Rev Biochem. 2001;70:535–602.

60.     Lin J, Yang R, Tarr PT, Wu P-H, Handschin C, Li S, et al. Hyperlipidemic effects of dietary saturated fats mediated through PGC-1beta coactivation of SREBP. Cell. 2005;120(2):261–73.

61.     Lin J, Handschin C, Spiegelman BM. Metabolic control through the PGC-1 family of transcription coactivators. Cell Metab. 2005;1(6):361–70.

62.    Zechner R, Zimmermann R, Eichmann TO, Kohlwein SD, Haemmerle G, Lass A, et al. FAT SIGNALS - Lipases and Lipolysis in Lipid Metabolism and Signaling. Cell Metab. 2012;15(3):279–91.

63.    Large V, Reynisdottir S, Langin D, Fredby K, Klannemark M, Holm C, et al. Decreased expression and function of adipocyte hormone-sensitive lipase in subcutaneous fat cells of obese subjects. J Lipid Res. 1999;40(11):2059–66.

64.    Berndt J, Kralisch S, Klöting N, Ruschke K, Kern M, Fasshauer M, et al. Adipose triglyceride lipase gene expression in human visceral obesity. Exp Clin Endocrinol Diabetes Off J Ger Soc Endocrinol Ger Diabetes Assoc. 2008;116(4):203–10.

65.    Hellström L, Langin D, Reynisdottir S, Dauzats M, Arner P. Adipocyte lipolysis in normal weight subjects with obesity among first-degree relatives. Diabetologia. 1996;39(8):921–8.

66.    Steinberg GR, Kemp BE, Watt MJ. Adipocyte triglyceride lipase expression in human obesity. Am J Physiol Endocrinol Metab. 2007;293(4):E958-964.

67.    Arce-Salinas C, Aguilar-Ponce JL, Villarreal-Garza C, Lara-Medina FU, Olvera-Caraza D, Alvarado Miranda A, et al. Overweight and obesity as poor prognostic factors in locally advanced breast cancer patients. Breast Cancer Res Treat. 2014;146(1):183–8.

68.    Osman MA, Hennessy BT. Obesity Correlation With Metastases Development and Response to First-Line Metastatic Chemotherapy in Breast Cancer. Clin Med Insights Oncol. 2015;9:105–12.

69.    Ewertz M, Jensen M-B, Gunnarsdóttir KÁ, Højris I, Jakobsen EH, Nielsen D, et al. Effect of obesity on prognosis after early-stage breast cancer. J Clin Oncol Off J Am Soc Clin Oncol. 2011;29(1):25–31.

70.    Du J, Sun C, Hu Z, Yang Y, Zhu Y, Zheng D, et al. Lysophosphatidic Acid Induces MDA-MB-231 Breast Cancer Cells Migration through Activation of PI3K/PAK1/ERK Signaling. PLoS ONE [Internet]. 2010 ;5(12). Disponível em: ttps://www.ncbi.nlm.nih.gov/pmc/articles/PMC3012724/

71.    Prostaglandin E2 production and metabolism in human breast cancer cells and breast fibroblasts. Regulation by inflammatory mediators. [Internet]. [2018]. Disponível em: https://www.ncbi.nlm.nih.gov/pmc/articles/PMC2034098/

72.    Mukhopadhyay P, Ramanathan R, Takabe K. S1P promotes breast cancer progression by angiogenesis and lymphangiogenesis. Breast Cancer Manag. 2015;4(5):241–4.

73.    Navarro-Tito N, Soto-Guzman A, Castro-Sanchez L, Martinez-Orozco R, Salazar EP. Oleic acid promotes migration on MDA-MB-231 breast cancer cells through an arachidonic acid-dependent pathway. Int J Biochem Cell Biol. 2010;42(2):306–17.

74.    Soto-Guzman A, Robledo T, Lopez-Perez M, Salazar EP. Oleic acid induces ERK1/2 activation and AP-1 DNA binding activity through a mechanism involving Src kinase and EGFR transactivation in breast cancer cells. Mol Cell Endocrinol. 2008;294(1–2):81–91.

75.     Shen C-J, Chan S-H, Lee C-T, Huang W-C, Tsai J-P, Chen B-K. Oleic acid-induced ANGPTL4 enhances head and neck squamous cell carcinoma anoikis resistance and metastasis via up-regulation of fibronectin. Cancer Lett. 2017;386:110–22.

76.     Georgiadi A, Lichtenstein L, Degenhardt T, Boekschoten MV, Bilsen M van, Desvergne B, et al. Induction of Cardiac Angptl4 by Dietary Fatty Acids Is Mediated by Peroxisome Proliferator-Activated Receptor β/δ and Protects Against Fatty Acid–Induced Oxidative Stress. Circ Res. 2010;106(11):1712–21.

77.     Lichtenstein L, Mattijssen F, de Wit NJ, Georgiadi A, Hooiveld GJ, van der Meer R, et al. Angptl4 Protects against Severe Proinflammatory Effects of Saturated Fat by Inhibiting Fatty Acid Uptake into Mesenteric Lymph Node Macrophages. Cell Metab. 2010;12(6):580–92.

78.     Li S, Zhou T, Li C, Dai Z, Che D, Yao Y, et al. High Metastaticgastric and Breast Cancer Cells Consume Oleic Acid in an AMPK Dependent Manner. PLoS ONE [Internet]. 2014 [ 2018];9(5). Disponível em: https://www.ncbi.nlm.nih.gov/pmc/articles/PMC4019637/

79.     Hardy S, St-Onge GG, Joly E, Langelier Y, Prentki M. Oleate promotes the proliferation of breast cancer cells via the G protein-coupled receptor GPR40. J Biol Chem. 2005;280(14):13285–91.

80.     Ivanova PT, Cerda BA, Horn DM, Cohen JS, McLafferty FW, Brown HA. Electrospray ionization mass spectrometry analysis of changes in phospholipids in RBL-2H3 mastocytoma cells during degranulation. Proc Natl Acad Sci U S A. 2001;98(13):7152–7.

81.     Shevchenko A, Simons K. Lipidomics: coming to grips with lipid diversity. Nat Rev Mol Cell Biol. 2010;11(8):593–8.

82.     Astigarraga E, Barreda-Gómez G, Lombardero L, Fresnedo O, Castaño F, Giralt MT, et al. Profiling and imaging of lipids on brain and liver tissue by matrix-assisted laser desorption/ ionization mass spectrometry using 2-mercaptobenzothiazole as a matrix. Anal Chem. 2008;80(23):9105–14.

83.     Wenk MR. The emerging field of lipidomics. Nat Rev Drug Discov. 2005;4(7):594–610.

84.     Poirier H, Shapiro JS, Kim RJ, Lazar MA. Nutritional supplementation with trans-10, cis-12-conjugated linoleic acid induces inflammation of white adipose tissue. Diabetes. 2006;55(6):1634–41.

85.     LaRosa PC, Miner J, Xia Y, Zhou Y, Kachman S, Fromm ME. Trans-10, cis-12 conjugated linoleic acid causes inflammation and delipidation of white adipose tissue in mice: a microarray and histological analysis. Physiol Genomics. 2006;27(3):282–94.

86.     Fonseca FC, Orlando RM, Turchetti-Maia RM, de Francischi JN. Comparative effects of the ω3 polyunsaturated fatty acid derivatives resolvins E1 and D1 and protectin DX in models of inflammation and pain. J Inflamm Res. 2017;10:119–33.

87.     Fabian CJ, Kimler BF, Hursting SD. Omega-3 fatty acids for breast cancer prevention and survivorship. Breast Cancer Res BCR. 2015;17:62.

88.     Simopoulos AP. The importance of the omega-6/omega-3 fatty acid ratio in cardiovascular disease and other chronic diseases. Exp Biol Med Maywood NJ. 2008;233(6):674–88.

89.     Chajès V, Torres-Mejía G, Biessy C, Ortega-Olvera C, Angeles-Llerenas A, Ferrari P, et al. ω-3 and ω-6 Polyunsaturated fatty acid intakes and the risk of breast cancer in Mexican women: impact of obesity status. Cancer Epidemiol Biomark Prev Publ Am Assoc Cancer Res Cosponsored Am Soc Prev Oncol. 2012;21(2):319–26.

90.     Howe LR, Subbaramaiah K, Hudis CA, Dannenberg AJ. Molecular pathways: adipose inflammation as a mediator of obesity-associated cancer. Clin Cancer Res Off J Am Assoc Cancer Res.  2013;19(22):6074–83.

91.     Maillard V, Bougnoux P, Ferrari P, Jourdan M-L, Pinault M, Lavillonnière F, et al. N-3 and N-6 fatty acids in breast adipose tissue and relative risk of breast cancer in a case-control study in Tours, France. Int J Cancer.  2002;98(1):78–83.

92.     Bougnoux P, Giraudeau B, Couet C. Diet, cancer, and the lipidome. Cancer Epidemiol Biomarkers Prev.  2006;15(3):416–21.

93.     Cífková E, Holčapek M, Lísa M, Vrána D, Gatěk J, Melichar B. Determination of lipidomic differences between human breast cancer and surrounding normal tissues using HILIC-HPLC/ESI-MS and multivariate data analysis. Anal Bioanal Chem. 2015;407(3):991–1002.

94.     Cífková E, Lísa M, Hrstka R, Vrána D, Gatěk J, Melichar B, et al. Correlation of lipidomic composition of cell lines and tissues of breast cancer patients using hydrophilic interaction liquid chromatography/electrospray ionization mass spectrometry and multivariate data analysis. Rapid Commun Mass Spectrom. 2017;31(3):253–63.

95.     Dória ML, Cotrim CZ, Simões C, Macedo B, Domingues P, Domingues MR, et al. Lipidomic analysis of phospholipids from human mammary epithelial and breast cancer cell lines. J Cell Physiol. 2013;228(2):457–68.

96.     Kim H-Y, Lee K-M, Kim S-H, Kwon Y-J, Chun Y-J, Choi H-K. Comparative metabolic and lipidomic profiling of human breast cancer cells with different metastatic potentials. Oncotarget. 2016;7(41):67111–28.

97.     Kang HS, Lee SC, Park YS, Jeon YE, Lee JH, Jung S-Y, et al. Protein and lipid MALDI profiles classify breast cancers according to the intrinsic subtype. BMC Cancer. 2011;11:465.

98.     Kawashima M, Iwamoto N, Kawaguchi-Sakita N, Sugimoto M, Ueno T, Mikami Y, et al. High-resolution imaging mass spectrometry reveals detailed spatial distribution of phosphatidylinositols in human breast cancer. Cancer Sci. 2013;104(10):1372–9.

99.     Chughtai K, Jiang L, Greenwood TR, Glunde K, Heeren RMA. Mass spectrometry images acylcarnitines, phosphatidylcholines, and sphingomyelin in MDA-MB-231 breast tumor models. J Lipid Res. 2013;54(2):333–44.

100.    Michalik L, Wahli W. PPARs Mediate Lipid Signaling in Inflammation and Cancer. PPAR Res [Internet]. 2008 ;2008. Disponível em: https://www.ncbi.nlm.nih.gov/pmc/articles/PMC2606065/

101.    Michalik L, Wahli W. Involvement of PPAR nuclear receptors in tissue injury and wound repair. J Clin Invest. 2006;116(3):598–606.

102.    Lehrke M, Lazar MA. The many faces of PPARgamma. Cell. 2005;123(6):993–9.

103.    Willson TM, Brown PJ, Sternbach DD, Henke BR. The PPARs: From Orphan Receptors to Drug Discovery. J Med Chem. 2000;43(4):527–50.

104.    Auwerx J, Martin G, Guerre-Millo M, Staels B. Transcription, adipocyte differentiation, and obesity. J Mol Med Berl Ger. 1996;74(7):347–52.

105.    Tontonoz P, Hu E, Spiegelman BM. Regulation of adipocyte gene expression and differentiation by peroxisome proliferator activated receptor gamma. Curr Opin Genet Dev. 1995;5(5):571–6.

106.    Oliveira ACP, Bertollo CM, Rocha LTS, Nascimento EB, Costa KA, Coelho MM. Antinociceptive and antiedematogenic activities of fenofibrate, an agonist of PPAR alpha, and pioglitazone, an agonist of PPAR gamma. Eur J Pharmacol. 2007;561(1–3):194–201.

107.    Aoyama T, Peters JM, Iritani N, Nakajima T, Furihata K, Hashimoto T, et al. Altered constitutive expression of fatty acid-metabolizing enzymes in mice lacking the peroxisome proliferator-activated receptor alpha (PPARalpha). J Biol Chem. 1998;273(10):5678–84.

108.    Hashimoto T, Fujita T, Usuda N, Cook W, Qi C, Peters JM, et al. Peroxisomal and mitochondrial fatty acid beta-oxidation in mice nullizygous for both peroxisome proliferator-activated receptor alpha and peroxisomal fatty acyl-CoA oxidase. Genotype correlation with fatty liver phenotype. J Biol Chem. 1999;274(27):19228–36.

109.    Schoonjans K, Staels B, Auwerx J. The peroxisome proliferator activated receptors (PPARS) and their effects on lipid metabolism and adipocyte differentiation. Biochim Biophys Acta. 1996;1302(2):93–109.

110.    Motojima K, Passilly P, Peters JM, Gonzalez FJ, Latruffe N. Expression of putative fatty acid transporter genes are regulated by peroxisome proliferator-activated receptor alpha and gamma activators in a tissue- and inducer-specific manner. J Biol Chem. 1998;273(27):16710–4.

111.    Kersten S, Seydoux J, Peters JM, Gonzalez FJ, Desvergne B, Wahli W. Peroxisome proliferator-activated receptor alpha mediates the adaptive response to fasting. J Clin Invest. 1999;103(11):1489–98.

112.    Leone TC, Weinheimer CJ, Kelly DP. A critical role for the peroxisome proliferator-activated receptor alpha (PPARalpha) in the cellular fasting response: the PPARalpha-null mouse as a model of fatty acid oxidation disorders. Proc Natl Acad Sci U S A. 1999;96(13):7473–8.

113.    Mascaró C, Acosta E, Ortiz JA, Marrero PF, Hegardt FG, Haro D. Control of human muscle-type carnitine palmitoyltransferase I gene transcription by peroxisome proliferator-activated receptor. J Biol Chem. 1998;273(15):8560–3.

114.    Brandt JM, Djouadi F, Kelly DP. Fatty acids activate transcription of the muscle carnitine palmitoyltransferase I gene in cardiac myocytes via the peroxisome proliferator-activated receptor alpha. J Biol Chem. 1998;273(37):23786–92.

115.     Kelly LJ, Vicario PP, Thompson GM, Candelore MR, Doebber TW, Ventre J, et al. Peroxisome proliferator-activated receptors gamma and alpha mediate in vivo regulation of uncoupling protein (UCP-1, UCP-2, UCP-3) gene expression. Endocrinology. 1998;139(12):4920–7.

116.     Tsuboyama-Kasaoka N, Takahashi M, Kim H, Ezaki O. Up-regulation of liver uncoupling protein-2 mRNA by either fish oil feeding or fibrate administration in mice. Biochem Biophys Res Commun. 1999;257(3):879–85.

117.     Wang MY, Lee Y, Unger RH. Novel form of lipolysis induced by leptin. J Biol Chem. 1999;274(25):17541–4.

118.     Schoonjans K, Watanabe M, Suzuki H, Mahfoudi A, Krey G, Wahli W, et al. Induction of the acyl-coenzyme A synthetase gene by fibrates and fatty acids is mediated by a peroxisome proliferator response element in the C promoter. J Biol Chem. 1995;270(33):19269–76.

119.     Tontonoz P, Hu E, Graves RA, Budavari AI, Spiegelman BM. mPPAR gamma 2: tissue-specific regulator of an adipocyte enhancer. Genes Dev. 1994;8(10):1224–34.

120.     Tontonoz P, Hu E, Devine J, Beale EG, Spiegelman BM. PPAR gamma 2 regulates adipose expression of the phosphoenolpyruvate carboxykinase gene. Mol Cell Biol. 1995;15(1):351–7.

121.     Martin G, Schoonjans K, Lefebvre AM, Staels B, Auwerx J. Coordinate regulation of the expression of the fatty acid transport protein and acyl-CoA synthetase genes by PPARalpha and PPARgamma activators. J Biol Chem. 1997;272(45):28210–7.

122.     PPARalpha and PPARgamma activators direct a distinct tissue-specific transcriptional response via a PPRE in the lipoprotein lipase gene. [Internet]. [citado 2018]. Disponível em: https://www.ncbi.nlm.nih.gov/pmc/articles/PMC452277/

123.     Tan NS, Michalik L, Noy N, Yasmin R, Pacot C, Heim M, et al. Critical roles of PPAR beta/delta in keratinocyte response to inflammation. Genes Dev. 2001;15(24):3263–77.

124.     Chawla A, Lee C-H, Barak Y, He W, Rosenfeld J, Liao D, et al. PPARδ is a very low-density lipoprotein sensor in macrophages. Proc Natl Acad Sci U S A. 2003;100(3):1268–73.

125.     Ito K, Carracedo A, Weiss D, Arai F, Ala U, Avigan DE, et al. A PML–PPAR-δ pathway for fatty acid oxidation regulates hematopoietic stem cell maintenance. Nat Med. 2012;18(9):1350–8.

126.     Yeo H, Lyssiotis CA, Zhang Y, Ying H, Asara JM, Cantley LC, et al. FoxO3 coordinates metabolic pathways to maintain redox balance in neural stem cells. EMBO J. 2013;32(19):2589–602.

127.     Khozoie C, Borland MG, Zhu B, Baek S, John S, Hager GL, et al. Analysis of the peroxisome proliferator-activated receptor-β/δ (PPARβ/δ) cistrome reveals novel co-regulatory role of ATF4. BMC Genomics.  2012;13:665.

128. Neschen S, Morino K, Dong J, Wang-Fischer Y, Cline GW, Romanelli AJ, et al. n-3 Fatty acids preserve insulin sensitivity in vivo in a peroxisome proliferator-activated receptor-alpha-dependent manner. Diabetes. 2007;56(4):1034–41.

129. Plutzky J. Peroxisome proliferator-activated receptors in vascular biology and atherosclerosis: emerging insights for evolving paradigms. Curr Atheroscler Rep. 2000;2(4):327–35.

130. Fruchart JC, Staels B, Duriez P. The role of fibric acids in atherosclerosis. Curr Atheroscler Rep. 2001;3(1):83–92.

131. Krey G, Braissant O, L'Horset F, Kalkhoven E, Perroud M, Parker MG, et al. Fatty acids, eicosanoids, and hypolipidemic agents identified as ligands of peroxisome proliferator-activated receptors by coactivator-dependent receptor ligand assay. Mol Endocrinol Baltim Md. 1997;11(6):779–91.

132. Volker D, Fitzgerald P, Major G, Garg M. Efficacy of fish oil concentrate in the treatment of rheumatoid arthritis. J Rheumatol. 2000;27(10):2343–6.

133. Kliewer SA, Sundseth SS, Jones SA, Brown PJ, Wisely GB, Koble CS, et al. Fatty acids and eicosanoids regulate gene expression through direct interactions with peroxisome proliferator-activated receptors alpha and gamma. Proc Natl Acad Sci U S A. 1997;94(9):4318–23.

134. Sheu S-H, Kaya T, Waxman DJ, Vajda S. Exploring the binding site structure of the PPAR gamma ligand-binding domain by computational solvent mapping. Biochemistry (Mosc). 2005;44(4):1193–209.

135. Lo Verme J, Fu J, Astarita G, La Rana G, Russo R, Calignano A, et al. The nuclear receptor peroxisome proliferator-activated receptor-alpha mediates the anti-inflammatory actions of palmitoylethanolamide. Mol Pharmacol. 2005;67(1):15–9.

136. Sethi S, Ziouzenkova O, Ni H, Wagner DD, Plutzky J, Mayadas TN. Oxidized omega-3 fatty acids in fish oil inhibit leukocyte-endothelial interactions through activation of PPAR alpha. Blood. 2002;100(4):1340–6.

137. Trombetta A, Maggiora M, Martinasso G, Cotogni P, Canuto RA, Muzio G. Arachidonic and docosahexaenoic acids reduce the growth of A549 human lung-tumor cells increasing lipid peroxidation and PPARs. Chem Biol Interact. 2007;165(3):239–50.

138. Heim M, Johnson J, Boess F, Bendik I, Weber P, Hunziker W, et al. Phytanic acid, a natural peroxisome proliferator-activated receptor (PPAR) agonist, regulates glucose metabolism in rat primary hepatocytes. FASEB J Off Publ Fed Am Soc Exp Biol. 2002;16(7):718–20.

139. Yang Z-H, Miyahara H, Iwasaki Y, Takeo J, Katayama M. Dietary supplementation with long-chain monounsaturated fatty acids attenuates obesity-related metabolic dysfunction and increases expression of PPAR gamma in adipose tissue in type 2 diabetic KK-Ay mice. Nutr Metab. 2013;10:16.

140. Dranoff G. Cytokines in cancer pathogenesis and cancer therapy. Nat Rev Cancer. 2004;4(1):11–22.

141.    Lin WW, Karin M. A cytokine-mediated link between innate immunity, inflammation, and cancer., A cytokine-mediated link between innate immunity, inflammation, and cancer. J Clin Investig J Clin Investig. 2007;117, 117(5, 5):1175, 1175–83.

142.    Jiang C, Ting AT, Seed B. PPAR-gamma agonists inhibit production of monocyte inflammatory cytokines. Nature.  1998;391(6662):82–6.

143.    Ricote M, Li AC, Willson TM, Kelly CJ, Glass CK. The peroxisome proliferator-activated receptor-gamma is a negative regulator of macrophage activation. Nature. 1998;391(6662):79–82.

144.    Daynes RA, Jones DC. Emerging roles of PPARs in inflammation and immunity. Nat Rev Immunol. 2002;2(10):748–59.

145.    Conzen SD. Minireview: nuclear receptors and breast cancer. Mol Endocrinol Baltim Md.  2008;22(10):2215–28.

146.    Menendez JA. Fine-tuning the lipogenic/lipolytic balance to optimize the metabolic requirements of cancer cell growth: molecular mechanisms and therapeutic perspectives. Biochim Biophys Acta. 2010;1801(3):381–91.

147.    Goel SK, Lalwani ND, Reddy JK. Peroxisome proliferation and lipid peroxidation in rat liver. Cancer Res. 1986;46(3):1324–30.

148.    Reddy JK, Goel SK, Nemali MR, Carrino JJ, Laffler TG, Reddy MK, et al. Transcription regulation of peroxisomal fatty acyl-CoA oxidase and enoyl-CoA hydratase/3-hydroxyacyl-CoA dehydrogenase in rat liver by peroxisome proliferators. Proc Natl Acad Sci U S A.  1986;83(6):1747–51.

149.    Furuta S, Miyazawa S, Hashimoto T. Biosynthesis of enzymes of peroxisomal beta-oxidation. J Biochem (Tokyo). 1982;92(2):319–26.

150.    Amirkhizi F, Siassi F, Djalali M, Shahraki SH. Impaired enzymatic antioxidant defense in erythrocytes of women with general and abdominal obesity. Obes Res Clin Pract. 2014;8(1):e26-34.

151.    Yeldandi AV, Rao MS, Reddy JK. Hydrogen peroxide generation in peroxisome proliferator-induced oncogenesis. Mutat Res.  2000;448(2):159–77.

152.    Chu S, Huang Q, Alvares K, Yeldandi AV, Rao MS, Reddy JK. Transformation of mammalian cells by overexpressing H2O2-generating peroxisomal fatty acyl-CoA oxidase. Proc Natl Acad Sci U S A.  1995;92(15):7080–4.

153.    Wang D, Wang H, Guo Y, Ning W, Katkuri S, Wahli W, et al. Crosstalk between peroxisome proliferator-activated receptor delta and VEGF stimulates cancer progression. Proc Natl Acad Sci U S A.  2006;103(50):19069–74.

154.    Vara JÁF, Casado E, de Castro J, Cejas P, Belda-Iniesta C, González-Barón M. PI3K/Akt signalling pathway and cancer. Cancer Treat Rev.  2004;30(2):193–204.

155.    Piqueras L, Reynolds AR, Hodivala-Dilke KM, Alfranca A, Redondo JM, Hatae T, et al. Activation of PPARbeta/delta induces endothelial cell proliferation and angiogenesis. Arterioscler Thromb Vasc Biol. 2007;27(1):63–9.

156. Yin Y, Russell RG, Dettin LE, Bai R, Wei Z-L, Kozikowski AP, et al. Peroxisome proliferator-activated receptor delta and gamma agonists differentially alter tumor differentiation and progression during mammary carcinogenesis. Cancer Res. 2005;65(9):3950–7.

157. Stephen RL, Gustafsson MCU, Jarvis M, Tatoud R, Marshall BR, Knight D, et al. Activation of peroxisome proliferator-activated receptor delta stimulates the proliferation of human breast and prostate cancer cell lines. Cancer Res. 2004;64(9):3162–70.

158. Girroir EE, Hollingshead HE, Billin AN, Willson TM, Robertson GP, Sharma AK, et al. Peroxisome proliferator-activated receptor-β/δ (PPARβ/δ) ligands inhibit growth of UACC903 and MCF7 human cancer cell lines. Toxicology. 2008;243(1–2):236–43.

159. Grommes C, Landreth GE, Heneka MT. Antineoplastic effects of peroxisome proliferator-activated receptor gamma agonists. Lancet Oncol. Julho de 2004;5(7):419–29.

160. Theocharis S, Margeli A, Vielh P, Kouraklis G. Peroxisome proliferator-activated receptor-gamma ligands as cell-cycle modulators. Cancer Treat Rev. 2004;30(6):545–54.

161. Chen GG, Lee JFY, Wang SH, Chan UPF, Ip PC, Lau WY. Apoptosis induced by activation of peroxisome-proliferator activated receptor-gamma is associated with Bcl-2 and NF-kappaB in human colon cancer. Life Sci. 2002;70(22):2631–46.

162. Yin F, Wakino S, Liu Z, Kim S, Hsueh WA, Collins AR, et al. Troglitazone inhibits growth of MCF-7 breast carcinoma cells by targeting G1 cell cycle regulators. Biochem Biophys Res Commun. 2001;286(5):916–22.

163. Clay CE, Namen AM, Atsumi G, Willingham MC, High KP, Kute TE, et al. Influence of J series prostaglandins on apoptosis and tumorigenesis of breast cancer cells. Carcinogenesis. 1999;20(10):1905–11.

164. Rey F, Alves E, Melo T, Domingues P, Queiroga H, Rosa R, et al. Unravelling polar lipids dynamics during embryonic development of two sympatric brachyuran crabs (Carcinus maenas and Necora puber) using lipidomics. Sci Rep. 2015;5:14549.

165. Kamikawa A, Ichii O, Yamaji D, Imao T, Suzuki C, Okamatsu-Ogura Y, et al. Diet-induced obesity disrupts ductal development in the mammary glands of nonpregnant mice. Dev Dyn. 238(5):1092–9.

166. Nutritional Comparison: Lard vs Oil, cocoa butter [Internet]. [citado 2018]. Disponível em: https://skipthepie.org/fats-and-oils/lard/compared-to/oil-cocoa-butter/

167. Prieur X, Mok CYL, Velagapudi VR, Núñez V, Fuentes L, Montaner D, et al. Differential lipid partitioning between adipocytes and tissue macrophages modulates macrophage lipotoxicity and M2/M1 polarization in obese mice. Diabetes. 2011;60(3):797–809.

168. Pamplona R, Portero-Otín M, Riba D, Ruiz C, Prat J, Bellmunt MJ, et al. Mitochondrial membrane peroxidizability index is inversely related to maximum life span in mammals. J Lipid Res. 1998;39(10):1989–94.

169. Vaca CE, Fang JL, Mutanen M, Valsta L. 32P-postlabelling determination of DNA adducts of malonaldehyde in humans: total white blood cells and breast tissue. Carcinogenesis. 1995;16(8):1847–51.

170. Wang M, Dhingra K, Hittelman WN, Liehr JG, de Andrade M, Li D. Lipid peroxidation-induced putative malondialdehyde-DNA adducts in human breast tissues. Cancer Epidemiol Biomark Prev Publ Am Assoc Cancer Res Cosponsored Am Soc Prev Oncol. 1996;5(9):705–10.

171. Badawi AF, El-Sohemy A, Stephen LL, Ghoshal AK, Archer MC. The effect of dietary n-3 and n-6 polyunsaturated fatty acids on the expression of cyclooxygenase 1 and 2 and levels of p21ras in rat mammary glands. Carcinogenesis. 1998;19(5):905–10.

172. Armoni M, Harel C, Bar-Yoseph F, Milo S, Karnieli E. Free fatty acids repress the GLUT4 gene expression in cardiac muscle via novel response elements. J Biol Chem. 2005;280(41):34786–95.

173. Kawashima A, Harada T, Imada K, Yano T, Mizuguchi K. Eicosapentaenoic acid inhibits interleukin-6 production in interleukin-1beta-stimulated C6 glioma cells through peroxisome proliferator-activated receptor-gamma. Prostaglandins Leukot Essent Fatty Acids. 2008;79(1–2):59–65.

174. Thoennes SR, Tate PL, Price TM, Kilgore MW. Differential transcriptional activation of peroxisome proliferator-activated receptor gamma by omega-3 and omega-6 fatty acids in MCF-7 cells. Mol Cell Endocrinol. 2000;160(1–2):67–73.

175. Imai T, Takakuwa R, Marchand S, Dentz E, Bornert J-M, Messaddeq N, et al. Peroxisome proliferator-activated receptor γ is required in mature white and brown adipocytes for their survival in the mouse. Proc Natl Acad Sci. 2004;101(13):4543–7.

176. Barak Y, Nelson MC, Ong ES, Jones YZ, Ruiz-Lozano P, Chien KR, et al. PPARγ Is Required for Placental, Cardiac, and Adipose Tissue Development. Mol Cell. 1999;4(4):585–95.

177. Sun K, Kusminski CM, Scherer PE. Adipose tissue remodeling and obesity. J Clin Invest. 2011;121(6):2094–101.

178. Gorla-Bajszczak A, Siegrist-Kaiser C, Boss O, Burger AG, Meier CA. Expression of peroxisome proliferator-activated receptors in lean and obese Zucker rats. Eur J Endocrinol. 2000;142(1):71–8.

179. Vidal-Puig AJ, Considine RV, Jimenez-Liñan M, Werman A, Pories WJ, Caro JF, et al. Peroxisome proliferator-activated receptor gene expression in human tissues. Effects of obesity, weight loss, and regulation by insulin and glucocorticoids. J Clin Invest. 1997;99(10):2416–22.

180. Badawi AF, Badr MZ. Expression of cyclooxygenase-2 and peroxisome proliferator-activated receptor-gamma and levels of prostaglandin E2 and 15-deoxy-delta12,14-prostaglandin J2 in human breast cancer and metastasis. Int J Cancer. 2003;103(1):84–90.

181. Auwerx J, Cock T-A, Knouff C. PPAR-γ: a thrifty transcription factor. Nucl Recept Signal [Internet]. 2003; 1. Disponível em: https://www.ncbi.nlm.nih.gov/pmc/articles/PMC1402226/

182. Wolczyk D, Zaremba-Czogalla M, Hryniewicz-Jankowska A, Tabola R, Grabowski K, Sikorski AF, et al. TNF-α promotes breast cancer cell migration and enhances the

concentration of membrane-associated proteases in lipid rafts. Cell Oncol Dordr. 2016;39(4):353–63.

183. Li K, Wei L, Huang Y, Wu Y, Su M, Pang X, et al. Leptin promotes breast cancer cell migration and invasion via IL-18 expression and secretion. Int J Oncol. 2016;48(6):2479–87.

184. Lee JO, Kim N, Lee HJ, Lee YW, Kim SJ, Park SH, et al. Resistin, a fat-derived secretory factor, promotes metastasis of MDA-MB-231 human breast cancer cells through ERM activation. Sci Rep. 2016;6:18923.

185. Pawar A, Jump DB. Unsaturated Fatty Acid Regulation of Peroxisome Proliferator-activated Receptor α Activity in Rat Primary Hepatoctes. J Biol Chem. 2003;278(38):35931–9.

186. Suchanek KM, May FJ, Robinson JA, Lee WJ, Holman NA, Monteith GR, et al. Peroxisome proliferator–activated receptor α in the human breast cancer cell lines MCF-7 and MDA-MB-231. Mol Carcinog. 2002;34(4):165–71.

187. López-Bascón MA, Calderón-Santiago M, Sánchez-Ceinos J, Fernández-Vega A, Guzmán-Ruiz R, López-Miranda J, et al. Influence of sample preparation on lipidomics analysis of polar lipids in adipose tissue. Talanta. 2018;177:86–93.

188. He D, Mustafi D, Fan X, Fernandez S, Markiewicz E, Zamora M, et al. Magnetic resonance spectroscopy detects differential lipid composition in mammary glands on low fat, high animal fat versus high fructose diets. PLOS ONE. 2018;13(1):e0190929.

189. Fonseca-Alaniz MH, Takada J, Alonso-Vale MIC, Lima FB. Adipose tissue as an endocrine organ: from theory to practice. J Pediatr (Rio J). 2007;83(5 Suppl):S192-203.

190. Furukawa S, Fujita T, Shimabukuro M, Iwaki M, Yamada Y, Nakajima Y, et al. Increased oxidative stress in obesity and its impact on metabolic syndrome. J Clin Invest. 2004;114(12):1752–61.

191. Murdolo G, Piroddi M, Luchetti F, Tortoioli C, Canonico B, Zerbinati C, et al. Oxidative stress and lipid peroxidation by-products at the crossroad between adipose organ dysregulation and obesity-linked insulin resistance. Biochimie. 2013;95(3):585–94.

192. Marnett LJ. Oxy radicals, lipid peroxidation and DNA damage. Toxicology. 2002;181–182:219–22.

193. Body DR. The lipid composition of adipose tissue. Prog Lipid Res. 1988;27(1):39–60.

194. Sok M, Sentjurc M, Schara M, Stare J, Rott T. Cell membrane fluidity and prognosis of lung cancer. Ann Thorac Surg. 2002;73(5):1567–71.

195. Pietiläinen KH, Róg T, Seppänen-Laakso T, Virtue S, Gopalacharyulu P, Tang J, et al. Association of Lipidome Remodeling in the Adipocyte Membrane with Acquired Obesity in Humans. PLOS Biol. 2011;9(6):e1000623.

196. Yea K, Kim J, Yoon JH, Kwon T, Kim JH, Lee BD, et al. Lysophosphatidylcholine activates adipocyte glucose uptake and lowers blood glucose levels in murine models of diabetes. J Biol Chem. 2009;284(49):33833–40.

197.     Samad F, Hester KD, Yang G, Hannun YA, Bielawski J. Altered Adipose and Plasma Sphingolipid Metabolism in Obesity: A Potential Mechanism for Cardiovascular and Metabolic Risk. Diabetes. 2006;55(9):2579–87.

198.     Błachnio-Zabielska AU, Pułka M, Baranowski M, Nikołajuk A, Zabielski P, Górska M, et al. Ceramide metabolism is affected by obesity and diabetes in human adipose tissue. J Cell Physiol. 2012;227(2):550–7.

199.     Jiang W, Ogretmen B. Ceramide stress in survival versus lethal autophagy paradox: ceramide targets autophagosomes to mitochondria and induces lethal mitophagy. Autophagy. 2013;9(2):258–9.

200.     Truman J-P, García-Barros M, Obeid LM. "Evolving concepts in cancer therapy through targeting sphingolipid metabolism". Biochim Biophys Acta. Agosto de 2014;1841(8):1174–88.

201.     Beckham TH, Lu P, Jones EE, Marrison T, Lewis CS, Cheng JC, et al. LCL124, a Cationic Analog of Ceramide, Selectively Induces Pancreatic Cancer Cell Death by Accumulating in Mitochondria. J Pharmacol Exp Ther. 2013;344(1):167–78.

202.     Hou Q, Jin J, Zhou H, Novgorodov SA, Bielawska A, Szulc ZM, et al. Mitochondrially targeted ceramides preferentially promote autophagy, retard cell growth, and induce apoptosis. J Lipid Res. 2011;52(2):278–88.

203.     Ling B, Chen L, Alcorn J, Ma B, Yang J. Sphingosine-1-phosphate: a potential therapeutic agent against human breast cancer. Invest New Drugs. 2011;29(2):396–9.

204.     Vance JE. Phosphatidylserine and phosphatidylethanolamine in mammalian cells: two metabolically related aminophospholipids. J Lipid Res. 2008;49(7):1377–87.

205.     van den Brink-van der Laan E, Killian JA, de Kruijff B. Nonbilayer lipids affect peripheral and integral membrane proteins via changes in the lateral pressure profile. Biochim Biophys Acta. 2004;1666(1–2):275–88.

206.     Maeba R, Ueta N. A novel antioxidant action of ethanolamine plasmalogens in lowering the oxidizability of membranes. Biochem Soc Trans. 2004;32(1):141–3.

207.     Zoeller RA, Lake AC, Nagan N, Gaposchkin DP, Legner MA, Lieberthal W. Plasmalogens as endogenous antioxidants: somatic cell mutants reveal the importance of the vinyl ether. Biochem J. 1999;338 ( Pt 3):769–76.

208.     Stark G. Functional consequences of oxidative membrane damage. J Membr Biol. 2005;205(1):1–16.

# 12. Supplementary information

## 12.1 Diets

**Description**
Rodent Diet with 10% kcal% fat.

**Used in Research**
Obesity
Diabetes

**Packaging**
Product is packed in 12.5 kg box.
Each box is identified with the
product name, description, lot
number and expiration date.

**Lead Time**
D12450H in 5-7 business days.

**Gamma-Irradiation**
D12450Hi available on request.
Add 10 days to delivery time.

**Form**
Pellet, Powder, Liquid

**Shelf Life**
Most diets require storage in a cool
dry environment. Stored correctly
they should last 6 months.

**Control Diets**
Used as a control diet for D12451

**Sucrose Content**
D12451 Match
17% Sucrose

## Formula

| Product #D12450H | | gm% | kcal% |
|---|---|---|---|
| Protein | | 19.2 | 20 |
| Carbohydrate | | 67.3 | 70 |
| Fat | | 4.3 | 10 |
| | Total | | 100 |
| | kcal/gm | 3.85 | |

| Ingredient | gm | kcal |
|---|---|---|
| Casein, 30 Mesh | 200 | 800 |
| L-Cystine | 3 | 12 |
| Corn Starch | 452.2 | 1808.8 |
| Maltodextrin 10 | 75 | 300 |
| Sucrose | 172.8 | 691.2 |
| Cellulose, BW200 | 50 | 0 |
| Soybean Oil | 25 | 225 |
| Lard* | 20 | 180 |
| Mineral Mix S10026 | 10 | 0 |
| DiCalcium Phosphate | 13 | 0 |
| Calcium Carbonate | 5.5 | 0 |
| Potassium Citrate, 1 H2O | 16.5 | 0 |
| Vitamin Mix V10001 | 10 | 40 |
| Choline Bitartrate | 2 | 0 |
| FD&C Yellow Dye #5 | 0.04 | 0 |
| FD&C Red Dye #40 | 0.01 | 0 |
| **Total** | **1055.05** | **4057** |

*Typical analysis of cholesterol in lard = 0.72 mg/gram.
Cholesterol (mg)/4057 kcal = 54.4
Cholesterol (mg)/kg = 51.6

*Figure C.1 – Data sheet from the normal diet*

## Description

High fat rodent diet with 1.25% cholesterol.

## Used in Research

Atherosclerosis
Often used with Apo E or LDLR knockout mice

## Replaces

D12108 with used alcohol-extracted casein, which is not believed to be important in inducing an athero phenotype.

## Packaging

Product is packed in 12.5 kg box. Each box is identified with the product name, description, lot number and expiration date.

## Lead Time

D12108C in 5-7 business days.

## Gamma-Irradiation

D12108C1 available on request. Add 10 days to delivery time.

## Form

Pellet, Powder

## Shelf Life

Most diets require storage in a cool dry environment. Stored correctly they should last 6 months. Because of the high fat content is best if kept frozen.

## Formula

| Product # D12108C | | gm% | kcal% |
|---|---|---|---|
| Protein | | 23 | 20 |
| Carbohydrate | | 45 | 40 |
| Fat | | 20 | 40 |
| | Total | | 100 |
| | kcal/gm | 4.5 | |

| Ingredient | gm | kcal |
|---|---|---|
| Casein, 30 Mesh | 200 | 800 |
| L-Cystine | 3 | 12 |
| Corn Starch | 212 | 848 |
| Maltodextrin 10 | 71 | 284 |
| Sucrose | 113 | 452 |
| Cellulose, BW200 | 50 | 0 |
| Soybean Oil | 25 | 225 |
| Cocoa Butter | 155 | 1395 |
| Mineral Mix S10021 | 10 | 0 |
| Dicalcium Phosphate | 13 | 0 |
| Calcium Carbonate | 5.5 | 0 |
| Potassium Citrate | 16.5 | 0 |
| Vitamin Mix V10001 | 10 | 40 |
| Choline Bitartrate | 2 | 0 |
| Cholesterol | 11.25 | 0 |
| Blue Dye, FD&C #1 | 0.05 | 0 |
| Yellow Dye, FD&C #5 | 0.05 | 0 |
| Red Dye, FD&C #40 | 0 | 0 |
| Total | 897.35 | 4056 |

*Figure C.2 – Data sheet for the High Cholesterol Diet*

**Description**
Rodent Diet with 45% kcal% fat.

**Used in Research**
Fatty Liver
Inflammation
Obesity
Diabetes

**Packaging**
Product is packed in 12.5 kg box. Each box is identified with the product name, description, lot number and expiration date.

**Lead Time**
D12451 IN-STOCK.
Ready for next day shipment.

**Gamma-Irradiation**
D12451i available on request. Add 10 days to delivery time.

**Form**
Pellet, Powder, Liquid

**Shelf Life**
Most diets require storage in a cool dry environment. Stored correctly they should last 6 months.

**Control Diets**
D12450B, D12450H, D12450K

## Formula

| Product #D12451 | gm% | kcal% |
|---|---|---|
| Protein | 24 | 20 |
| Carbohydrate | 41 | 35 |
| Fat | 24 | 45 |
| Total | | 100 |
| Total kcal/gm | 4.73 | |

| Ingredient | gm | kcal |
|---|---|---|
| Casein, 30 Mesh | 200 | 800 |
| L-Cystine | 3 | 12 |
| Corn Starch | 72.8 | 291 |
| Maltodextrin 10 | 100 | 400 |
| Sucrose | 172.8 | 691 |
| Cellulose, BW200 | 50 | 0 |
| Soybean Oil | 25 | 225 |
| Lard* | 177.5 | 1598 |
| Mineral Mix S10026 | 10 | 0 |
| DiCalcium Phosphate | 13 | 0 |
| Calcium Carbonate | 5.5 | 0 |
| Potassium Citrate, 1 H2O | 16.5 | 0 |
| Vitamin Mix V10001 | 10 | 40 |
| Choline Bitartrate | 2 | 0 |
| FD&C Red Dye #40 | 0.05 | 0 |
| **Total** | **858.16** | **4057** |

Formulated by E. A. Ulman, Ph.D., Research Diets, Inc., 8/26/98 and 3/11/99.

*Typical analysis of cholesterol in lard - 0.72 mg/gram.
Cholesterol (mg)/4057 kcal - 167.8
Cholesterol (mg)/kg - 195.5

*Figure C.3 – Data sheet from High Fat Diet*

## 12.2 Phospholipids identified in LC-MS and LC-MS/MS

*Table C.1 - LC-MS- and MS/MS-based identification of the phospholipid molecular species that were quantified in the present study in the positive ion mode. PLs – phospholipids; FA – fatty acids; RT – retention time*

| Class | nr. | PLs | FAs composition | m/z tab. | m/z obs. | RT |
|---|---|---|---|---|---|---|
| **PE** | 1 | PE(30:3) | | 658.4450 | 658.4430 | 4.54 |
| | 2 | PE(32:0) | | 692.5230 | 692.5212 | 4.31 |
| | 3 | PE(32:1) | | 690.5070 | 690.5069 | 4.49 |
| | 4 | PE(32:4) | | 684.4600 | 684.4621 | 4.12 |
| | 5 | PE(34:1) | PE(18:1/16:0) | 718.5390 | 718.5367 | 4.37 |
| | 6 | PE(34:2) | PE(18:2/16:0) PE(18:1/16:1) | 716.5230 | 716.5203 | 4.54 |
| | 7 | PE(34:3) | PE(16:1/18:2) | 714.5070 | 714.5084 | 4.41 |
| | 8 | PE(34:4) | | 712.4920 | 712.4955 | 4.31 |
| | 9 | PE(34:6) | | 708.4600 | 708.4594 | 4.48 |
| | 10 | PE(36:4) | | 740.5230 | 740.5230 | 4.30 |

| | | | | | |
|---|---|---|---|---|---|
| 11 | PE(38:1) | PE(20:0/18:1) PE(20:1/18:0) | 774.6010 | 774.5976 | 3.67 |
| 12 | PE(38:4) | PE(20:4/18:0) | 768.5540 | 768.5541 | 4.26 |
| 13 | PE(38:5) | PE(20:4/18:1) | 766.5390 | 766.5376 | 5.47 |
| 14 | PE(38:6) | | 764.5230 | 764.5235 | 4.30 |
| 15 | PE(38:8) | | 760.4920 | 760.4904 | 4.68 |
| 16 | PE(40:4) | PE(18:2/22:2) PE(18:3/22:1) PE(18:0/22:4) | 796.5800 | 796.5839 | 4.09 |
| 17 | PE(40:5) | PE(18:1/22:4) | 794.5700 | 794.5687 | 4.17 |
| 18 | PE(40:6) | | 792.5540 | 792.5554 | 4.19 |
| 19 | PE(40:8) | PE(18:2/22:6) PE(18:3/22:5) | 788.5230 | 788.5212 | 4.22 |
| 20 | PE(40:9) | | 786.5070 | 786.5034 | 4.28 |
| 21 | PE(40:10) | | 784.4920 | 784.4900 | 4.88 |
| 22 | PE(42:5) | | 822.6010 | 822.6021 | 3.98 |
| 23 | PE(42:9) | | 814.5390 | 814.5352 | 4.20 |
| 24 | PE(42:10) | | 812.5230 | 812.5206 | 4.22 |
| 25 | PE(44:10) | | 840.5540 | 840.5513 | 4.21 |
| 26 | PE(P-34:1) | | 702.5440 | 702.5454 | 4.79 |
| 27 | PE(P-34:2) | | 700.5280 | 700.5287 | 4.36 |
| 28 | PE(P-36:1) | | 730.5750 | 730.5721 | 4.44 |
| 29 | PE(P-36:2) | | 728.5590 | 728.5593 | 4.32 |
| 30 | PE(P-36:3) | | 726.5440 | 726.5404 | 5.10 |
| 31 | PE(P-38:1) | | 758.6060 | 758.6043 | 3.70 |
| 32 | PE(P-38:2) | | 756.5910 | 756.5887 | 4.31 |
| 33 | PE(P-38:4) | | 752.5590 | 752.5622 | 3.95 |
| 34 | PE(P-38:5) | | 750.5440 | 750.5429 | 4.33 |
| 35 | PE(P-40:1) | | 786.6380 | 786.6396 | 3.00 |
| 36 | PE(P-40:3) | | 782.6060 | 782.6027 | 3.98 |
| 37 | PE(P-40:4) | | 780.5910 | 780.5900 | 4.25 |
| 38 | PE(P-40:5) | | 778.5750 | 778.5752 | 4.16 |
| 39 | PE(P-40:7) | | 774.5440 | 774.5423 | 4.20 |
| 40 | PEo(36:5) | | 724.5280 | 724.5276 | 4.30 |
| 41 | PEo(38:3) | | 756.5910 | 756.5887 | 4.31 |
| 42 | PEo(38:5) | | 752.5590 | 752.5622 | 3.95 |
| 43 | PEo(38:8) | | 746.5130 | 746.5111 | 4.32 |
| 44 | PEo(40:2) | | 786.6380 | 786.6396 | 3.00 |
| 45 | PEo(40:4) | | 782.6060 | 782.6027 | 3.98 |
| 46 | PEo(40:6) | | 778.5750 | 778.5752 | 4.16 |
| 47 | PEo(40:7) | | 776.5590 | 776.5612 | 2.84 |
| 48 | PEo(40:8) | | 774.5440 | 774.5423 | 4.20 |
| 49 | PEo(40:9) | | 772.5280 | 772.5253 | 4.20 |
| 50 | PEo(40:10) | | 770.5130 | 770.5103 | 4.36 |
| **LPE** 51 | LPE(14:0) | LPE(14:0) | 426.2614 | 426.2620 | 5.44 |

| | | | | | | |
|---|---|---|---|---|---|---|
| | 52 | LPE(16:1) | LPE(16:1) | 452.2777 | 452.2777 | 5.37 |
| | 53 | LPE(18:0) | LPE(18:0) | 482.3247 | 482.3246 | 5.23 |
| | 54 | LPE(18:1) | LPE(18:1) | 480.3091 | 480.3090 | 5.24 |
| | 55 | LPE(18:2) | LPE(18:2) | 478.2929 | 478.2933 | 5.18 |
| | 56 | LPE(20:0) | LPE(20:0) | 510.3563 | 510.3559 | 4.18 |
| | 57 | LPE(20:1) | LPE(20:1) | 508.3404 | 508.3403 | 3.92 |
| | 58 | LPE(20:2) | LPE(20:2) | 506.3252 | 506.3246 | 4.84 |
| | 59 | LPE(20:4) | LPE(20:4) | 502.2931 | 502.2933 | 5.16 |
| | 60 | LPE(22:1) | LPE(22:1) | 536.3718 | 536.3716 | 5.26 |
| | 61 | LPE(22:2) | LPE(22:2) | 534.3564 | 534.3559 | 4.36 |
| | 62 | LPE(22:4) | LPE(22:4) | 530.3241 | 530.3246 | 4.90 |
| | 63 | LPE(22:6) | LPE(22:6) | 526.2927 | 526.2933 | 5.10 |
| | 64 | LPE(24:3) | LPE(24:3) | 560.3728 | 560.3716 | 4.51 |
| | 65 | LPE(O-16:0) | LPE(O-16:0) | 440.3141 | 440.3141 | 5.54 |
| | 66 | LPE(O-18:0) | LPE(O-18:0) | 468.3457 | 466.3304 | 5.57 |
| | 67 | LPE(P-16:0) | LPE(P-16:0) | 438.2979 | 436.2836 | 5.21 |
| | 68 | LPE(P-18:0) | LPE(P-18:0) | 466.3298 | 466.3297 | 5.10 |
| | 69 | LPE(P-20:0) | LPE(P-20:0) | 494.3607 | 494.3611 | 5.10 |
| **PC** | 70 | PC(30:0) | PC(14:0/16:0) | 706.5389 | 706.5390 | 9.98 |
| | 71 | PC(30:1) | PC(14:0/16:1) | 704.5243 | 704.5230 | 10.50 |
| | 72 | PC(32:0) | PC(16:0/16:0) | 734.5710 | 734.5700 | 9.83 |
| | 73 | PC(32:1) | PC(16:0/16:1) | 732.5531 | 732.5540 | 10.26 |
| | 74 | PC(32:2) | PC(14:0/18:2) PC(16:1/16:1) | 730.5382 | 730.5390 | 9.71 |
| | 75 | PC(34:0) | | 762.5986 | 762.6010 | 10.82 |
| | 76 | PC(34:1) | PC(16:0/18:1) | 760.5854 | 760.5860 | 9.66 |
| | 77 | PC(34:2) | PC(16:0/18:2) | 758.5699 | 758.5700 | 9.49 |
| | 78 | PC(34:3) | PC(16:1/18:3) | 756.5537 | 756.5540 | 9.71 |
| | 79 | PC(34:4) | PC(14:0/20:4) | 754.5388 | 754.5390 | 9.63 |
| | 80 | PC(36:2) | PC(18:0/18:2) | 786.6011 | 786.6010 | 9.38 |
| | 81 | PC(36:3) | PC(18:1/18:2) PC(16:0/20:3) | 784.5854 | 784.5860 | 9.38 |
| | 82 | PC(36:4) | PC(16:0/20:4) PC(18:2/18:2) | 782.5693 | 782.5700 | 9.00 |
| | 83 | PC(36:5) | PC(16:1/20:4) | 780.5521 | 780.5540 | 9.51 |
| | 84 | PC(36:6) | | 778.5383 | 778.5390 | 9.31 |
| | 85 | PC(38:2) | | 814.6317 | 814.6330 | 9.09 |
| | 86 | PC(38:3) | | 812.6143 | 812.6170 | 9.04 |
| | 87 | PC(38:4) | | 810.6024 | 810.6010 | 8.97 |
| | 88 | PC(38:5) | | 808.5845 | 808.5860 | 8.92 |
| | 89 | PC(38:6) | PC(16:0/20:6) PC(18:2/20:4) | 806.5699 | 806.5700 | 8.92 |
| | 90 | PC(38:7) | PC(16:1/22:6) PC(20:4/18:3) | 804.5523 | 804.5540 | 9.03 |
| | 91 | PC(38:8) | PC(18:1/20:5) PC(18:2/20:4) | 802.5358 | 802.5390 | 9.02 |
| | 92 | PC(40:1) | | 844.6803 | 844.6800 | 8.93 |

| 93 | PC(40:4) | | 838.6309 | 838.6330 | 8.90 |
|---|---|---|---|---|---|
| 94 | PC(40:5) | | 836.6157 | 836.6170 | 8.83 |
| 95 | PC(40:6) | | 834.6019 | 834.6010 | 8.72 |
| 96 | PC(40:7) | | 832.5843 | 832.5860 | 8.81 |
| 97 | PC(40:8) | | 830.5683 | 830.5700 | 8.75 |
| 98 | PC(40:9) | | 828.5524 | 828.5540 | 8.77 |
| 99 | PC(40:10) | | 826.5378 | 826.5390 | 8.84 |
| 100 | PC(42:1) | PC(18:1/24:0) | 872.7106 | 872.7110 | 8.86 |
| 101 | PC(42:2) | | 870.6973 | 870.6950 | 8.85 |
| 102 | PC(42:5) | | 864.4692 | 864.6480 | 8.70 |
| 103 | PC(42:6) | | 862.6324 | 862.6330 | 8.74 |
| 104 | PC(42:7) | | 860.6150 | 860.6170 | 8.66 |
| 105 | PC(42:8) | | 858.5979 | 858.6010 | 8.67 |
| 106 | PC(42:9) | | 856.5832 | 856.5860 | 8.64 |
| 107 | PC(42:10) | | 854.5696 | 854.5700 | 8.61 |
| 108 | PC(42:11) | | 852.5516 | 852.5540 | 8.63 |
| 109 | PC(44:4) | | 894.6995 | 894.6950 | 8.49 |
| 110 | PC(44:8) | | 886.6307 | 886.6330 | 8.54 |
| 111 | PC(44:10) | PC(20:4/22:6) | 882.5996 | 882.6010 | 8.56 |
| 112 | PC(44:11) | | 880.5833 | 880.5860 | 8.51 |
| 113 | PC(44:12) | | 878.5698 | 878.5700 | 8.43 |
| 114 | PC(O-30:0) | | 692.5599 | 692.5590 | 10.20 |
| 115 | PC(P-30:0) | | 690.5446 | 690.5440 | 9.91 |
| 116 | PC(O-32:0) | | 720.5905 | 720.5910 | 10.16 |
| 117 | PC(P-32:0) | | 718.5753 | 718.5750 | 9.92 |
| 118 | PC(P-34:0) | | 746.6062 | 746.6060 | 9.82 |
| 119 | PC(P-34:1) | | 744.5885 | 744.5910 | 10.20 |
| 120 | PC(P-34:2) | | 742.5737 | 742.5750 | 9.50 |
| 121 | PC(P-34:3) | | 740.5573 | 740.5590 | 9.85 |
| 122 | PC(P-36:0) | | 774.6387 | 774.6380 | 9.75 |
| 123 | PC(P-36:2) | | 770.6038 | 770.6060 | 9.49 |
| 124 | PC(P-36:3) | | 768.5897 | 768.5910 | 9.38 |
| 125 | PC(P-36:4) | | 766.5757 | 766.5750 | 8.93 |
| 126 | PC(P-38:3) | | 796.6198 | 796.6220 | 9.14 |
| 127 | PC(P-38:4) | | 794.6056 | 794.6060 | 9.07 |
| 128 | PC(P-38:5) | | 792.5911 | 792.5910 | 8.96 |
| 129 | PC(P-40:3) | | 824.6523 | 824.6530 | 9.06 |
| 130 | PC(P-40:4) | | 822.6359 | 822.6380 | 9.08 |
| 131 | PC(P-40:5) | | 820.6202 | 820.6220 | 8.96 |
| 132 | PC(P-42:3) | | 852.6830 | 852.6850 | 8.79 |
| 133 | PC(P-42:4) | | 850.6680 | 850.6700 | 8.92 |

| | | | | | | |
|---|---|---|---|---|---|---|
| | 134 | PC(P-42:5) | | 848.6527 | 848.6530 | 8.97 |
| | 135 | PC(P-32:1) | | 716.5586 | 716.5590 | 9.63 |
| | 136 | PC(P-36:5) | | 764.5602 | 764.5590 | 9.06 |
| | 137 | PC(P-38:6) | | 790.5749 | 790.5750 | 8.70 |
| | 138 | PC(P-40:6) | | 818.6048 | 818.6060 | 8.88 |
| | 139 | PC(P-44:6) | | 874.6690 | 874.6690 | 8.90 |
| **SM** | 140 | SM(d32:1) | | 675.5444 | 675.5441 | 11.93 |
| | 141 | SM(d32:2) | | 673.5288 | 673.5284 | 11.90 |
| | 142 | SM(d34:0) | | 705.5900 | 705.5910 | 11.25 |
| | 143 | SM(d34:1) | SM(d18:1/16:0) | 703.5748 | 703.5754 | 11.68 |
| | 144 | SM(d34:2) | | 701.5591 | 701.5597 | 11.69 |
| | 145 | SM(d36:0) | | 733.6219 | 733.6223 | 11.19 |
| | 146 | SM(d36:1) | | 731.6065 | 731.6067 | 11.41 |
| | 147 | SM(d36:2) | | 729.5916 | 729.5910 | 11.75 |
| | 148 | SM(d36:3) | | 727.5735 | 727.5754 | 11.28 |
| | 149 | SM(d38:1) | | 759.6378 | 759.6380 | 11.20 |
| | 150 | SM(d38:2) | | 757.6219 | 757.6223 | 11.17 |
| | 151 | SM(d38:3) | | 755.6041 | 755.6067 | 11.20 |
| | 152 | SM(d40:1) | SM(d18:1/22:0) | 787.6691 | 787.6693 | 10.97 |
| | 153 | SM(d40:2) | | 785.6535 | 785.6536 | 10.93 |
| | 154 | SM(d40:3) | | 73.6370 | 783.6380 | 11.06 |
| | 155 | SM(d42:1) | | 815.6996 | 815.7006 | 10.72 |
| | 156 | SM(d42:2) | SM(d18:1/24:1) | 813.6850 | 813.6849 | 10.81 |
| | 157 | SM(d42:3) | | 811.6686 | 811.6693 | 10.83 |
| | 158 | SM(d44:1) | | 843.7311 | 843.7319 | 10.51 |
| | 159 | SM(d44:2) | | 841.7157 | 841.7162 | 10.62 |
| **Cer** | 160 | Cer(d20:1) | | 342.3003 | 342.3008 | 3.19 |
| | 161 | Cer(d32:1) | | 510.4885 | 510.4886 | 3.34 |
| | 162 | Cer(d34:1) | | 538.5201 | 538.5199 | 3.34 |
| | 163 | Cer(d34:2) | | 536.5044 | 536.5043 | 3.35 |
| | 164 | Cer(d36:1) | | 566.5506 | 566.5512 | 3.33 |
| | 165 | Cer(d36:2) | | 564.5354 | 564.5356 | 3.33 |
| | 166 | Cer(d38:1) | | 594.5814 | 594.5825 | 3.13 |
| | 167 | Cer(d38:2) | | 592.5675 | 592.5669 | 3.25 |
| | 168 | Cer(d40:1) | | 622.6133 | 622.6138 | 3.32 |
| | 169 | Cer(d40:2) | | 620.5980 | 620.5982 | 3.32 |
| | 170 | Cer(d42:1) | | 650.6420 | 650.6451 | 3.37 |
| | 171 | Cer(d42:2) | | 648.6291 | 648.6295 | 3.34 |
| **LPC** | 172 | LPC(14:0) | LPC(14:0) | 468.3088 | 468.3090 | 14.83 |
| | 173 | LPC(16:0) | LPC(16:0) | 496.3379 | 496.3403 | 14.19 |
| | 174 | LPC(16:1) | LPC(16:1) | 494.3245 | 494.3247 | 14.35 |

| | | | | | |
|---|---|---|---|---|---|
| 175 | LPC(18:0) | LPC(18:0) | 524.3723 | 524.3716 | 13.57 |
| 176 | LPC(18:1) | LPC(18:1) | 522.3565 | 522.3560 | 13.82 |
| 177 | LPC(18:2) | LPC(18:2) | 520.3405 | 520.3403 | 14.48 |
| 178 | LPC(18:4) | LPC(18:4) | 516.3066 | 516.3090 | 14.37 |
| 179 | LPC(20:0) | LPC(20:0) | 552.4033 | 552.4029 | 13.30 |
| 180 | LPC(20:1) | LPC(20:1) | 550.3880 | 550.3873 | 13.32 |
| 181 | LPC(20:3) | LPC(20:3) | 546.3548 | 546.3560 | 13.65 |
| 182 | LPC(20:4) | LPC(20:4) | 544.3401 | 544.3403 | 13.57 |
| 183 | LPC(20:5) | LPC(20:5) | 542.3227 | 542.3247 | 14.09 |
| 184 | LPC(22:1) | LPC(22:1) | 578.4191 | 578.4186 | 13.08 |
| 185 | LPC(22:4) | LPC(22:4) | 572.3720 | 572.3716 | 13.31 |
| 186 | LPC(22:5) | LPC(22:5) | 570.3568 | 570.3560 | 13.38 |
| 187 | LPC(22:6) | LPC(22:6) | 568.3406 | 568.3403 | 13.35 |
| 188 | LPC(24:0) | LPC(24:0) | 608.4657 | 608.4655 | 12.34 |
| 189 | LPC(24:1) | LPC(24:1) | 606.4506 | 606.4487 | 12.76 |
| 190 | LPC(O-16:0) | LPC(O-16:0) | 482.3608 | 482.3611 | 15.71 |
| 191 | LPC(P-16:0) | LPC(P-16:0) | 480.3462 | 480.3454 | 13.55 |
| 192 | LPC(O-18:0) | LPC(O-18:0) | 510.3930 | 510.3924 | 15.03 |
| 193 | LPC(O-18:1) | LPC(O-18:1) | 506.3621 | 506.3611 | 13.16 |
| 194 | LPC(P-18:0) | LPC(P-18:0) | 508.3768 | 508.3767 | 15.22 |
| 195 | LPC(O-20:0) | LPC(O-20:0) | 538.4231 | 538.4237 | 14.42 |

*Table C.2 – LC-MS and MS/MS-based identification of the phospholipid molecular species that were quantified in the present study in the negative ion mode. PLs – phospholipids; FA – fatty acids; RT – retention time*

| Class | nr. | PLs | Faz composition | m/z tab. | m/z obs. | RT |
|---|---|---|---|---|---|---|
| PE | 1 | PE(32:0) | | 690.5070 | 690.5068 | 4.46 |
| | 2 | PE(32:2) | | 686.4760 | 686.4758 | 4.10 |
| | 3 | PE(34:1) | PE(18:1/18:0) | 716.5230 | 716.5223 | 4.41 |
| | 4 | PE(34:2) | PE(18:2/16:0) PE(18:1/16:1) | 714.5070 | 714.5076 | 4.39 |
| | 5 | PE(34:3) | PE(16:1/18:2) | 712.4920 | 712.4933 | 4.38 |
| | 6 | PE(38:1) | PE(20:0/18:1) PE(20:1/18:0) | 772.5860 | 772.5848 | 4.35 |
| | 7 | PE(38:4) | PE(20:4/18:0) | 766.5390 | 766.5394 | 4.23 |
| | 8 | PE(38:5) | PE(20:4/18:1) | 764.5230 | 764.5239 | 4.21 |
| | 9 | PE(38:7) | | 760.4920 | 760.4925 | 4.22 |
| | 10 | PE(40:3) | PE(18:2/22:1) PE(18:1/22:2) | 796.5800 | 796.5784 | 4.25 |
| | 11 | PE(40:4) | PE(18:2/22:2) PE(18:2/22:1) PE(18:0/22:4) | 794.5700 | 794.5709 | 4.21 |
| | 12 | PE(40:5) | PE(18:1/22:4) | 792.5540 | 792.5524 | 4.19 |
| | 13 | PE(40:7) | PE(18:2/22:5) PE(18:1/22:6) | 788.5230 | 788.5235 | 4.18 |
| | 14 | PE(40:8) | PE(18:2/22:6) PE(18:3/22:5) | 786.5070 | 786.5076 | 4.18 |
| | 15 | PE(P-32:1) | | 672.4970 | 672.4980 | 4.43 |
| | 16 | PE(P-34:1) | | 700.5280 | 700.5290 | 4.39 |

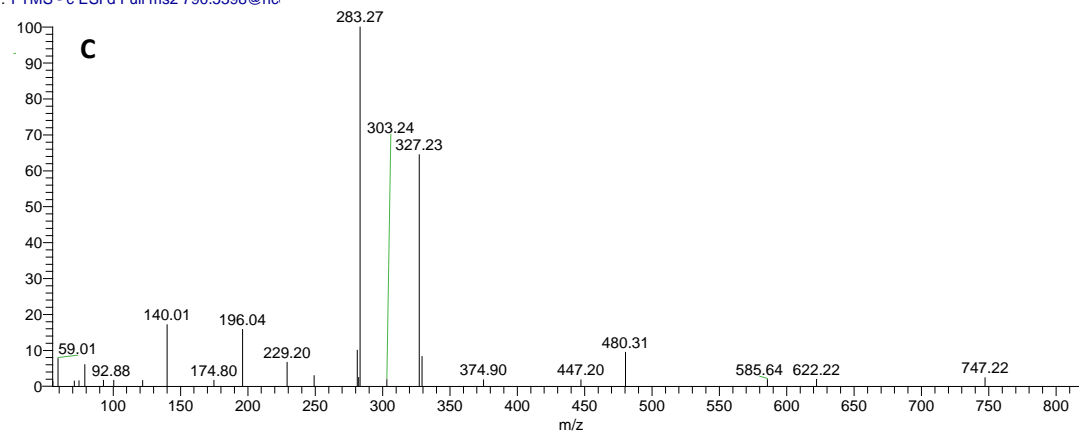| | | | | | |
|---|---|---|---|---|---|
| | 17 | PE(P-36:1) | | 728.5590 | 728.5596 | 4.36 |
| | 18 | PE(P-36:2) | | 726.5440 | 726.5458 | 4.35 |
| | 19 | PE(P-36:4) | | 722.5130 | 722.5135 | 4.27 |
| | 20 | PE(P-36:5) | | 720.4970 | 720.4975 | 4.28 |
| | 21 | PE(P-38:4) | | 750.5440 | 750.5449 | 4.21 |
| | 22 | PE(P-38:6) | | 746.5130 | 746.5134 | 4.20 |
| | 23 | PE(P-40:3) | | 780.5910 | 780.5871 | 4.23 |
| | 24 | PE(P-40:4) | | 778.5750 | 778.5749 | 4.19 |
| | 25 | PE(P-40:6) | | 774.5440 | 774.5445 | 4.17 |
| | 26 | PE(P-40:7) | | 772.5280 | 772.5289 | 4.22 |
| | 27 | PEo(38:3) | | 754.5750 | 754.5741 | 4.32 |
| | 28 | PEo(40:6) | | 776.5590 | 776.5585 | 4.18 |
| **LPE** | 29 | LPE(14:0) | LPE(14:0) | 424.2464 | 424.2478 | 5.47 |
| | 30 | LPE(16:0) | LPE(16:0) | 452.2777 | 452.2786 | 5.33 |
| | 31 | LPE(16:1) | LPE(16:1) | 450.2621 | 450.2629 | 5.37 |
| | 32 | LPE(18:0) | LPE(18:0) | 480.3090 | 480.3094 | 5.25 |
| | 33 | LPE(18:1) | LPE(18:1) | 478.2934 | 478.2943 | 5.22 |
| | 34 | LPE(18:2) | LPE(18:2) | 476.2777 | 476.2786 | 5.28 |
| | 35 | LPE(20:1) | LPE(20:1) | 506.3247 | 506.3254 | 5.20 |
| | 36 | LPE(20:2) | LPE(20:2) | 504.3090 | 504.3068 | 5.48 |
| | 37 | LPE(20:4) | LPE(20:4) | 500.2777 | 500.2788 | 5.17 |
| | 38 | LPE(20:5) | LPE(20:5) | 498.2621 | 498.2619 | 5.24 |
| | 39 | LPE(22:4) | LPE(22:4) | 528.3090 | 528.3095 | 5.10 |
| | 40 | LPE(22:5) | LPE(22:5) | 526.2934 | 526.2951 | 5.18 |
| | 41 | LPE(22:6) | LPE(22:6) | 524.2777 | 524.2786 | 5.14 |
| | 42 | LPE(O-16:0) | LPE(O-16:0) | 438.2985 | 438.2995 | 5.60 |
| | 43 | LPE(O-18:0) | LPE(O-18:0) | 466.3298 | 466.3304 | 5.52 |
| | 44 | LPE(P-16:0) | LPE(P-16:0) | 436.2828 | 436.2836 | 5.20 |
| | 45 | LPE(P-18:0) | LPE(P-18:0) | 464.3141 | 464.3153 | 5.13 |

## 12.3   Phospholipids MS and MS/MS spectra examples
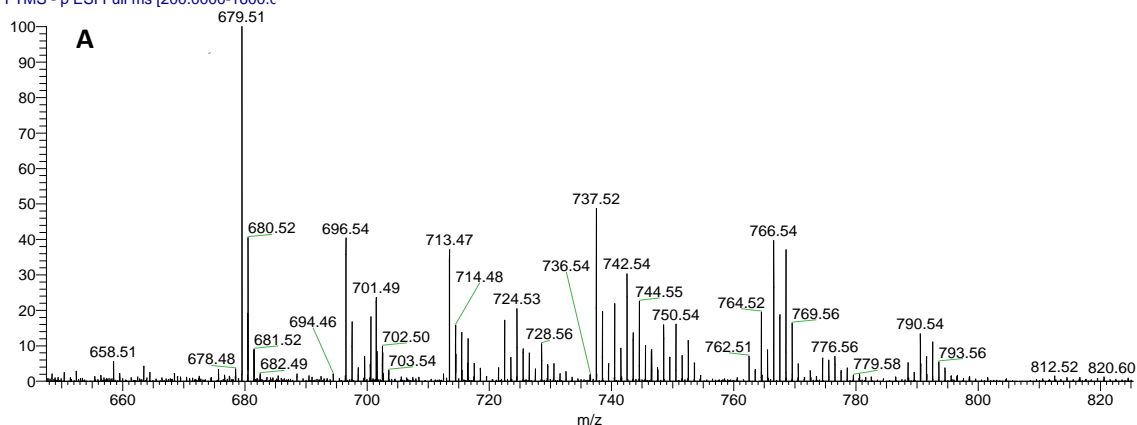


*Figure C.4 – A – Example LC-MS spectra of PE;  B – LC-MS/MS spectra of PE in the positive mode; C -  LC-MS/MS spectra of PE in the negative mode*
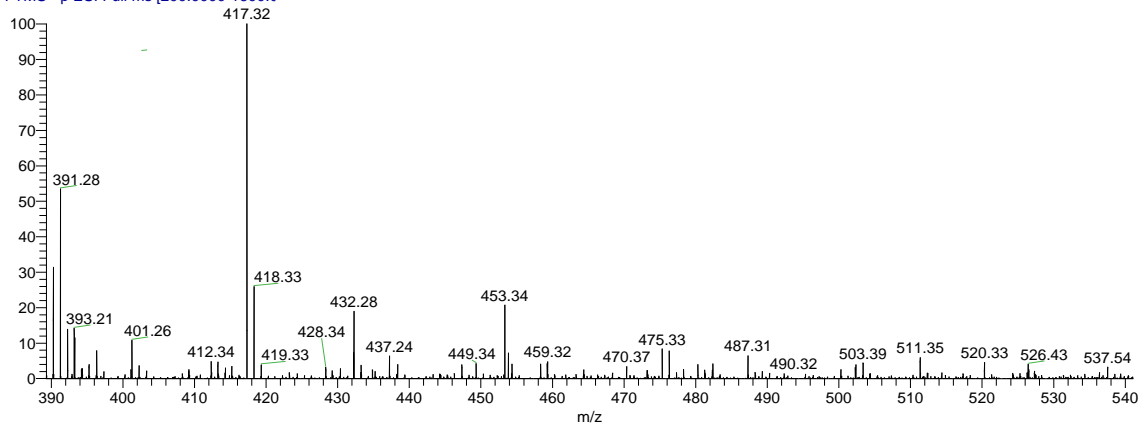
Figure C.5 - Example LC-MS spectra of LPE in negative mode.
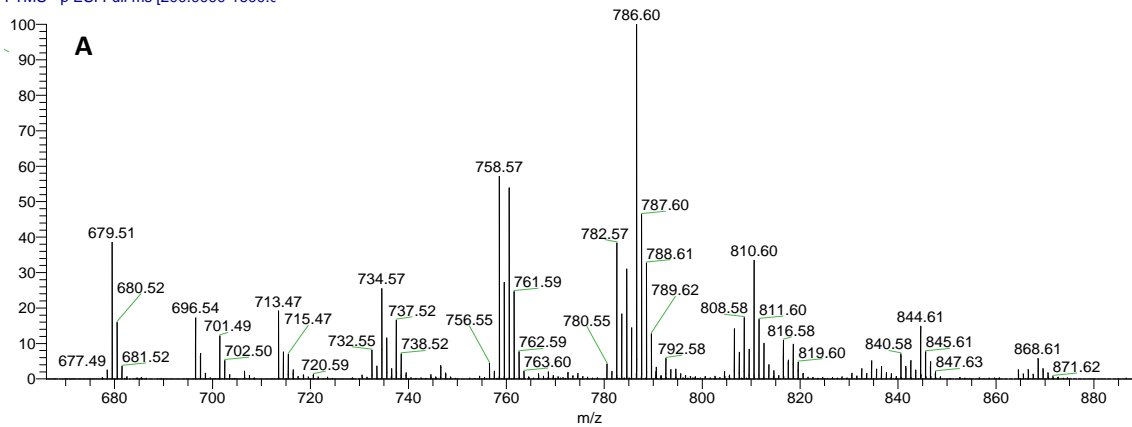


Figure C.6 - A – Example LC-MS spectra of PC; B – MS/MS spectra of PC in the positive mode;

RHChD_Mix #4562-5314  RT: 13.03-15.12  AV: 68  NL: 3.53E6
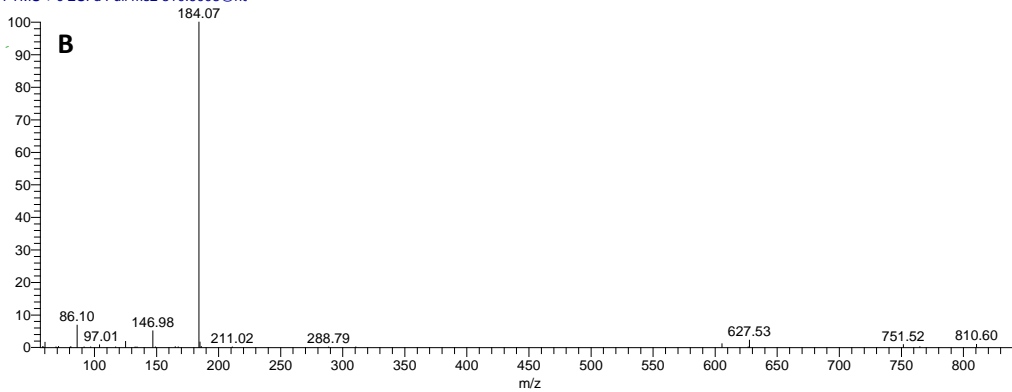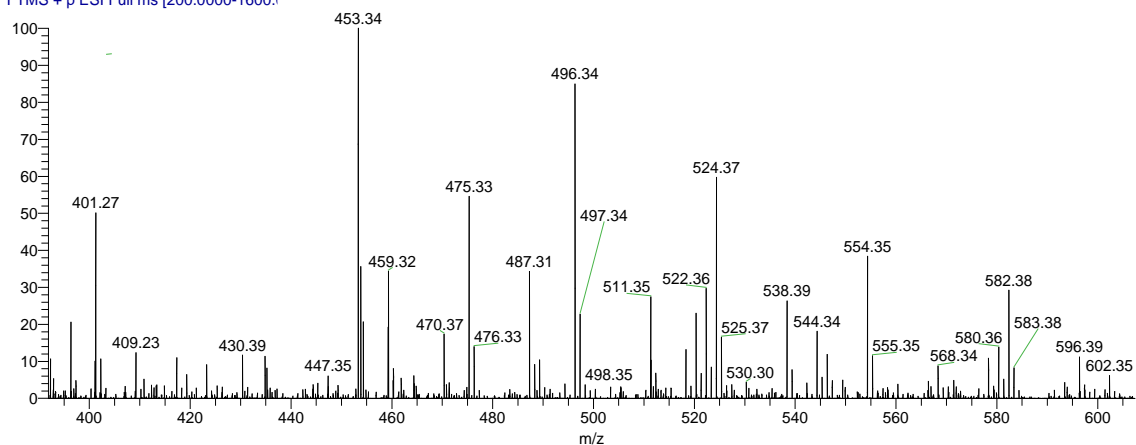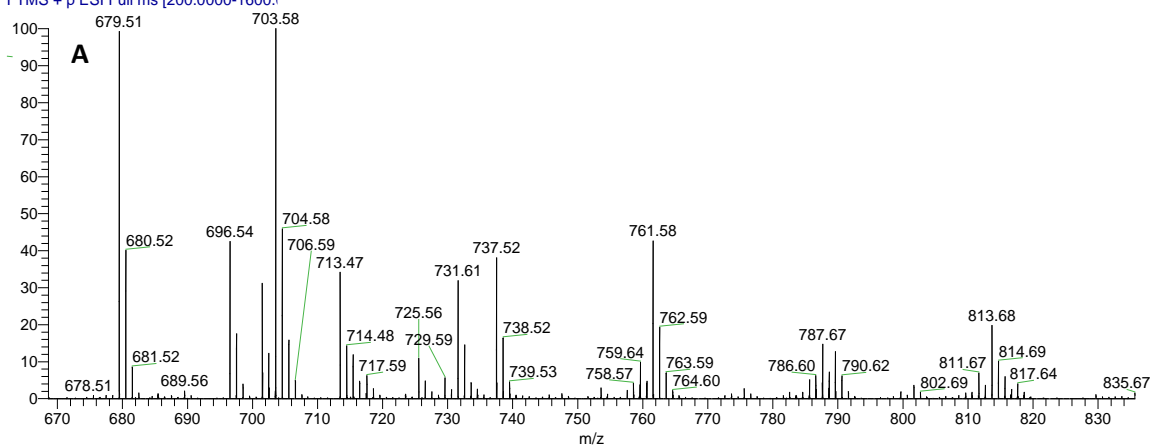T: FTMS + p ESI Full ms [200.0000-1600.0



*Figure C.7 – Example LC- MS spectra of LPC in positive mode.*

RHChD_Mix #3809-4149  RT: 10.91-11.85  AV: 31  NL: 1.51E7
T: FTMS + p ESI Full ms [200.0000-1600.0



HFD_Mix #3888  RT: 11.12  AV: 1  NL: 6.92E5
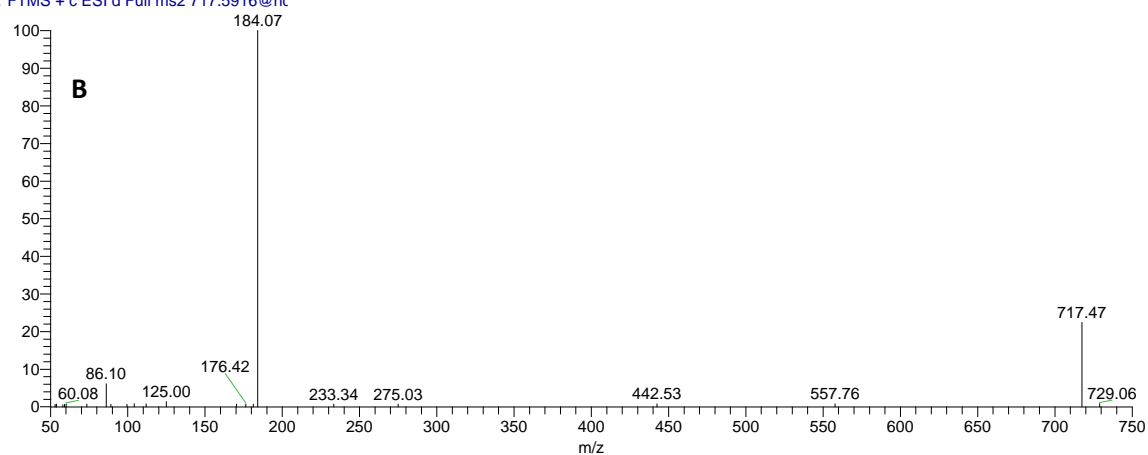T: FTMS + c ESI d Full ms2 717.5916@hc



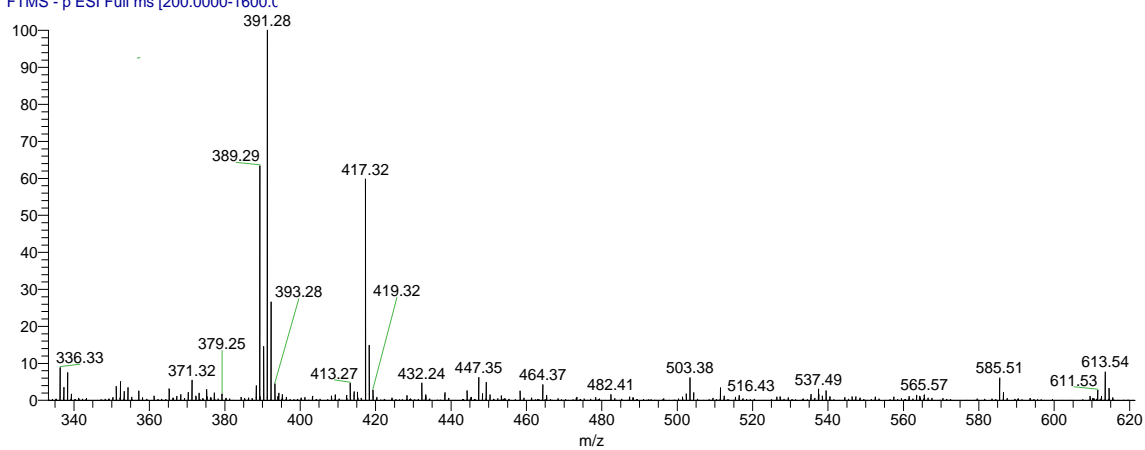*Figure C.8 - A – Example MS spectra of SM resulting from the LC-MS;  B – LC-MS/MS spectra of SM in the positive mode;*

*Figure C.9 - Example MS spectra of Cer resulting from the LC-MS*